POLYMER WHITE LIGHT EMITTING DIODES APPLICATIONS OF
BENZOTRIAZOLE AND FLUORENE DERIVATIVES

A THESIS SUBMITTED TO
THE GRADUATE SCHOOL OF NATURAL AND APPLIED SCIENCES
OF
MIDDLE EAST TECHNICAL UNIVERSITY

BY

GÜLER KOÇAK

IN PARTIAL FULFILLMENT OF THE REQUIREMENTS
FOR
THE DEGREE OF MASTER OF SCIENCE
IN
CHEMISTRY

SEPTEMBER 2015

Approval of the thesis:

POLYMER WHITE LIGHT EMITTING DIODES APPLICATIONS OF BENZOTRIAZOLE AND FLUORENE DERIVATIVES

submitted by **GÜLER KOÇAK** in partial fulfillment of the requirements for the degree of **Master of Science in Chemistry Department, Middle East Technical University** by,

Prof. Dr. Gülbin Dural Ünver   _____
Dean, Graduate School of **Natural and Applied Sciences**

Prof. Dr. Cihangir Tanyeli   _____
Head of Department, **Chemistry**

Assoc. Prof. Dr. Ali Çırpan   _____
Supervisor, **Chemistry Dept., METU**

Examining Committee Members:

Prof. Dr. Levent Toppare   _____
Chemistry Dept., METU

Assoc. Prof. Dr. Ali Çırpan   _____
Chemistry Dept., METU

Assoc. Prof. Dr. Ayşen Yılmaz   _____
Chemistry Dept., METU

Assist. Prof. Dr. İrem Erel Göktepe   _____
Chemistry Dept., METU

Assoc. Prof. Dr. Yasemin Arslan Udum   _____
Advanced Technologies Dept., Gazi University

Date: _____

I hereby declare that all information in this document has been obtained and presented in accordance with academic rules and ethical conduct. I also declare that, as required by these rules and conduct, I have fully cited and referenced all material and results that are not original to this work.

Name, Last Name: GÜLER KOÇAK

Signature   :

ABSTRACT

POLYMER WHITE LIGHT EMITTING DIODES APPLICATIONS OF BENZOTRIAZOLE AND FLUORENE DERIVATIVES

Koçak, Güler

M.S., Department of Chemistry

Supervisor: Assoc. Prof. Dr. Ali Çırpan

September 2015, 113 pages

In this thesis, white polymer light emitting diodes (WPLEDs) were constructed using benzotriazole and fluorene containing conjugated polymers. For this purpose, three different blue and four different orange emitting conjugated polymers with different end cappers were used. The method that was used throughout the thesis included mixing of two polymers (blue and orange emitting) having different weight ratios in a common solvent. These solutions were coated on ITO-glass substrates by spin-coating technique which is the most common method for polymer coating. The different ratios of the two polymers were optimized according to the luminance efficiency of OLED devices. Moreover, an optimization study was conducted for different solvents such as toluene and chloroform. The polymers that were synthesized throughout the thesis were characterized by means of NMR, GPC, TGA and DSC. Polymers were also characterized for determining their fluorescence quantum yield prior to the device

fabrication. In addition, all polymers and polymer blends were spin coated onto silicon wafers in order to examine the active layer thickness via Atomic Force Microscopy (AFM). After determination of the optimum film thickness, WPLED devices were constructed. The flexible WPLED device experiments were also conducted, and all constructed devices were characterized by means of their luminance, color coordinates and luminance efficiency. As a result, WPLEDs from fluorescent polymer blends showed effective CIE color coordinates of x=0.31, y=0.33 which are very close to the pure white color (x=0.33, y=0.33), and all devices showed high stability and have voltage invariant electroluminescence spectra.

Keywords: Conjugated Polymers, Benzotriazole, Polymer White Light Emitting Diodes, Optoelectronics

ÖZ

BENZOTRİAZOL VE FLOREN TÜREVLERİ İÇEREN POLİMERLERİN BEYAZ IŞIK YAYAN DİYOT UYGULAMALARI

Koçak, Güler

Yüksek Lisans, Kimya Bölümü

Tez Yöneticisi: Doç. Dr. Ali Çırpan

Eylül 2015, 113 sayfa

Gerçekleştirilen bu tez çalışmasında, beyaz polimerik ışık yayan diyotlar, benzotriazol ve floren türevi içeren konjüge polimerler kullanılarak elde edilmiştir. Tez çalışmasında, üç farklı mavi ve dört farklı turuncu ışık yayan farklı son gruplara sahip polimerler kullanılmıştır. Kullanılan yöntem, farklı çözücüler içinde, farklı oranlarda mavi ve turuncu ışık yayan iki polimerin karıştırılmasını içerir. Bu polimer karışımları, ITO-cam alttaş üzerine polimer kaplama için en yaygın yöntem olan dönel kaplama yöntemi ile kaplanmıştır. Ayrıca, toluen ve kloroform gibi değişik çözücüler kullanılarak da bir optimizasyon çalışması yapılmıştır. Sentezlenen polimerler, NMR, GPC, TGA ve DSC kullanılarak karakterize edilmiştir. Bunların yanında polimerlerin floresans kuantum verimleri de hesaplanmıştır. Buna ek olarak, tüm polimerler ve polimer karışımları, aktif tabaka kalınlığını belirlemek için silisyum plakalar üzerine dönel kaplama yardımıyla

kaplanmıştır. Aktif tabaka kalınlıkları belirlendikten sonra WPLED'ler üretilmiştir. Esnek WPLED deneyleri de gerçekleştirilmiştir; üretilen tüm cihazlar; parlaklıkları, renk koordinatları ve güç verimleri açısından karakterize edilmiştir. Sonuç olarak, üretilen WPLED'lerin CIE renk koordinatları (x=0.31, y=0.33) saf beyaz ışık renk koordinatlarına (x=0.33, y=0.33) çok yakın bulunmuştur. Aynı zamanda, üretilen tüm cihazlar yüksek dayanıklılığa sahiptir ve cihazlardan gerilime bağlı olmayan elektrolüminesans spektrumu elde edilmiştir.

Anahtar Kelimeler: Konjüge Polimerler, Benzotriazol, Polimerik Beyaz Işık Yayan Diyotlar, Optoelektronik

To my family…

ACKNOWLEDGMENTS

I would like to thank to my supervisor Assoc. Prof. Dr. Ali Çırpan for his constant support and valuable guidance. His mentorship has created great influence on my academic life.

I would like to express my appreciation to Prof. Dr. Levent Toppare for his astonishing and invaluable support.

I am also grateful for my friend Ozan Erlik for the synthesis of the polymers.

Moreover, all Toppare and Çırpan Research Group Members supported me continuously, their friendship and cooperation were exceptionally encouraging.

I also appreciate the METU Central Laboratory for the technical support provided.

Finally, I would like to thank to my family for all the love and invaluable encouragement.

TABLE OF CONTENTS

CHAPTERS

LIST OF TABLES

TABLES

LIST OF FIGURES

FIGURES

LIST OF ABBREVIATIONS

ACN	Acetonitrile
AFM	Atomic force microscopy
Alq3	Tris(8-hydroxyquinoline) aluminum
AMOLED	Active matrix organic light emitting diode
BE	Blue emitting
CA-CN	Mixed cellulose
CB	Conduction band
CIE	Commission internationale de I'Eclairage
CP	Conjugated polymer
CsF	Cesium fluoride
CV	Cyclic voltammetry
DCM	Dichloromethane
DSC	Differential scanning calorimetry
EL	Electroluminescence
Eg	Band gap energy
EQE	External quantum efficiency
EML	Emissive layer
ETL	Electron transport layer
Fc	Ferrocene
FRET	Förster resonance energy transfer
GPC	Gel permeation chromatography
HOMO	Highest occupied molecular orbital
HTL	Hole transport layer
ITO	Indium tin oxide
LE	Luminance efficiency
LED	Light emitting diode
LiF	Lithium fluoride

LUMO	Lowest unoccupied molecular orbital
Mn	Number average molecular weight
Mw	Weight average molecular weight
NHE	Normal hydrogen electrode
NIR	Near infrared
NMR	Nuclear magnetic resonance
OLED	Organic light emitting diode
PDI	Polydispersity index
PEDOT:PSS	Poly (3,4-ethylenedioxythiophene):poly(styrenesulfonate)
PEN	Polyethylene naphthalate
PET	Polyethylene terephthalate
PF	Polyfluorene
PHOLEDs	Phosphorescent organic light emitting diode
PL	Photoluminescence
PLED	Polymer light emitting diode
PMOLED	Passive matrix organic light emitting diode
PPV	Polyphenylene vinylene
PTh	Polythiophene
PVK	Poly(9-vinylcarbazole)
QS	Quinine sulfate
QY	Quantum yield
RGB	Red-green-blue
SSL	Solid state lighting
TBAPF$_6$	Tetrabutylammonium hexafluorophosphate
TEM	Transmission electron microscopy
TGA	Thermogravimetric analysis
UPS	Ultraviolet photoelectron spectroscopy
UV	Ultraviolet
WF	Work function
WOLED	White organic light emitting diode
WPLED	White polymer light emitting diode

CHAPTER 1

INTRODUCTION

1.1 Conjugated Polymers

Polymers have been realized as good electrical insulators since their early practice. Owing to their easy processing, flexibility, low weight, and chemical inertness in addition to their insulating qualities, they are used for significant purposes such as cable sheathing. A novel approach for altering the electrical conductivity and mechanical characteristics of the polymers was constantly being studied by many researchers in order to achieve a resilient material. Among these researchers; Heeger, MacDiarmid, and Shirakawa combined their efforts to examine the electronic characteristics through treating polyacetylene films by certain amounts of gas-phase Cl_2, Br_2, I_2 and AsF_5 doping [1]. The outcome of the study is the presence of mobile charges in a conjugated polymer system, in other words, the conductivity in polymers. This study received Nobel Prize in 2000, and it has led up to well-characterized, solution processable polymers with sound structural control that have become better alternatives and widely used materials for many applications. The conjugation accomplished in these systems is due to the formation of the delocalized double bond over the main chain of the polymer. The orbital overlap forms the π bonds assisting the electrons to move freely along the chain as depicted in **Figure 1.1** [2]. Bearing p-electron systems, conjugated polymers exhibit remarkable electronic properties. Eventually, along the polymer chain, current is carried through species of holes and electrons [2, 3].
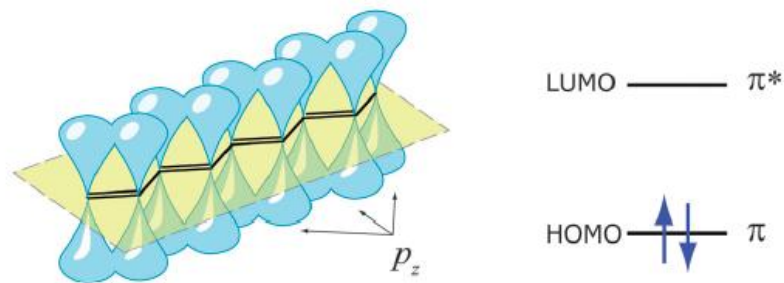
Figure 1.1 Conjugated backbone with overlapping p_z orbitals [3].

The utilization of these electrically conductive and conjugated polymers is numerous. The promising technology of the polymer electronics is prevalent. In particular, conjugated polymers which are utilized for the production of flexible polymer light emitting diodes are the key materials for the future lighting and display technologies [4].

1.1.1 Light Emission by Conjugated Polymers

As atoms or molecules absorb energy, the energy level of electrons change accordingly. There are several ways to form excited states through energy absorption. In photoexcitation, electron absorbs a photon and gains the energy of the photon. In electrical excitation, the primary electron absorbs the energy of another energetic electron. Lastly, thermal energy also rises the electron to a higher energy state where collisions are formed between the sample atoms causing the electrons of the atom to be excited. Thus, as the electron returns to the ground (lower energy) state for a relaxation, light is emitted. If the excited state decays under the emission of visible light, the corresponding emission is called luminescence [5]. **Figure 1.2** presents a selection of the light emitting polymers possessing a conjugated π electron system, other polymers with saturated backbones bearing conjugated side groups exist, as well [6].
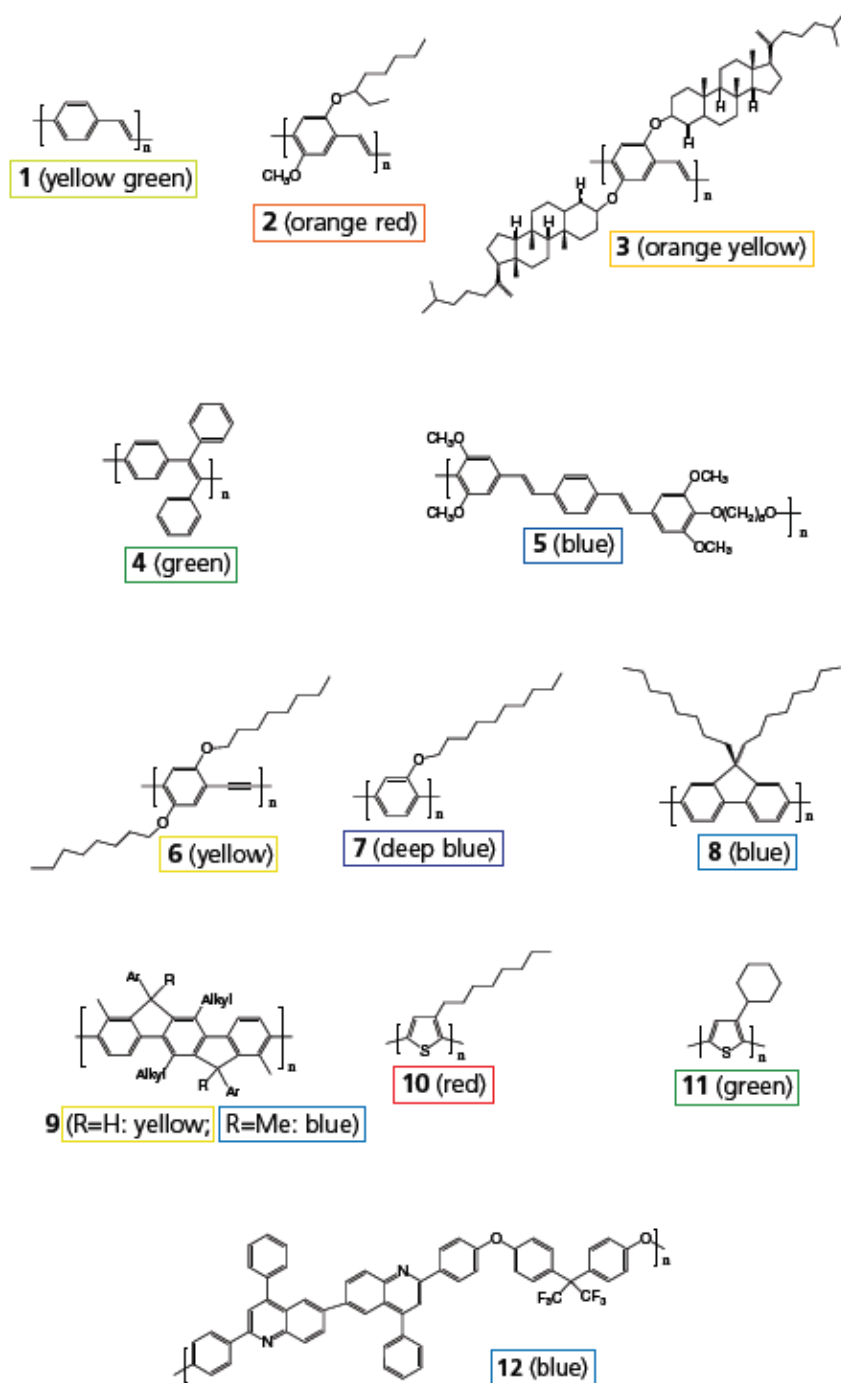
Figure 1.2 Light emitting conjugated polymers [6].

1.2 Luminescence

Figure 1.3 Luminescence from light emitting materials [8].

Since the new era of energy has brought the problems of the waste of power, shortage of electricity, and non-disposable lighting tools; a novel lighting system has come forefront as a better alternative. This system is made use of luminescence instead of incandescence which produces light from heat energy. The common light bulbs, in which the tungsten filament is heated to glow, are not environment friendly. Nevertheless, luminescence, which is a form of cool light, does not use any hot sources. It is resulted due to the electron movement from more energetic states to less energetic states of the substances [7]. Luminescence is observed from many inorganic and organic substances, examples for luminophores are as shown in **Figure 1.3** [8], and could be generated by various physical processes. Two possible mechanisms are the absorption of photons, which leads to photoluminescence, or the recombination of injected charges, which is called electroluminescence.

1.2.1   Photoluminescence (PL)

When sufficient light energy is directed on a molecule, photons are absorbed and excited states are formed instantly. Ultimately, the relaxation occurs and the electrons go back to

the ground state. If the relaxation is radiative, the phenomenon is photoluminescence [9]. Due to the energy loss, the absorption wavelength is shorter than the emission energy state. The PL spectrum presents the transition energies which are advantageous in determining the electronic energy levels.

1.2.1.1 Fluorescence

Fluorescence phenomenon is the result of the process called electron excitation. As a selection of atoms are subjected to the ultraviolet (UV) light, a photon initiate for the transfer of electrons in the lower energy shell to move to the higher energy shell. When it relaxes while dropping from the higher energy level, it releases the additional energy [10]. **Figure 1.4** exemplifies the energy level diagram for the absorption of a photon by a luminescent molecule (Jablonski Diagram) [11].
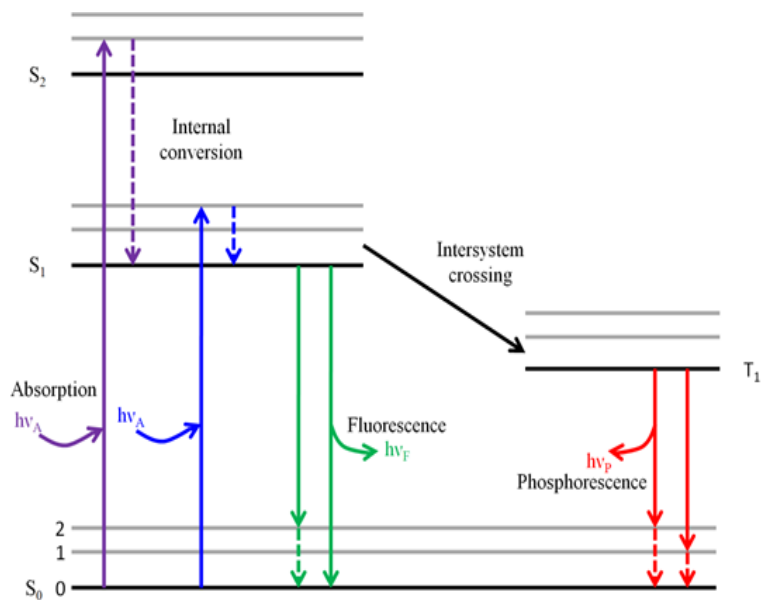
Figure 1.4 Jablonski Diagram [11].

By an absorption of a molecule, electrons move to the excited S_1, S_2 levels from the singlet electronic ground level. As the molecule has an excessive energy in these excited states, it is needed to be relaxed via returning to the ground state. Emission of the photon occurs with a particular energy E and thus it will be observed at a precise wavelength (λ_{em}) [12].

1.2.1.2 Phosphorescence

A similar process is phosphorescence. The relaxation step differs in this phenomenon. A phosphorescent material re-emits the absorbed energy much slower than the fluorescent material as depicted in **Figure 1.4**. The time difference is due to the transition in forbidden energy states [13]. A molecule in the excited triplet state is less likely to carry out triplet to triplet transition than singlet to singlet transition.

1.2.2   Electroluminescence (EL)

Electroluminescence (EL) was discovered by H. J. Round who used carborundum (SiC) crystals in 1907 [14]. The luminescence is due to the externally applied voltage in EL. In photoluminescence, charge carriers (electrons and holes) are photo excited by a light source and the luminescence emission occurs from the radiative recombination of the carriers. Whereas, in EL, the carriers are produced by current injection and the performance is measured on a device [22]. Electroluminescence phenomena is based on electron-hole pair formation in a molecule as an external current applied as depicted in **Figure 1.5**, which is a more basic form of Jablonski energy diagram. The ground state of the organic molecules is electrically neutral and has zero spin. Excitons (hole-electron pairs) are electrically neutral, and have an existing potential energy that is used when returning to the ground state. Excitons with total spin of zero are called singlet (S_0, S_1), and triplet excitons (T_1) have total spin of one. Fluorescence and phosphorescence

6

emissions collect different percentages of excitons. Fluorescence has a 25% restriction of singlet exciton production efficiency. Nevertheless, exciton production ratio upon excitation from electrical current is 1:3 for the singlet-to-triplet exciton. Hence, phosphorescence materials are crucial for high EL efficiency in which exciton production efficiency is 100%. Thus, second generation organic light emitting diodes benefit from phosphorescent molecules that also harvest triplet excitons for higher device efficiency.
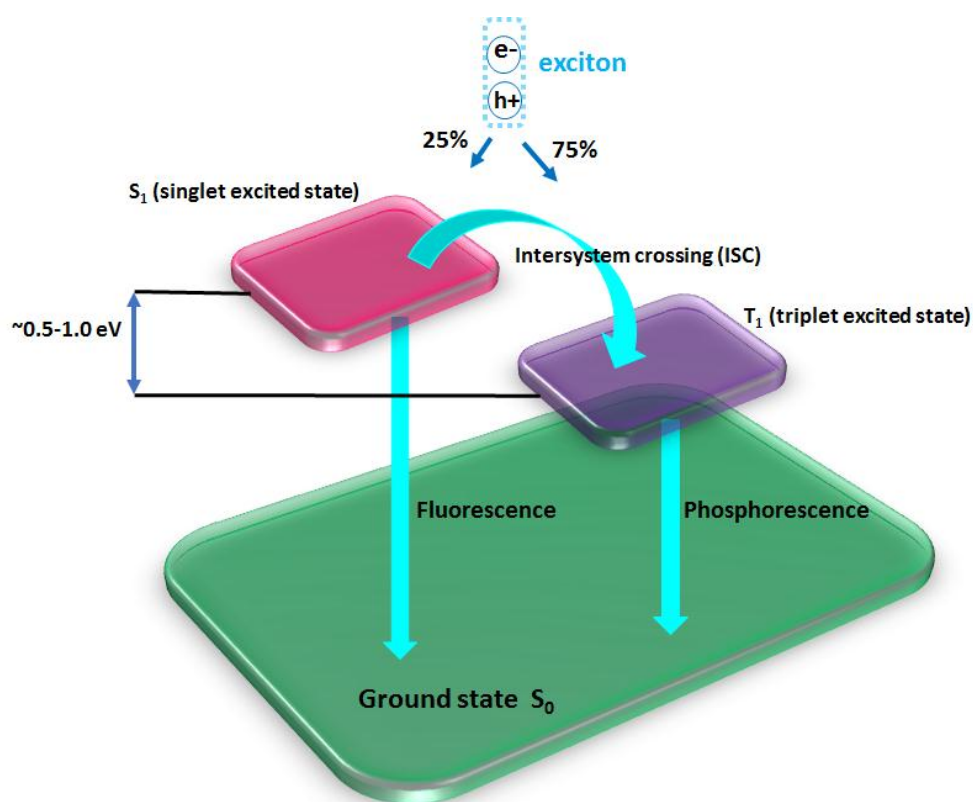
Figure 1.5 Electroluminescence from fluorescent and phosphorescent molecules.

The developments of electroluminescence from organic materials are also summarized in Table 1.1.

Table 1.1 History of investigations in the field of electroluminescence in organic materials

Year	EL Source and Emission
1963	EL from antracene crystals [15]
1976	EL from tetracene crystals [16]
1983	EL from polymers [17]
1987	Double layer organic solid LED [18]
1990	Single layer PLED [19]
1993	Double layer PLED [20]
2007	Flexible OLED display [21]

1.3 Energy Transfer Mechanisms

Energy transfer phenomenon is the other path that excited molecules could take along with the relaxation. A hole-electron pair (exciton) can be displaced from an excited donor molecule to an acceptor molecule through a non-radiative energy transfer route. After this energy transfer, the donor molecule remains in the ground state and the acceptor molecule is located in the excited state. High band gap donor materials produce excitons that are transferred to any lower band gap acceptor materials via long range Förster resonance energy transfer (coulombic interaction) of singlet excitons or Dexter transfer of triplet excitons. The exciton formation is due to the coulombic forces in energy transfer phenomena and its formation varies with molecules' having triplet states. These states could be used as triplet excitons when the molecule is excited. As indicated before, Dexter transfer uses these triplet excitons and they possess shorter interaction ranges [23, 24, 25].

1.3.1   Förster Energy Transfer (FRET)

The Fluorescence Resonance Energy Transfer (FRET) is an imperative method for analyzing the exciton formation and its applicability on organic electronics [26, 27]. In FRET, a high band gap donor (D) transfers its absorbed energy to the neighboring acceptor (A) without a radiative energy transfer, as explained in Equation 1.1.

$$D^* + A \longrightarrow D + A^*$$

$$A^* \longrightarrow A + h\,v$$
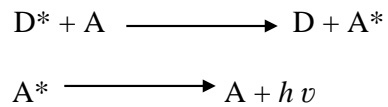
Equation. 1.1

FRET mechanism is also given in **Figure 1.6**. It can be seen that the donor material transfers its excitation energy to the acceptor, and successively, the light is emitted from the acceptor molecule when the charges are recombined.
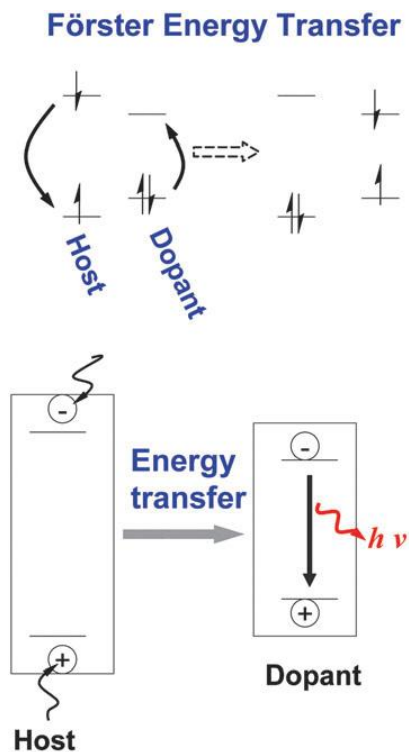
Figure 1.6 Förster energy transfer mechanism.

The Förster mechanism is principally based on the criteria of overlapping of the absorption spectra of the acceptor with the photoluminescence spectra of the donor.
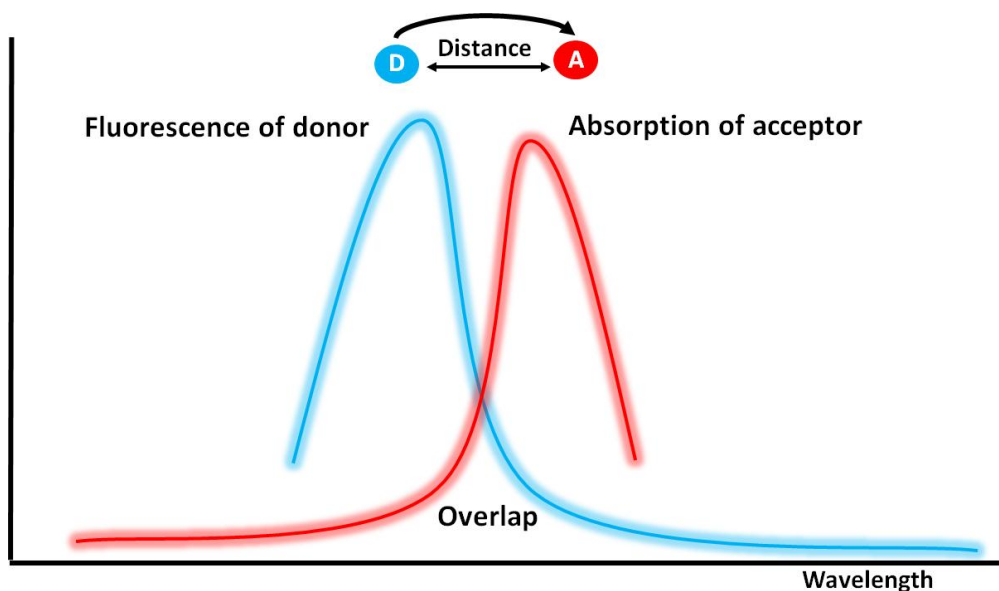
Figure 1.7 Overlap of the emission spectrum of the donor and the excitation spectrum of the acceptor.

The efficiency of FRET also depends on the distance between donor and acceptor, it is observed generally in 1-5 nm ranges as illustrated in **Figure 1.7**. Hence, several parameters have come forefront for an efficient FRET; the spectral overlap of the emission spectrum of the donor and the absorption of the acceptor, and the specific distance (Förster radius) at which the non-radiative energy transfer occurs [28].

1.3.2   Dexter Energy Transfer

The Dexter Energy Transfer is another non-radiative electron exchange mechanism as stated earlier and depicted in **Figure 1.8**. The transfer is established through electrons that are inter-changed between donor and acceptor [29]. The distance that is required for an efficient Dexter energy transfer is shorter than that of FRET. The triplet excitons are

made use of in this phenomena and the metal complexes such as iridium complexes are the most commonly used examples of triplet emitters [30].
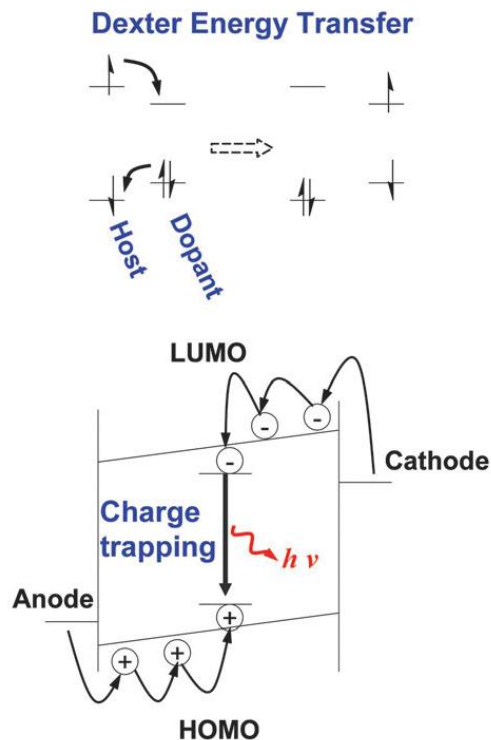
Figure 1.8 Dexter energy transfer mechanism.

1.4 Organic Light Emitting Diodes (OLEDs)

An OLED is a solid state electronic device constructed by depositing a series of thin layers and as required voltage is applied, light is emitted as shown in **Figure 1.9** [31]. Principally, in OLEDs, the emissive layer (EML) that is responsible for the specifications of the light emitted is in between electrodes. EML is required to possess high photoluminescence quantum efficiency and high optical and thermal stabilities due to its exposure to increasing driving voltages.
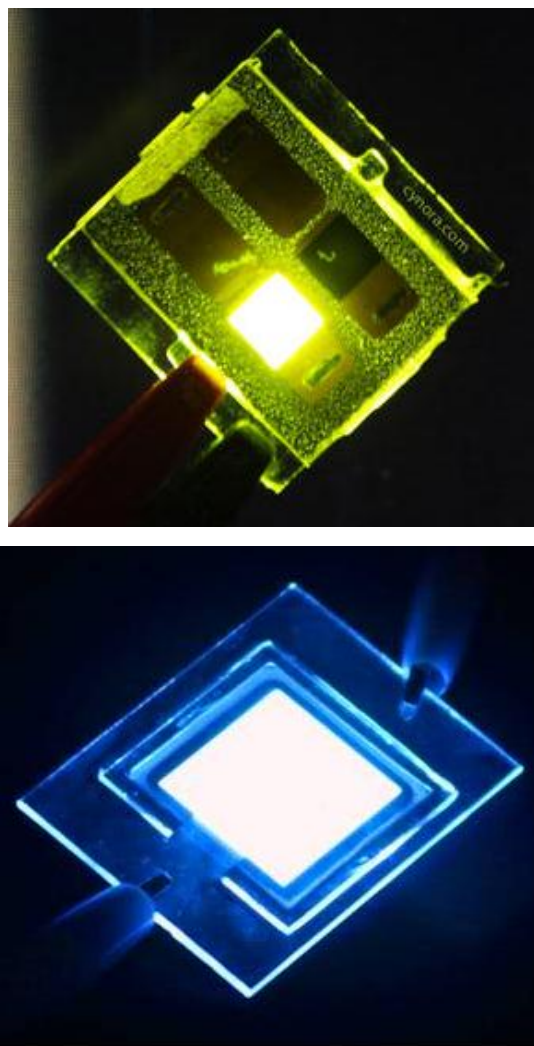
Figure 1.9 Green and Blue OLED Modules.

1.4.1 History of OLEDs

In 1987, the first organic light emitting diodes (OLEDs) were built as stated earlier in investigations of electroluminescence, based on thin molecular films (Alq3) with conducting and luminescent properties and reasonable operating voltages less than 10V, although with very small external quantum efficiencies as 1%. Indeed, electroluminescence from organic molecules was first discovered by Martin Pope and his group in 1963, yet the operating voltage and the efficiency of the device were quite

low. In 1990, along with the extensive research, the PPV based OLED was made, as well. The device was called as Polymer-LED or PLED. The ongoing research is promising particularly in illumination industry, advancements of OLEDs for lighting are also given by year in **Figure 1.10** [32].
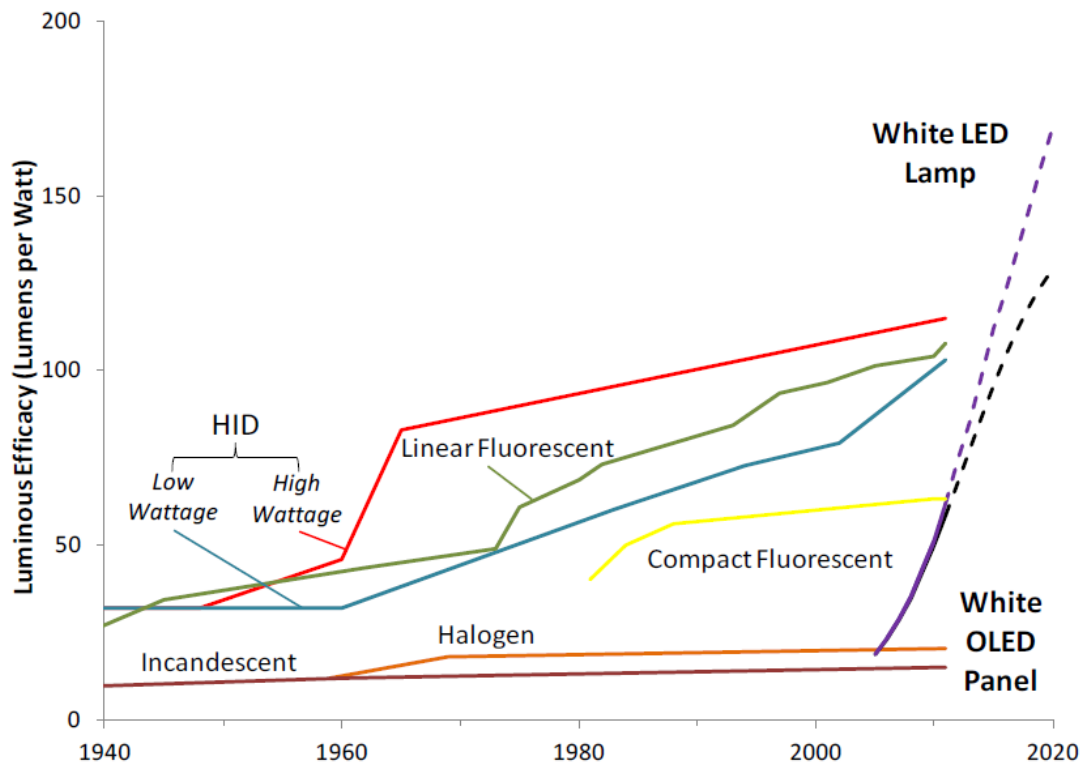
Figure 1.10 Advancements in Lighting [32].

1.4.2   OLED Working Principle

The light generation from an OLED takes place in four fundamental step as shown in **Figure 1.11**. The first step is the injection of the charge carriers (holes and electrons) from anode and cathode, respectively. Second step is the transport of the charge carriers into the organic materials by coulombic attraction. Then, excitons (hole and electron pairs) are formed. Finally, light is emitted by radiative decay.

13
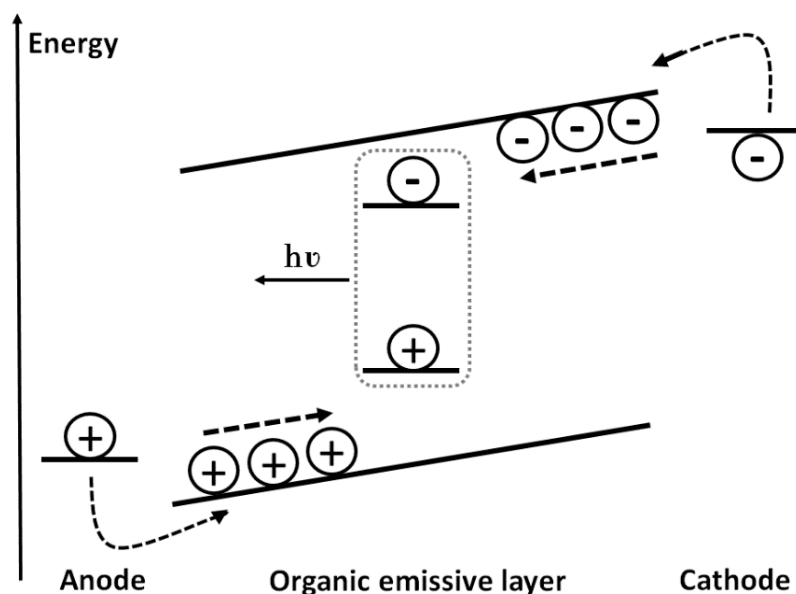
Figure 1.11 Operation of an OLED.

When a proper voltage is applied into the electrodes of the OLED, the electrons from cathode are removed and injected into the LUMO energy level of the emissive layer components, simultaneously, the holes are injected from anode and transported via hole transport agents such as PEDOT:PSS or PVK as they possess high electron donating properties which cause them to be excellent hole transport materials. Low work function (WF) metals are used since the electron transport materials due their energy level's closeness to the vacuum level have compatible WF with the LUMO of the emissive layer components. There may exist some energy barriers resulting from many successive layers, particularly with extremely different energy levels of organic layer as and the electrodes [33].

1.4.3 Advantages and Disadvantages of OLEDs

The main advantages of OLEDs compared to inorganic devices are OLEDs' being ultra-thin, lighter, flexible, and in some cases semitransparent. Their applicability to be applied on any substrate and on large area are other advantages. They are more readily accessible technology and have lower production costs. Yet, their performance increasing and dominating other technologies. Recent advances in new OLEDs based on phosphorescent materials (PHOLEDs) are reaching efficiencies close to 100% [34].

The main disadvantages of OLEDs are currently under investigation; the sensitivity to ambient conditions, their reaction with oxygen and moisture, and exposure towards UV are among OLEDs' weaknesses.

1.4.4 Device Configuration

The architecture of polymer based OLED is illustrated in **Figure 1.12**.
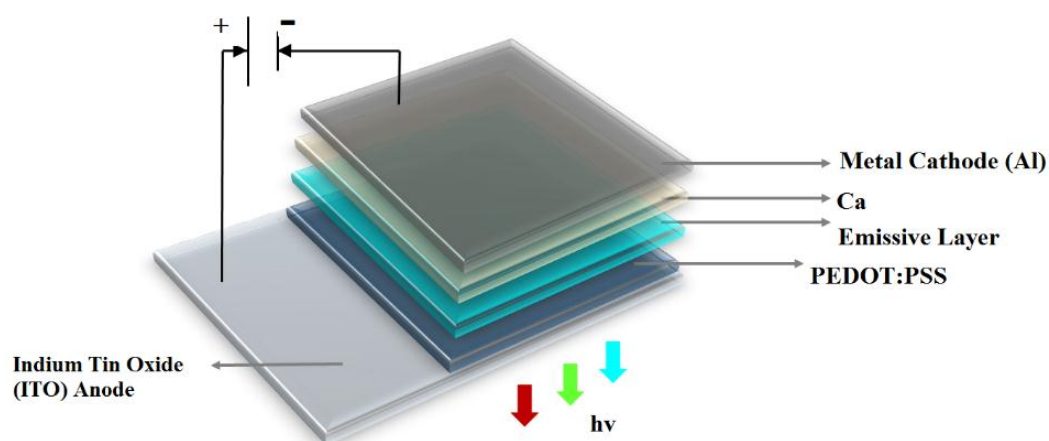
Figure 1.12 Architecture of polymer based OLED or PLED.

1.4.4.1 Glass/Plastic Substrates

The substrate supports the OLED. Glass and transparent plastics are the most common examples.

1.4.4.2 Anode Materials

Anode materials are responsible for the injection of holes when voltage is applied. The anode materials are generally formed on the substrate (plastic or glass) and must have some characteristic constraints [35], they need to be highly conductive in order to decrease the contact resistance. They must have high work function (WF) in order to assist to the injection of holes into the organic emissive layers. Good film forming and wettability are also essential in order to have good contact with adjacent organic layers. Thermal and chemical stability should be high. Lastly, high transparency is needed in order to ensure the emitted light is able to leave the device efficiently. The most commonly used anode material is indium tin oxide (ITO) as it has great conductivity, high transparency, and a proper work function value to be a hole injection material. ITO surface can be altered in terms of its work function value through several methods such as oxygen plasma cleaning or acid or base treatments [36].

1.4.4.3 Cathode Materials

Cathode materials are metal alloys or pure metals. The selection of material is done considering the purpose of diminishing the energy barrier between the electrode and the neighboring organic layer. The cathode materials should have some basic properties [37], they must have high conductivity. They should have relatively low work function (Φ) in order to stimulate injection of electrons into the organic emissive layers. Good

film forming and wettability are significant in order to have good contact with adjacent organic layers. High thermal and chemical stability are required, as well. The metals such as calcium (Ca), magnesium (Mg), aluminum (Al) and their alloys are used as cathode. Since these metals have low work functions that are close to the vacuum level, they are extremely vulnerable to air and moisture. Cathode materials decompose by the expansion of non-emissive dark spots. In order to get rid of this undesirable issue, a very thin layer (≤0.6 nm) of LiF or CsF can be added [38].

1.4.4.4 Emissive Layers

Light emitting materials, i.e. conjugated polymers are used as emissive layers as stated in section 1.1.1.

1.5   OLED Fabrication

1.5.1   ITO-Substrate Cleaning

ITO surface is exposed to several steps of cleaning as it is one of the most critical step in device fabrication. Aqueous and organic solvents are made use of for the initial cleaning, later in order to remove the remaining contaminants, either oxygen plasma treatment or UV irradiation is utilized. The ITO surface is significantly affected from the cleaning steps, therefore, the duration of the initial cleaning steps and the power of the oxygen plasma needs further carefulness.

1.5.2   Spin-Coating of HTL (PEDOT:PSS Layer) and Emissive Layers

The PEDOT:PSS layer performs three functions [39]; It assists on good quality coating of the emissive layer by smoothing the ITO surface, it has a hole transporting property due to its compatible HOMO energy level with the work function of ITO and the

emissive layer HOMO level. PEDOT:PSS coating is done after guaranteeing that the ITO-surface is very clean and hydrophilic. The contact angle of the PEDOT:PSS on ITO surface is greatly diminished after oxygen plasma treatment. It is generally spin-coated to be adjusted for a thickness of 40 nm. For best performance, the PEDOT:PSS should be annealed on a hot plate. After PEDOT:PSS treatment, the light emitting polymer is filtered and dissolved in a proper solvent. The coating is done in O_2 and moisture free Glove Box System. The spinning rate and the solvent choices are critical in this step. AFM studies showed that the emissive layer that was prepared by casting from chloroform which is a more volatile solvent than toluene, has greater film thickness. This may be attributed to the spin-coating technique and the altering polymer behavior in the corresponding solvent.

1.5.3 Thermal Evaporation of Cathode Materials

The evaporation of the metals are also performed in high-vacuum Glove Box systems. Ca/Al (20nm/80nm) metals are made use of in this step. Calcium is made use of as the cathode since it possess low work function that enhance the injection of electrons into the LUMO of the organic layer. Due to its sensitivity towards moisture and oxygen, Aluminum (Al) metal is also evaporated in order to avoid the device to degrade and to protect Ca electron injection layer [40]. In ultra-high vacuum systems, also metals evaporate at lower temperatures, so that the polymers used do not decompose.

1.5.4 Encapsulation

The prolongation of the life time of the device is the most critical purpose in the fabrication step. After deposition of metals, the active area of the device is encapsulated with epoxy around a glass cap so as not to expose it to O_2 and moisture.

1.6 OLED Characterization

OLEDs can function only when an electric field, a potential difference, is applied between the two metallic electrodes. The voltage that the OLED is started to emit any detectable color is named as turn-on voltage. The energy barriers between the layers are related with the turn-on voltage of the device. Lower turn-on voltages is better than higher ones since at higher voltages, the organic materials start to degrade eventually [41].

The terms for the characterization of OLEDs are explained as [42];

- Luminance (L): The luminance is the brightness of the device within a certain area which is given as cd/m^2.
- Candela (cd): The unit of luminance intensity emitted by a light source.
- Color/Chromaticity: The color coordinates of light is determined by CIE chromaticity diagram which provides a broad color range, and denotes the equal energy white point with a coordinates of x=0.33, y=0.33. There is also a region of white color that is regarded as white light [43].
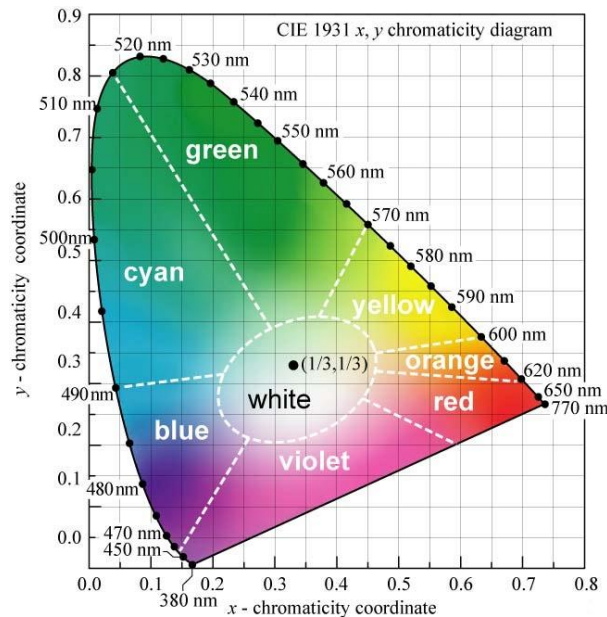
Figure 1.13 CIE 1931, x, y chromaticity diagram [43].

- Lumen (lm): Lumen is the unit of light intensity 1 lm = 1 cd x steradian (sr)
- Power Efficiency: The power efficiency is recognized as the luminance efficiency which is candela per ampere (cd/A) or lumens per watt (lm/W). It specifies the output of light power per electrical power input.
- External Quantum Efficiency (EQE): Efficiency is the most significant issue as energy consumption is concerned. The ability of devices to operate at lower voltages with a certain luminance is directly related with EQE. As the device starts to operate at lower voltages (turn-on voltage), resistive heating, which occurs through the passage of an electric current by a conductor, diminishes greatly and life time of the device increases accordingly [44].
- Light out-coupling loss: All the photons generated inside the device could escape from the device. Large percent of the light out-coupling loss is due to the internal absorption and wave guiding in a simple planar device as depicted in **Figure 1.14**.
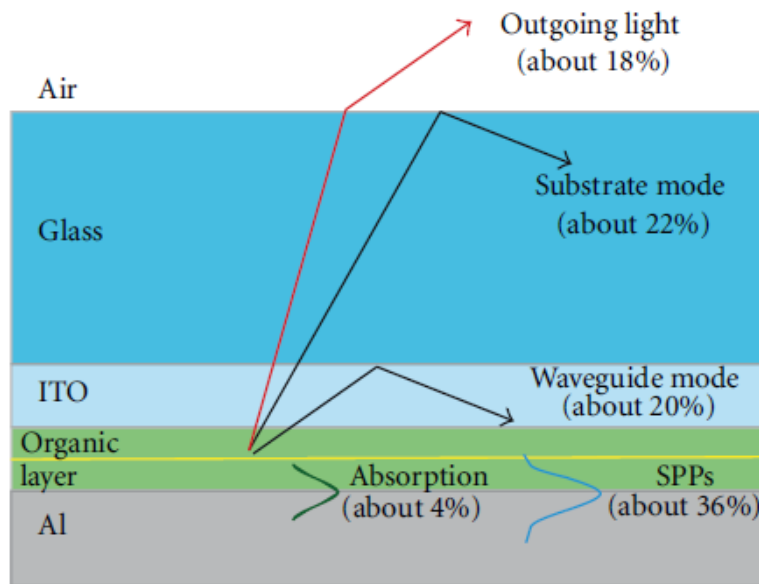
Figure 1.14 Light out-coupling losses (Internal reflections) in an OLED [45].

The light out-coupling losses cause a poor power efficacy. Yet, it is predicted that the future studies will lead to an improvement up to 60-80% EQE [44].

1.6.1 Electroluminescence Spectrum and Color Quality

Using certain spectrophotometers and power source, voltages are applied to the device, the electroluminescence data are obtained.

1.6.2 Device Efficiency

The light output as a result of the recombination of electrically injected charges is characterized through a spectrophotometer and a fiber optic cable-integrating sphere set-up. The measurements must be taken in a dark room. Lastly, the applied voltage and the luminance (cd/m^2) is plotted against each other as a scattered diagram. The luminance is precisely related to the current density. Therefore; the brighter the devices are, the shorter is their life [46]. The Luminance efficiency characterization provides a well-known parameter for the determination of device efficiency. The process of converting electrical power into optical power is investigated. The low luminance efficiencies are generally related to the non-radiative processes (thermal relaxation of excitons, internal reflection and absorption of the photons) [47].

1.6.3 Device Operational Lifetime

Presently, the OLED society defines the end of life as a point at which the luminance decays to 50% of the value at t=0. It is agreed that the first level target should be 20000 hours with a maximum 20% loss of luminance starting at 850 cd/m^2. The life time of an OLED is affected by several factors such as chemical and thermal degradation, charge transporting components, oxygen and moisture [48].

1.7 OLED Applications

1.7.1 Future Display Technology

Most desirable applications for OLED technology are ultra-light TV screens, flexible displays (electronic paper), and ambient lighting panels. Television does not demand a very superior resolution, yet good color distinctness, wide vision angle and high contrast, all are typical OLED features [49]. The world's largest OLED TV was introduced by LG, recently [50]. This particular TV by LG has a display of 77 inches and allows its users to be in charge of the angle of curvature by employing the remote control. It does this by factoring the screen size and the distance from which they are viewing the TV in order to generate the optimum viewing experience (**Figure 1.15**).

Figure 1.15 LG Ultra HD Curved OLED TV [50]

1.7.1.1 Passive Matrix OLED (PMOLED)

In order to construct a passive-matrix display, the electrode material has to be deposited in a row-column matrix. An OLED is formed at each joint point of the matrix. Illumination of each OLED (i.e. every pixel) is obtained by driving the appropriate row and column. Consequently, to create a video image, all rows and columns have to be examined so that all pixels required to form each frame are rapidly turned on and off. Therefore, with growing display size and so the pixel number, the scan rates are getting quicker and the time the pixel is in the ON state decreases. This directs to an intrinsic reduction of brightness that must be reimbursed with a higher pixel illumination. Additionally, column and row lengths frequently cause voltage drops, which make driver design more challenging. This trade-off between size and lighting restrains PMOLEDs performance and restricts them to small displays [51].The arrangement is given below in **Figure 1.16**.
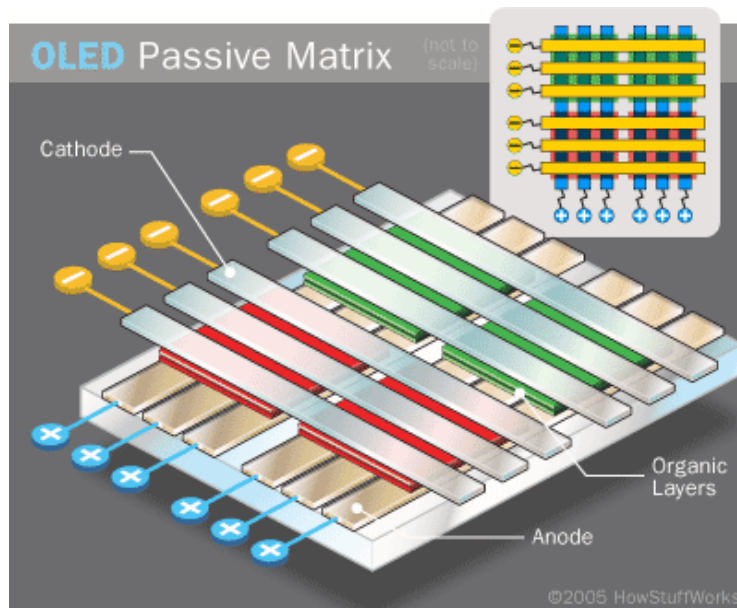
Figure 1.16 Passive Matrix OLED Configuration [51].

1.7.1.2 Active Matrix OLED (AMOLED)

Active-matrix displays benefit from thin film transistors (TFT) to drive each pixel. Every OLED cell is manipulated with at least two transistors, nonetheless more complex patterns are presently under research [52]. Each transistors in the array are separately accessible in a row-column format. Different than the passive-matrix display, transistor circuits preserve the state (on/off) and level (intensity) information programmed by the display driver. Hence, the light output of every pixel is utilized unceasingly, rather than being pulsed with high currents. Active-matrix displays are considerably more expensive than passive displays, except they are brighter, have sharper images and consume less power. One of the newest flexible AMOLED display technology was presented by Samsung [53] (**Figure 1.18**). AMOLEDs utilize less energy and are sufficient for larger areas [54]. The configuration is given below in **Figure 1.17**.
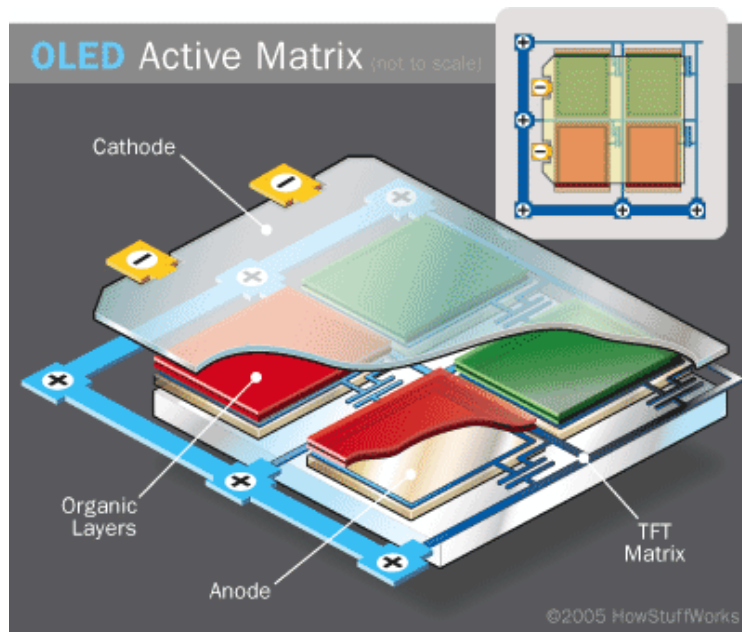
Figure 1.17 Active Matrix OLED Configuration [52].

Figure 1.18 Samsung Flexible AMOLED Display for Smartphones [53].

1.7.2 Future Solid-State Lighting

At present time solid state lighting (SSL) is beginning to take charge over conventional lighting technologies. According to the US Department of Energy, by 2025, SSL efficiency would be one order of magnitude higher than incandescent lamps and double of fluorescent tubes. OLEDs and LEDs are much more cost-effective than traditional incandescent light sources; in fact, they could reach comparable values to those of the fluorescent tubes. Luminance of a typical fluorescent tube is approximately 2000 cd/m^2. The possibility of extending the light source to wider areas and adjusting the color brings in an innovative perception of ambient lighting [55]. These panels are superior for the environment, since they could save approximately 50% of all energy spent on lighting [56]. Great effort is being made to progress effective, long lifetime white OLEDs (WOLEDs). Recently, scientists from Philips Research have developed the first-ever organic light emitting diode (OLED) module that can be powered directly from a

mains electricity supply, as well. It is a great advancement for illumination applications of WOLEDs [57]. (**Figure 1.19**)
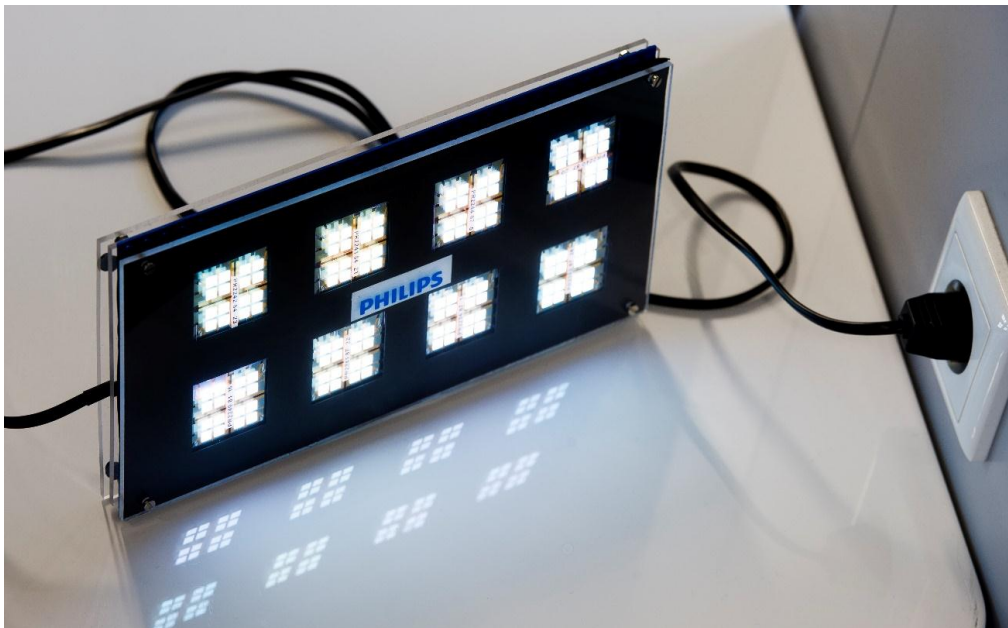
Figure 1.19 World's First 230V AC-powered White OLED module-Philips [57].

1.8 White Organic Light Emitting Diodes (WOLEDs)

There have been a lot of studies in order to develop more efficient organic materials. The priority in obtaining a specific color is given to the blue emission. Intense blue colored emission, long life time and efficiency are challenging to accomplish. This challenge leads to numerous difficulties with generating white light, as well. Accordingly, obtaining efficient white OLEDs (WOLEDs) is restricted by the blue emission. This inconvenience in blue emission is its intrinsic wide bandgap which usually requires higher turn-on and operating voltages which ultimately increases the degradation and reduces lifetime [58].

1.8.1 Crucial Issues and Challenges of WOLEDs

OLED technology is to be used widely and effectively, thus a variety of obstacles are present that need to be overcome. The primary difficulty is the operational life time maintenance. It is particularly challenging for blue OLEDs to operate for long hours. The market necessitates both enduring and stable devices that could be tested under strict circumstances. The other major issue is the cost per lumen in the fabrication of OLEDs. The demanded lighting parameters are declared that the brightness of 50–500 cd/m^2 at an efficiency of higher than 10 lm/W for a functioning lifetime of at least 10000 h are essentially needed. In addition, larger panels with moderate cost and efficiencies are also required [59]. The losses from internal reflections are an additional issue to be minimized by several structural design modifications or material alternatives.

1.9   White Polymer Light Emitting Diodes (WPLEDs)

The basic principles of WOLEDs and WPLEDs are compatible with each other provided that small molecules used in WPLEDs should be appropriate for the polymer medium and solution processable.

The major models of WPLEDs are classified as illustrated in **Figure 1.20** and listed as:

1. Polymer donor systems doped with fluorescent or phosphorescent molecules

2. Multiple stacked emissive hetero-layers

3. Polymer blends

4. Single component light emitting copolymer systems
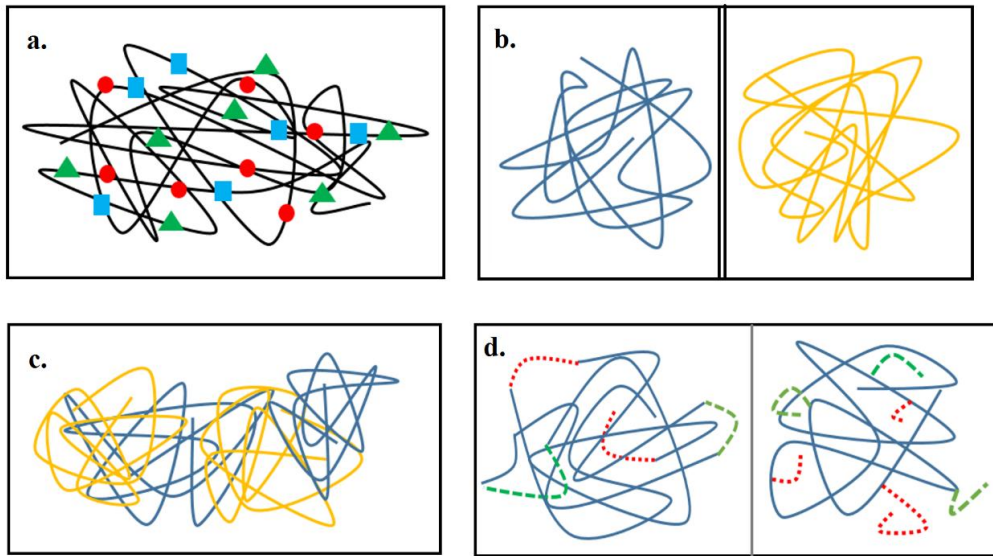
Figure 1.20 Types of WPLEDs.

a. 🔴▲🟦 : Red, green and blue fluorescent or phosphorescent molecules on polymer chain

b. ⬡ : Blue emitting polymer ⬡ : Orange emitting polymer   (Stacked hetero-layer)

c. ⬡ : Blue emitting polymer and orange emitting polymer blend

d. ⬡ : Red and green chromophore in single polymer chain

⬡ : Red and green chromophore in sidechain of a single polymer

1.9.1 WPLEDs from Polymer Donor systems Doped with Fluorescent or Phosphorescent Molecules

WPLEDs based on polymer donor systems doped with fluorescent or phosphorescent molecules are utilized mostly with components with high photoluminescence quantum efficiencies. Phosphorescent emitters have predominance over fluorescent ones due to their ability to harvest excitons with 100% efficiency. Blue emitting donor polyfluorene derivative and orange emitting acceptor rubrene were reported to be an example of this WPLED type [60]. A further balanced charge transport was accomplished by incorporating an electron-transporting material 2-(4-biphenylyl)-5-(4-tert- butylphenyl) - 1,3,4-oxadiazole (PBD) into the PF-rubrene system which ultimately gave rise to an amplified device efficiency. Through adjusting the blend ratio of PBD, a peak luminance efficiency of 17.9 cd/A were fulfilled with CIE coordinates of (0.33, 0.43) at 25 mA/cm^2. Recently, researchers also used a donor novel small molecule 9-(4'-(2''-ethylhexyloxyphenyl))-2,9- dipyrenylfluorene for orange-emitting polymer MEH-PPV [61]. The pyrene-functioned diarylfluorenes exhibited a powerful collected emission. The thin film emission is a broad peak at around 460 nm. Using this blend as the emissive layer, a luminance efficiency (LE) of 1.84 cd/A and luminance of 5700 cd/m^2 were obtained. As remarked before, WPLEDs based on phosphorescent dye-dispersed polymer blends are to be expected having much higher efficiencies [62].

1.9.2 WPLEDs from Multiple Stacked Emissive Hetero-layers

The multiple stacked emissive hetero-layers are more demanding than single layers. The components of the emissive layer are needed to be coated sequentially. The challenges for coating a layer on another layer are mainly due to the high possibility of dissolving of the bottom layer as the new layer is coated on [63]. In 2010, it was declared that two fluorescent emitting polymers having corresponding emission colors (a yellow PPV derivative and a blue polyfluorene) were utilized with a complete wet treatment method

for a bilayer polymer system. For this purpose, yellow emitting PPV derivative was thermally cross-linked. The device exhibited a maximum efficiency of 6.1 cd/A and a white light color having CIE coordinates of x=0.32, y=0.34 which are very close to equal energy white color point x=0.33, y=0.33 [64].

1.9.3 WPLEDs from polymer blends

Mostly, WPLEDs are fabricated in a thin film assembled type arrangement, namely, the light emitting layer is introduced in the middle of anode and cathode electrodes. On the basis of this, additional operational layers that are capable of enabling charge injection and transport are usually utilized to optimize the electroluminescent properties. For instance, PEDOT: PSS and LiF or CsF are commonly used at the anode and cathode side for charge-carrier injection. In spite of the advantages of the WPLEDs based on single-component White LEPs, it is not easy to precisely control the doping concentration of each organic dye during the polymerization and reduce the batch-to-batch deviation, particularly in mass production. On the other hand, physically blending based on a donor–acceptor system could provide an alternative approach towards white organic light-emitting devices, which could offer easy fabrication, excellent reproducibility and high efficiency. The method involves the blending of several dyes (acceptors) with different band gaps and forming a homogenous distribution of the dyes into the polymer matrix. A novel and efficient blue emitting polymer of poly((9,9-bis(4-(2-ethylhexyloxy)phenyl)fluorene-co-(3,7-dibenziothiene-S) with green-emitting and orange-red-emitting polymers were blended. This polymer blend was reported to be optimized for a blend ratio of 100:0.8:0.5 (B:G:R) by weight, and then it was utilized in constructing WPLEDs with good CIE color quality of x=0.34, y=0.35 and significantly high luminance efficiency LE of 14.0 cd/A [65].

1.9.4   WPLEDs from single component light emitting copolymer systems

White emission from conjugated polymer can be obtained via the insertion of different chromophores either fluorescent and/or phosphorescent into donor conjugated polymers with a binary chromophores form (blue-orange) or a triple chromophores form (red-green-blue). The resulting single-component white light-emitting polymers could offer several unique advantages, such as reasonable chemical modification of the emission color, minor color shift upon varying of voltage or current density, and easy device fabrication over large area size. In addition, they could successfully prevent the phase separation that is usually observed in donor-acceptor blend systems. A single component polymer system with three chromophores in the polymer backbone were declared in 2010. Exhibiting color coordinates of x=0.37, y= 0.42, it was reported that a power efficiency of 10.4 lm/W was obtained [66].

1.10 Aim of the thesis

The objective of the thesis is to investigate the performances of the white polymer light emitting diode (WPLED) applications of benzotriazole and fluorene derivatives. The method used throughout the studies includes blending two fluorescent polymers (blue and orange emitting) having different weight ratios in a common solvent. Different commercial blue emitting polymers and synthesized orange emitting polymers having different end cappers were used in the thesis study. Blue emitting polymers used in the experiments are; Poly (9,9-dioctylfluorenyl-2,7-diyl)-end capped with dimethylphenyl (**BE1**), Poly (9,9-dioctylfluorenyl-2,7-diyl)-end capped with N,N-bis(4-methylphenyl)-aniline (**BE2**), and Poly (9,9-dioctylfluorenyl-2,7-diyl)-end capped with 2,5-diphenyl-1,2,4-oxadiazole (**BE3**). Orange emitting polymers are; Poly-9,9-dioctylfluorene)-2,7-diyl-(4,7 bis(thien-2-yl)2-dodecyl- benzo[1,2,3]triazole)) end capped with phenyl (**P1**), Poly-9,9-dioctylfluorene)-2,7-diyl-(4,7 bis(thien-2-yl)2-dodecyl- benzo[1,2,3]triazole)) end capped with triphenylamine (**P2**), Poly ((4-(5-(biphenyl-4-yl)-4-hexylthiophenyl-2-

yl)-2-dodecyl-7-(4-hexylthiophen-2-yl)-2H-benzo[d][1,2,3]triazole)) end capped with phenyl (**P3**), Poly ((4-(5-(biphenyl-4-yl)-4-hexylthiophenyl-2-yl)-2-dodecyl-7-(4-hexylthiophen-2-yl)-2H benzo [d] [1,2,3]triazole)) end capped with triphenylamine (**P4**). WPLEDs from polymer blends either could experience low luminance efficiency or insufficient white color coordinates. These were mostly attributed to the complex morphology of the polymer blends that affect device reproducibility, voltage-dependent color, and intrinsic phase separation. Thus, the best choice of WPLED production type is critical in the thesis study. Morphology of the emitting layer and careful control of the ratio of the components have a crucial role in the management of the energy transfer process and accordingly in the optimization of the optoelectronic properties of the WPLEDs from polymer blends. Therefore, binary blend system that was chosen in the thesis study is more advantageous than ternary blends due to the better control of components with intimate mixing. It may reasonably be expected that the stability of the devices were also improved by adjusting the emission color via choosing the correct blend ratios. In addition, since blue emitting polymers have poor color stability and low EL efficiency, in the thesis study, the appropriate donor-acceptor strategy was also aimed to be benefited in which an energy transfer mechanism enhances the color stability. Capping both ends of the polymer chain with electron donating moieties of phenyl and triphenylamine were effective in increasing the hole transporting ability of the devices, resulting in high efficiency. Choosing the proper cathode material to minimize the electron injection barrier is also significant in WPLEDs, so Ca/Al was used that possess a work function matching to the LUMO of emissive layer components. In conclusion, the pure white light emission was realized and it was discovered that constructed devices possess good color quality, and voltage-independent EL spectra along with high luminance efficiencies to the best of our knowledge.

CHAPTER 2

EXPERIMENTAL

2.1 Materials

The blue light emitting polymers are commercially available from American Dye Source. The structures are depicted in **Figure 2.1** Poly (9,9-dioctylfluorenyl-2,7-diyl)-end capped with dimethylphenyl (**BE1**); Poly (9,9-dioctylfluorenyl-2,7-diyl)-end capped with N,N-bis(4-methylphenyl)-aniline (**BE2**); Poly (9,9-dioctylfluorenyl-2,7-diyl)-end capped with 2,5-diphenyl-1,2,4-oxadiazole (**BE3**). Weight average molecular weights (Mw) (vs polystyrene standards) of **BE1**, **BE2**, and **BE3** polymers are 68000, 87000, and 86000, respectively.

(Poly(3,4-ethylenedioxythiophene):polystyrene sulfonate) (PEDOT:PSS) was used as purchased (Clevios PH500), ITO-glass and ITO-PEN were purchased from VisionTek Systems. Toluene, chlorofom, acetone and 2-propanol (Aldrich) were used without further purification. Ca and Al were selected as cathode metals (Kurt J. Lesker).
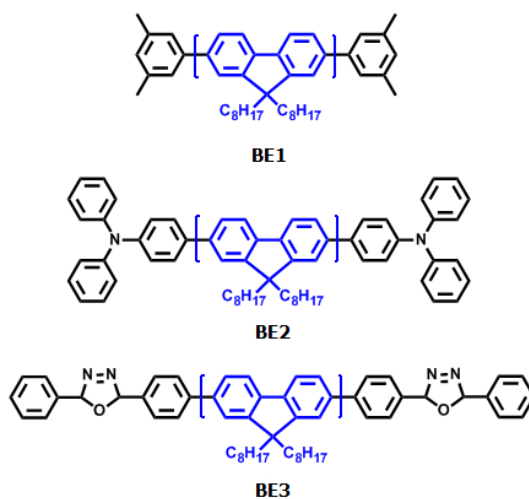
Figure 2.1 Chemical structure of blue light emitting polymers

33

2.2 Equipments

Electrochemical studies were carried out in a set up containing a reference electrode of Ag wire, a working electrode of indium tin oxide coated glass slide, and a counter electrode of Pt (platinum) wire. Average molecular weight was found by gel permeation chromatography (GPC) using METU Central Laboratory GPC 220 with dry THF being the effluent. The Voltalab 50 potentiostat was made use of for the measurements under ambient circumstances. Normal Hydrogen Electrode (NHE) was used as -4.75 eV [67]. ^{1}H-NMR spectra were recorded in $CDCl_3$ on Bruker Spectrospin Avance DPX-400 Spectrometer. Varian Cary 11 5000 UV–Vis spectrophotometer was made use of in order to accomplish the spectroelectrochemical analysis. Differential scanning calorimetry (DSC) and thermogravimetric analysis (TGA) were performed on Perkin Elmer Diamond DSC and Perkin Elmer Pyris 1 TGA. Atomic Force Microscopy (AFM) and Transmission Electron Microscopy (TEM) imaging techniques are achieved at METU Central Laboratory. Bandelin Sonorex Ultrasonic Bath were used for ITO substrate surface cleaning. Harrick Plasma Cleaner was also used for further cleaning of the ITO-anode surface of the devices. Spin-coating of the organic layers were conducted using SAWATEC Spinner Module of the glove box system (MBraun). INFICON SQC-310 Thin Film Deposition Controller was used for the depostion of the cathode metals after evaporated in the glove box evaporation chamber (MBRAUN MB EVAP). The current density-voltage (I–V) measurements were conducted in a glove box system (H_2O <0.1 ppm; O_2 <0.1 ppm). Current-voltage and Luminance-voltage characteristics were recorded using a Keithley 2400 Source, Maya2000PRO Spectrophotometer and a Newport Integrated Sphere Setup.

2.3 Synthesis

The orange light emitting polymers are; Poly-(9,9-dioctylfluorene)-2,7-diyl-(4,7 bis(thien-2-yl)2-dodecyl- benzo[1,2,3]triazole)) end capped with phenyl (**P1**), Poly-(9,9-dioctylfluorene)-2,7-diyl-(4,7 bis(thien-2-yl)2-dodecyl- benzo[1,2,3]triazole)) end capped with triphenylamine (**P2**), Poly ((4-(5-(biphenyl-4-yl)-4-hexylthiophenyl-2-yl)-2-dodecyl-7-(4-hexylthiophen-2-yl)-2H-benzo[d][1,2,3]triazole)) end capped with phenyl (**P3**), Poly ((4-(5-(biphenyl-4-yl)-4-hexylthiophenyl-2-yl)-2-dodecyl-7-(4-hexylthiophen-2-yl)-2H-benzo[d][1,2,3]triazole)) end capped with triphenylamine (**P4**). **P1** and **P2** without their end cappers were synthesized and characterized as described previously [68], and also **P3** and **P4** without their end cappers were synthesized and characterized as described previously in detail [69].

The additions of the end cappers to the polymers are carried out throughout this thesis work and described below:

2.3.1 Synthesis of poly-(9,9-dioctylfluorene)-2,7-diyl-(4,7 bis(thien-2-yl)2-dodecyl- benzo[1,2,3]triazole)) end capped with phenyl (P1)

In a 50 mL two-neck round bottom flask K_2CO_3 solution (2M, 0.5 mL) was added and the system was purged with argon for 30 minutes. Then, freshly dried toluene (5mL) was added to the mixture while argon purging was continued. 4,7-Bis(5-bromothiophen-2-yl)-2-dodecyl-2H-benzo[d][1,2,3]triazole (200 mg, 0.328 mmol), 9,9-dioctylfluorene-2,7-diboronic acid bis(1,3-propanediol) ester (183 mg, 0.328 mmol) and a catalytic amount of tetrahexylammonium iodide were then added to the reaction followed by argon purging for an additional 30 minutes. After that, tris(dibenzylideneacetone)dipalladium(0) (5.0 mol %, 15mg) and tris(o-tolyl)phosphine (11 mol %, 33.00 mg) were added to the reaction mixture. The temperature was raised to 105 °C from room temperature. Polymerization reaction

was sustained at this temperature under argon atmosphere for 40 hours. 4-Bromotriphenylamine (213 mg, 0.657 mmol) and extra catalyst (4.50 mg) were then added and the mixture was stirred for four hours. Then 4-(diphenylamino) phenylboronic acid, (380 mg, 1.314 mmol) was added and the mixture was stirred at 105 °C overnight. The reaction mixture was cooled to room temperature and precipitated in methanol. The mixture was filtered and precipitate was purified by Soxhlet extractor. Firstly, the precipitate was washed with acetone for 12 hours and then with hexane for 24 hours to remove oligomers and small molecules. The polymer was collected by chloroform and the solvent was evaporated. The residue was precipitated in methanol and pure polymer was obtained by vacuum filtration (135 mg, yield 35 %). GPC: Mn = 15700, Mw = 27900, PDI = 1.7

2.3.2 Synthesis of poly-(9,9-dioctylfluorene)-2,7-diyl-(4,7 bis(thien-2-yl)2-dodecyl- benzo[1,2,3]triazole)) end capped with triphenylamine (P2)

The same procedure with synthesis of **P1** was applied to synthesize **P2**. In this manner 4,7-bis(5-bromothiophen-2-yl)-2-dodecyl-2H-benzo[d][1,2,3]triazole (147 mg, 0.241 mmol), 9,9-dioctylfluorene-2,7-diboronic acid bis(1,3-propanediol) ester (135 mg, 0.242 mmol), tetrakis(triphenylphosphine)palladium(0) as the catalyst (5.0 mol %, 14.0 mg) and tris(o-tolyl)phosphine as the co-catalyst (10 mol %, 8.07 mg) were taken in determined amounts. End cappers bromobenzene and phenylboronic acid were taken as 180.0 mg (1.14 mmol) and 235.0 mg (1,93 mmol) respectively. Polymers collected with chloroform made ready for further applications. The amount of the polymer was 105 mg (yield 37 %). GPC: Mn = 6900, Mw = 17500, PDI = 2.5

2.3.3 Synthesis of poly ((4-(5-(biphenyl-4-yl)-4-hexylthiophenyl-2-yl)-2-dodecyl-7-(4- hexylthiophen-2-yl)-2H-benzo[d][1,2,3]triazole)) end capped with phenyl (P3)

36

The same procedure with synthesis of **P1** was applied to synthesize **P3**. In this manner 4,7-bis(5-bromo-4-hexylthiophen-2-yl)-2-dodecyl-2H-benzo[d][1,2,3]triazole (108 mg, 0.139 mmol), biphenyl-4,4'-diboronic acid bis(neopentyl glycol) ester (53 mg, 0.140 mmol), tetrakis(triphenylphosphine)palladium(0) as a catalyst (5.0 mol %, 8.03 mg) and tris(o-tolyl)phosphine as the co-catalyst (11 mol %, 4.65 mg) were taken in determined amounts. End cappers 4-bromotriphenylamine and 4-(diphenylamino)phenylboronic acid were taken as 180.0 mg (0.555 mmol) and 235.0 mg (1.11 mmol) respectively. Polymers collected with chloroform was quantified and made ready for further applications. The amount of the polymer was 65 mg (yield 42 %). GPC: Mn = 8600, Mw = 32600, PDI = 3.7

2.3.4 Synthesis of poly ((4-(5-(biphenyl-4-yl)-4-hexylthiophenyl-2-yl)-2-dodecyl-7-(4-hexylthiophen-2-yl)-2H-benzo[d][1,2,3]triazole)) end capped with triphenylamine (P4)

The same procedure with synthesis of **P1** was applied to synthesize **P4**. In this manner 4,7-bis(5-bromo-4-hexylthiophen-2-yl)-2-dodecyl-2H-benzo[d][1,2,3]triazole (100 mg, 0.129 mmol), biphenyl-4,4'-diboronic acid bis(neopentyl glycol) ester (49 mg, 0.130 mmol), tris(dibenzylideneacetone)dipalladium(0) as tyhe catalyst (5.0 mol %, 6.00 mg) and tris(o-tolyl)phosphine as the co-catalyst (11 mol %, 4.35 mg) were taken in determined amounts. End cappers bromobenzene and phenylboronic acid were taken as 82.0 mg (0.520 mmol) and 127.0 mg (1.04 mmol) respectively. Polymers collected with chloroform was quantified and made ready for further applications. The amount of the polymer was 50 mg (yield 34 %). GPC: Mn = 45000, Mw = 183000, PDI = 4

2.4 Characterization of the Polymers

2.4.1   Electrochemical Studies

2.4.1.1 Cyclic Voltammetry

Cyclic Voltammetry is a valuable tool for electrochemical analysis where the working electrode potential is swept versus a limited time. The potential at a working electrode is swept over a range and back again while the current is recorded. Redox potentials can be realized promptly via CV. In **Figure 2.2**, the voltage scan is depicted with a constant rate. [70], as the voltage is at V_2, the scan is reversed.
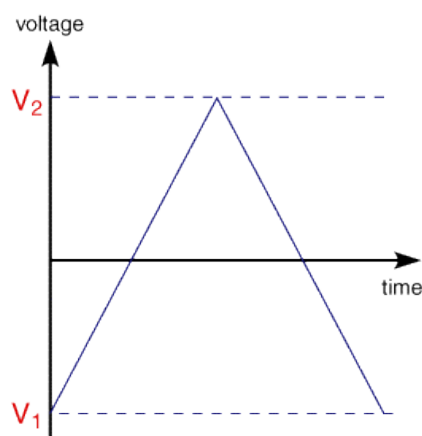
Figure 2.2 Cyclic voltammetry waveform.

During this voltage sweep scan, the currents are recorded by a potentiostat. **Figure 2.3** reveals the result of the reversible redox pair in a single scan. The voltage is determined from the voltage difference of the reference electrode and the working electrode, and the

current is determined from the current difference of the working electrode and the counter electrodes. Finally, current is plotted against voltage after these measurements.
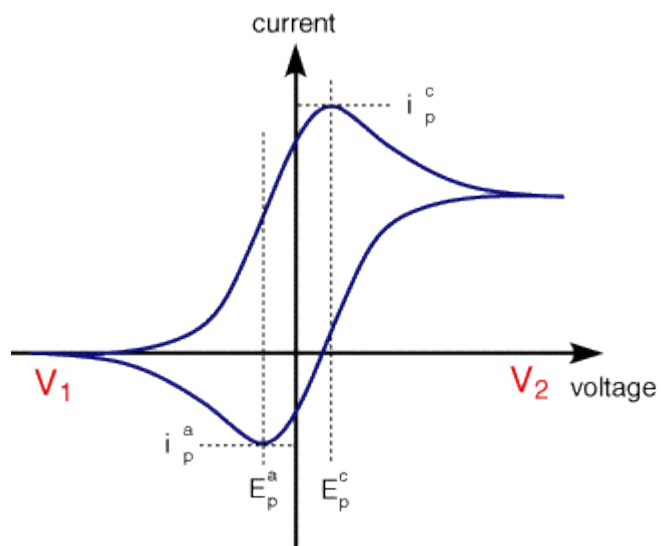
Figure 2.3 Cyclic voltammogram for a reversible redox process.

2.4.2 Spectroelectrochemistry

Spectroelectrochemistry is an advantageous technique which instantaneously unites the methods of electrochemistry and spectroscopy. At the surface of electrode surface, and through alterations in electronic transitions, absorbance variations are also realized. Through using this method, it is possible to provide information about the band gap energy, maximum absorption wavelength, polarons and bipolarons, and finally colors of the polymer.

2.4.3 Gel Permeation Chromatography (GPC)

Gel permeation chromatography is a separation method where the fragments are isolated in terms of their magnitude. In this technique, organic solvents constitute the active phase, and beads of porous polymeric material are the stationary phase. In the thesis study, the average molecular weights (Mn and Mw) of

polymers were determined at METU Central Laboratory, by GPC 220 calibrated with universal standard polystyrene.

2.4.4 Thermal Properties

The thermal properties are essential in determining the device stability prior to the device fabrication. In this thesis study, thermal analysis was examined by Perkin Elmer diamond differential scanning calorimetry (DSC) and Perkin Elmer Pyris 1 thermogravimetric analysis (TGA) instruments. DSC is used to identify the alterations in polymers with utilized heat. Glass transition temperature (Tg), melting temperature (Tm), and crystallinity temperature (Tc) are the parameters that were characterized by means of DSC. TGA investigations make use of applied heat in order to create physical adjustments and reactions in polymers. Using this technique, it is feasible to acquire the mass differences with regard to the thermal decomposition in polymers. Through employing TGA, decomposition temperature of polymers can be discovered. The TGA analysis was carried out under N_2 between 25-800 °C, and with 10 °C/minute periods.

2.4.5 Photo-physical Properties

UV-VIS Spectrometry is an easy and advantageous method for the absorption studies of the polymers. The excitation wavelengths for the PL experiments determined by this technique.

2.4.5.1 Photoluminescence Experiments

These experiments primarily include the measurements of the fluorescence quantum yields of the synthesized polymers before the device production step. The solutions for the absorption and fluorescence studies were dissolved in toluene and diluted excessively. Thin film samples were prepared from the exact dilute solutions with the same concentration. PL spectra were recorded on a Perkin-Elmer LS 55

luminescence spectrometer. The measurements were accomplished with excitation wavelength of λ_{exc}= 480 nm for the blended systems. The methods for the fluorescence quantum yield determination are explained in the discussion part of the thesis.

2.5 Device Fabrication
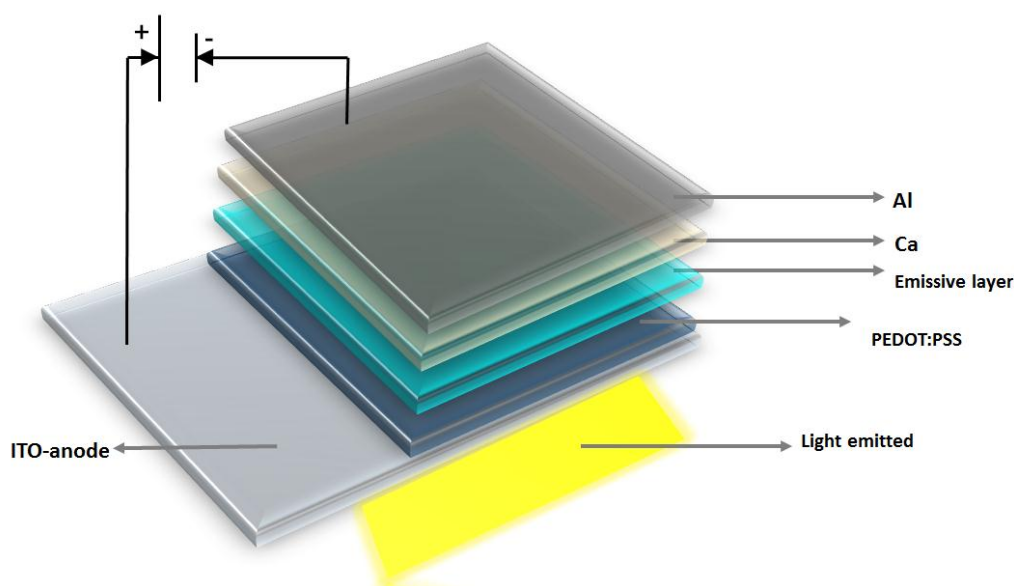
Figure 2.4 Device structure.

2.5.1　ITO-Glass WPLED Fabrication

Step-1: ITO-glass cutting and etching: ITO-coated glass sheets were used as substrates. The resistance of the ITO sheets are 15ohm/sq. In order for the substrates to be appropriate for the metal evaporation mask, the substrates are cut into 2.45 cm x 2.45 cm sizes. ITO used as anode needs to be etched in order to avoid short circuit

problems. Hence, by protecting the certain part of ITO as an active area, the sides of anode were etched carefully. Etching process includes 37% fuming/concentrated HCl acid (12M) which is heated up to 100°C.

Step-2: ITO-glass surface cleaning: It is very crucial to remove the contamination from the surface in order to fabricate OLEDs. Thus, prior to the coating processes, the ITO surface was treated with organic and aqueous solutions; using a sonicator bath, the substrates are cleaned in toluene, detergent (Hellmanex III)-water, water, acetone and 2-propanol solvents for 15 minutes, respectively. After cleaning, substrates were dried with N_2 gas. Oxygen plasma cleaning method in which the plasma is formed via radio frequency waves in low pressures, was applied to remove organic contaminates remained on the surface of ITO-glass. The purposes of this plasma cleaning are increasing the work function of ITO to ease the injection of holes and changing the surface tension of ITO and making it more hydrophilic to coat the PEDOT:PSS hole transport layer efficiently and smoothly.

Step-3: PEDOT:PSS hole transport layer spin-coating: PEDOT:PSS was filtered through 0.45 μm CA-CN filters. Then, by spin-coating method, PEDOT:PSS was coated with 5000 rpm speed for 1 minute duration onto pre-cleaned ITO substrates. After coating, in order to remove water, PEDOT:PSS coated ITO substrates were heated at 150°C for 10 minutes. The PEDOT:PSS layer film thicknesses were around 40 nm as averaged from Atomic Force Microscopy measurements and as given in Appendix D. So, substrates were made ready for use and kept in Glove Box systems.

Step-4: Emissive layer spin-coating:
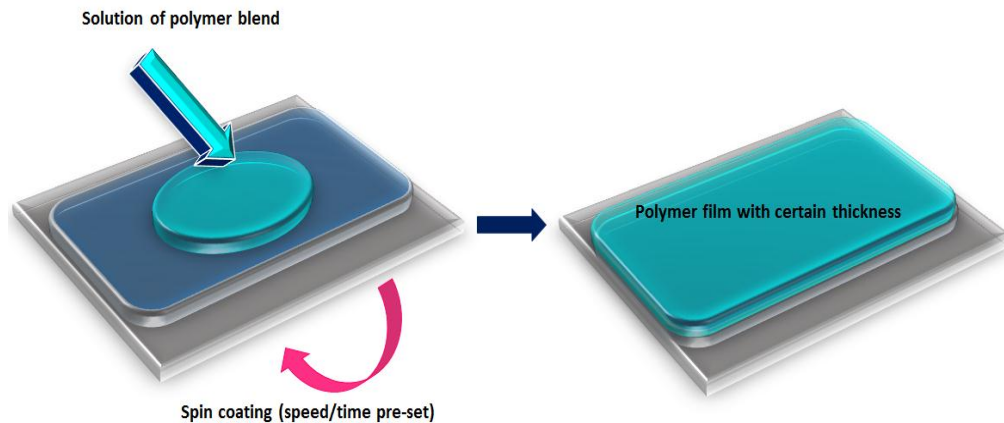
Figure 2.5 Spin-coating of polymer blend.

Blue-emitting polymers and orange emitting polymers are blended and dissolved in 1 mL toluene with a weight percentage ratio of 99:1, respectively. The polymer blend solutions were prepared with a concentration of 20 mg/mL. Solutions were filtered through 0.22 µm CA-CN filters and were then spin-coated by 2750 rpm speed for 1 minute onto dried PEDOT: PSS/ITO substrates that were kept in the glove box system (**Figure 2.5**). The emissive layer film thicknesses were around 100 nm as averaged from Atomic Force Microscopy measurements as given in Appendix D.

Step-5: Cathode (Ca/Al) Evaporation: Cathode metals were deposited at a pressure of 1×10^{-6} Torr in the evaporation chamber of Glove Box with 2x4 cm evaporation masks. Ca was deposited as 20 nm, Al was deposited as 80 nm. The device area of constructed PLEDs are 0.06 cm^2.

Step-6: Encapsulation: The fabricated OLED devices were encapsulated in glass with UV-curable epoxy resin immediately in an inert glove box environment (MBRAUN MB-200B Glove Box Systems).

The electroluminescence (EL) spectra were collected using a spectrophotometer (Maya2000PRO) connected with Spectra-Suite Software. The current density, voltage, and luminance characteristics were obtained using Keithley 2400 source-meter and Newport Integrated sphere.

2.5.2   ITO-PEN WPLED Fabrication

ITO-PEN etching and cleaning: ITO-coated PEN sheets were used as substrates. The sheet resistance is 15 ohm/sq. ITO-PEN substrates were etched dropwise with concentrated HCl acid, carefully. Prior to the coating processes, the ITO surface was treated solutions; the substrates were cleaned in ultrasonic bath with detergent (Hellmanex III)-water, water and 2-propanol solvents for 15 minutes, respectively. After dried with N_2 gas, oxygen plasma cleaning was conducted.

The remaining steps are exactly the same with ITO-glass WPLED fabrication steps.

CHAPTER 3

RESULTS AND DISCUSSION

3.1 Synthesis of the Polymers, P1, P2, P3, and P4

Dibrominated compound was added into the mixture of potassium carbonate $(K_2CO)_3$, and toluene. The mixture was refluxed under argon for one hour. Then, benzo [c] -1,2,3-thiadiazol-4,7-diyl-4,7-diboronic acid dipinacol ester, Pd (PPh3)$_4$ and tetrabutylammonium iodide, were added to the reaction medium. The mixture was refluxed under argon. In order to end the polymerization, end capper chemicals were added. After solvent evaporation, the remaining mixture was precipitated in methanol, and with the aid of Soxhlet, it was first cleaned with acetone, then with chloroform. Finally, the remaining ingredients namely polymers were obtained in chloroform. After the chloroform evaporated, the polymeric material was precipitated from methanol, and solid materials were taken again by vacuum filtration method. The polymer was ready for use after dried in a vacuum oven.
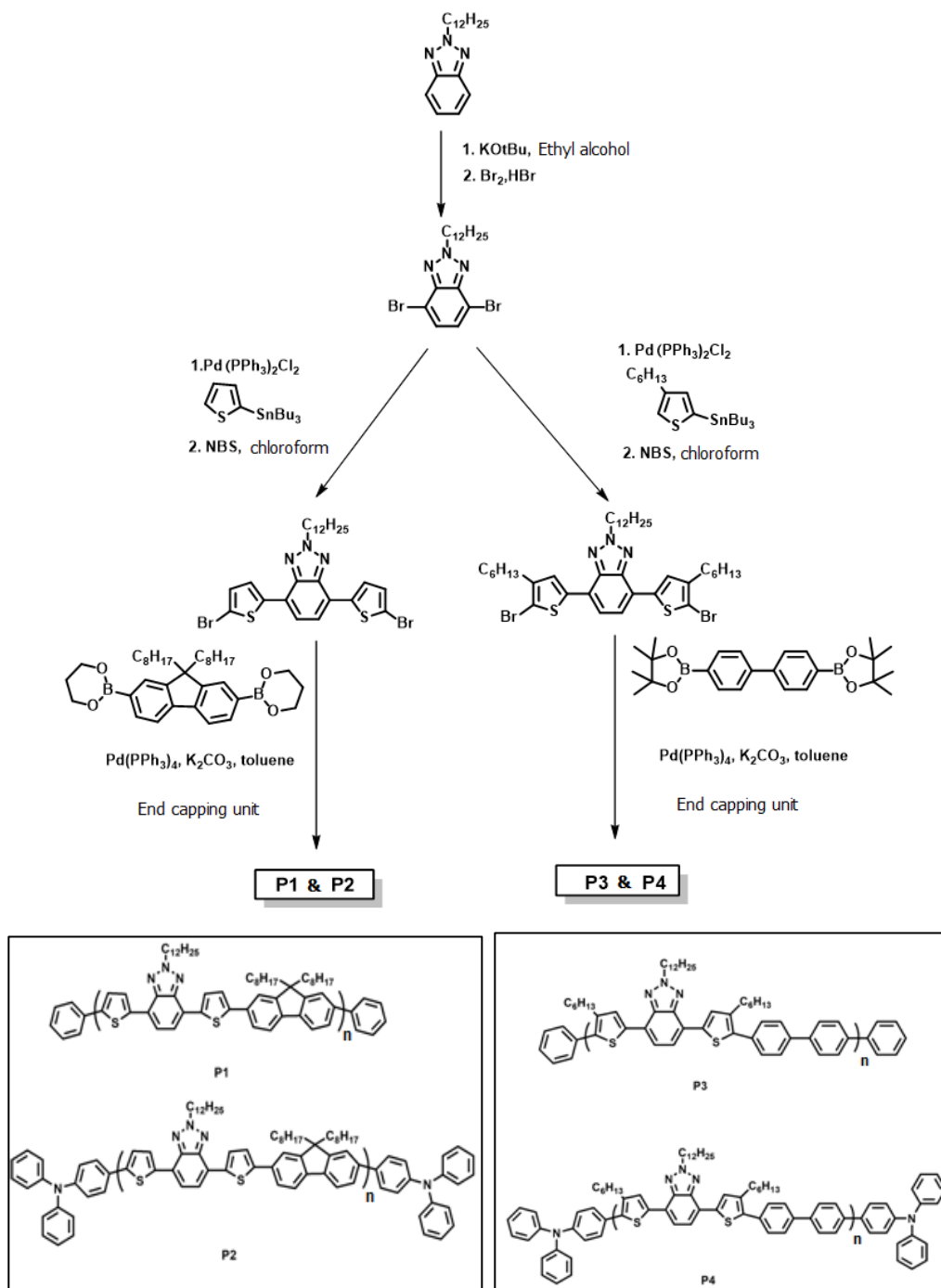
Figure 3.1 Synthetic Pathway of the Orange Emitting Polymers.

3.2 Electrochemical Properties

3.2.1 Cyclic Voltammetry

For electrochemical characterization, polymers were dissolved in chloroform and adjusted with a concentration of 5 mg/mL. The prepared solutions were spray coated on pre-cleaned indium tin oxide (ITO) coated glass slides. Then, the polymer films on ITO was characterized with cyclic voltammetry (CV) in ambient conditions in order to determine the redox potentials in 0.1 M tetrabutylammonium hexafluorophosphate (TBAPF6)/acetonitrile(ACN):dichloromethane (DCM) (9:1) supporting electrolyte solution, at a scan rate of 50 mV/s. The samples were located in the three electrode set-up, initially. Pt wire was the counter electrode, and the Ag wire was the pseudo-reference electrode.

The redox potentials of the polymers were determined as the potentials were swept between corresponding values versus Ag wire pseudo-reference electrode (50 mV versus Fc/Fc+). The performances of the polymers are given in **Figure**s **3.2- 3.5**.

In brief, **P1** film revealed reversible redox couple at positive potentials pointed at 1.10 and 0.81 V versus Ag wire pseudo-reference electrode. The negative potentials of **P1** are -1.94 and -1.67 V where it showed reversible redox couple. **P2** polymer showed reversible redox couple at positive potentials of 1.18 and 0.93 V, and negative potentials of -1.91 and -1.74 V. Similarly, for **P3**, the positive and negative potentials are 1.10/0.93 V and -1.83/-1.40 V, respectively. Finally, for **P4**, the positive and negative potentials are 1.08/0.91 V and 1.73/-1.41 V, respectively.

By single scan cyclic voltammetry which was taken in the 0.1 M TBAPF$_6$/ACN:DCM electrolyte solution, it was revealed that **P1**, **P2**, **P3** and **P4** exhibit both p-type and n-type dopable properties, due to the dual property of polymers, energy levels were calculated precisely. The reference electrode and the potentials were calibrated against Fc/Fc+, and the band energies were calculated by taking into account the value of NHE

is -4.75 eV versus vacuum. Electronic band gaps (E_g^{ec}) are also calculated from the difference between HOMO and LUMO energy level values as given in Equation 3.1.

$$\mathbf{E_{HOMO} = - (E_{onset,ox} + 4.75 + 0.3) \; (eV) \quad E_{LUMO} = - (E_{onset,red} + 4.75 + 0.3) \; (eV)}$$

$$\mathbf{E_g^{ec} = (E_{onset,ox} - E_{onset,red}) \; (eV)} \qquad \text{Equation 3.1}$$

Calculated electrochemical band gaps of the polymers were comparatively higher than the ones estimated from π-π* transition due to the creation of free ions by means of applied potential which requires higher energy than optical absorption [71]. Different end cappers of the polymers provided the polymers with different physical properties. Phenyl end group unit offers a more stable characteristic to the polymer than the triphenylamine end group unit. The E_g^{ec} of polymers **P1** and **P3** with phenyl groups are lower than others.

Figure 3.2 Cyclic voltammogram of **P1** for p type and n type doping in 0.1 M TBAPF6/ACN: DCM solution at a scan rate of 50 mV/s.
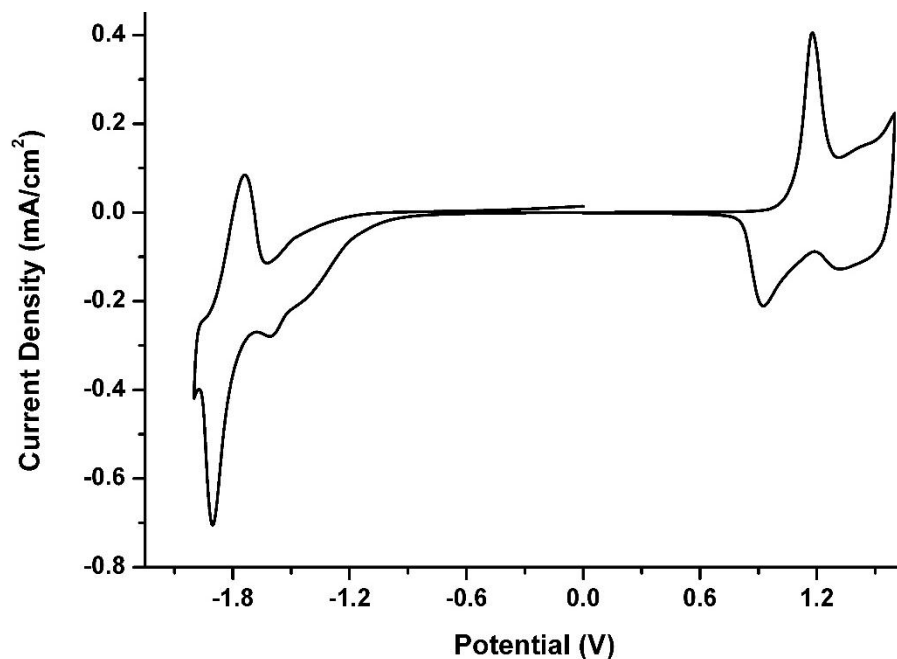
Figure 3.3 Cyclic voltammogram of **P2** for p type and n type doping in 0.1 M TBAPF6/ACN: DCM solution at a scan rate of 50 mV/s.
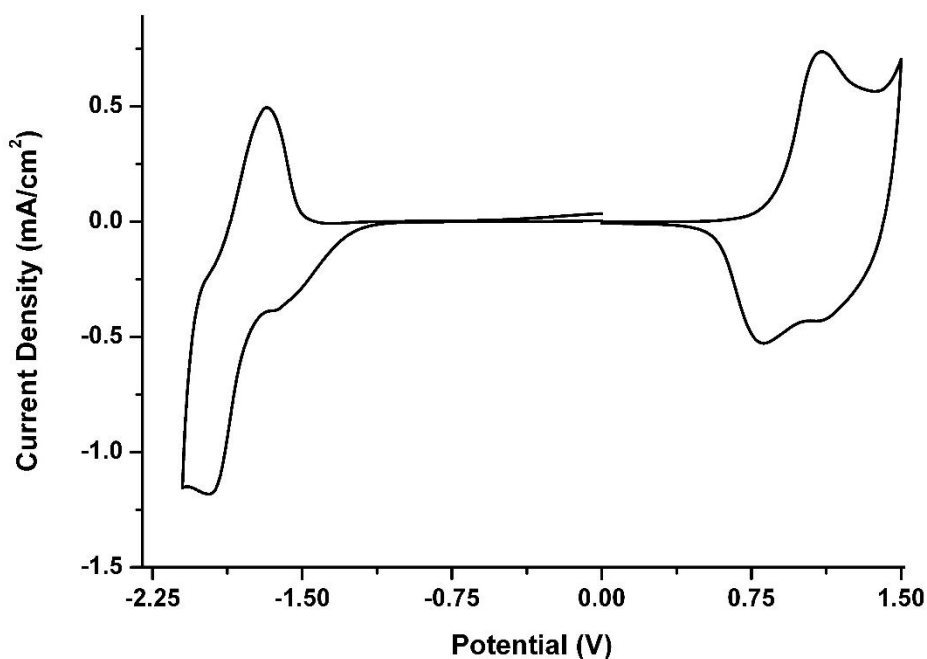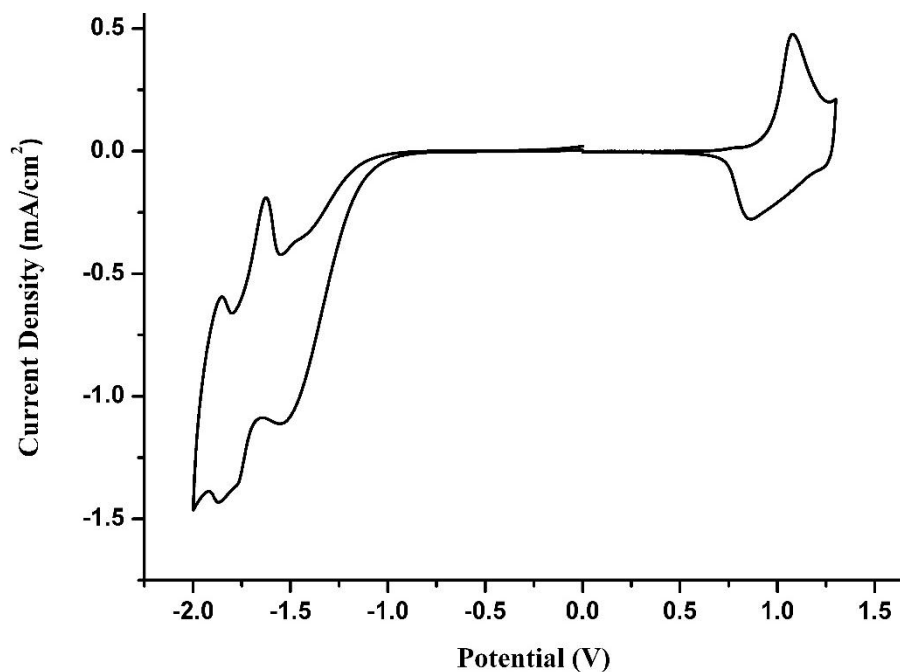

Figure 3.4 Cyclic voltammogram of **P3** for p type and n type doping in 0.1 M TBAPF6/ACN: DCM solution at a scan rate of 50 mV/s.
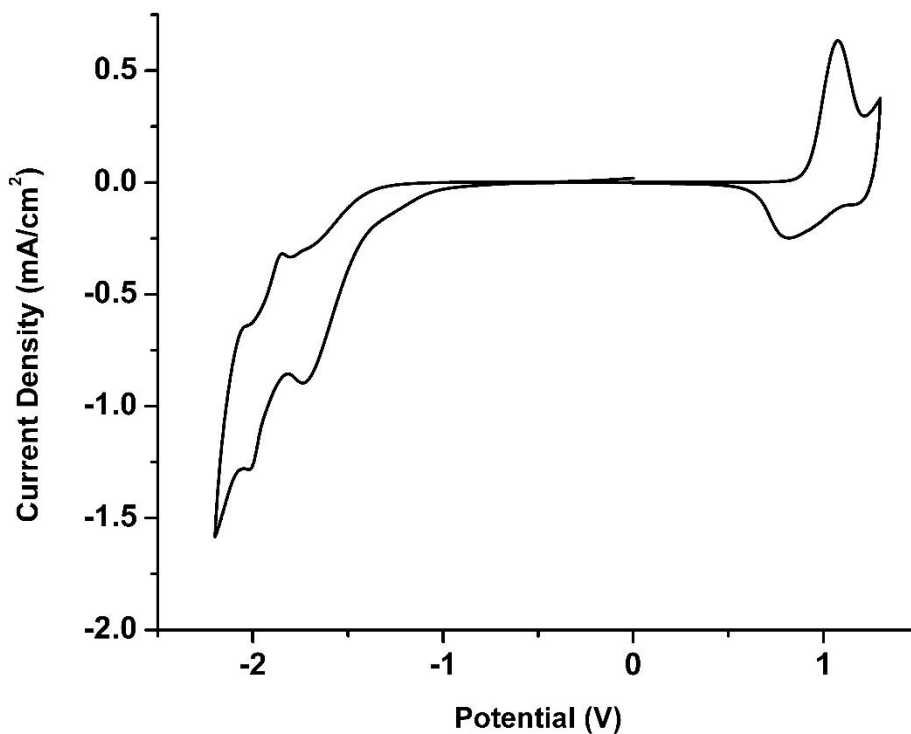
Figure 3.5 Cyclic voltammogram of **P4** for p type and n type doping in 0.1 M TBAPF6/ACN: DCM solution at a scan rate of 50 mV/s.

3.3 Spectroelectrochemistry

For the study of the optoelectronic properties of polymers, the spectral behavior of the polymers must be studied with the help of electronic absorption spectra under applied potential. For this reason, neutral polymer films, were coated on ITO coated glass slides by spray coating the solution that was originally in 5mg/ml chloroform solutions, and UV–vis–NIR spectrum was determined for corresponding polymer films in 0.1 M TBAPF6/ACN:DCM solution upon gradually increased external bias. Spray coating continued until homogeneous films were formed. After the produced films dried at room conditions, in order to determine the electrochemical stability before spectroelectrochemical analysis, they are subjected to continuous redox cycle with the help of CV. Using λ_{onset} obtained in the visible region of the polymer, optical bandgap is

calculated by formula ($E=1241/\lambda_{onset}$). Moreover, as a result of the spectroelectrochemical studies, it was discovered that the different end capper molecules affect the structure differently, and significantly alter the mechanisms of absorption and emission. For instance, the solid-phase state of **P1** is red-colored, yet the solid-phase state of **P2** was orange. When the neutral state absorption spectra obtained from the polymer solutions are analyzed, the maximum wavelengths that polymers absorb are revealed to be close to each other, and absorption is observed around 500 nm.
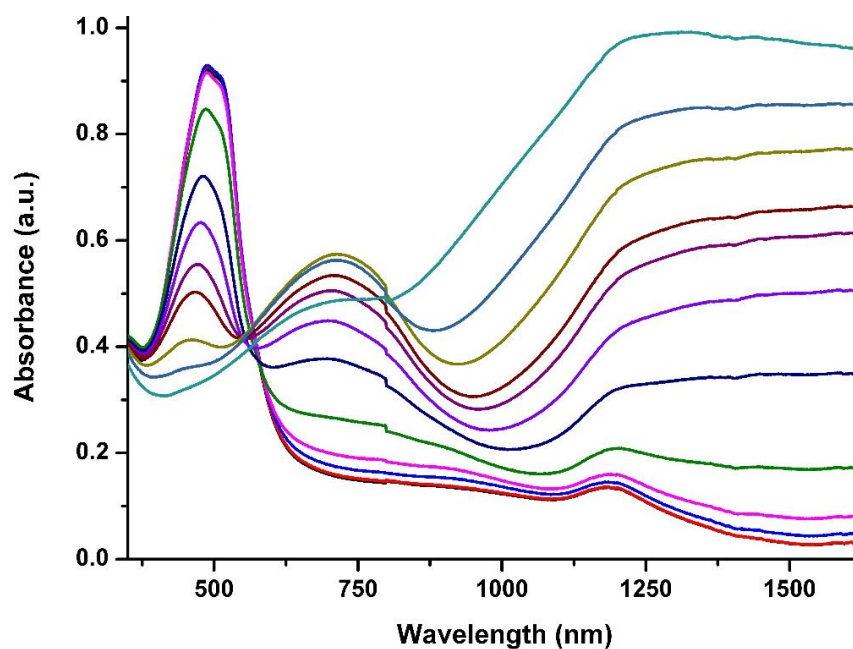
Figure 3.6 Electrochemical p-type doping electronic absorption spectra of **P1** (0-1.4V).
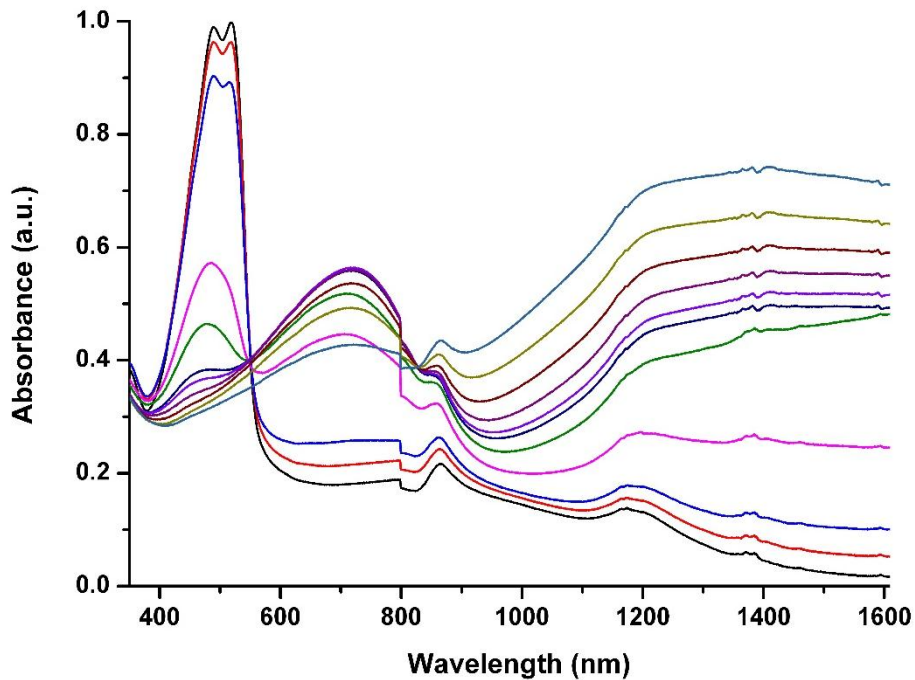
Figure 3.7 Electrochemical p-type doping electronic absorption spectra of **P2** (0-1.4V).
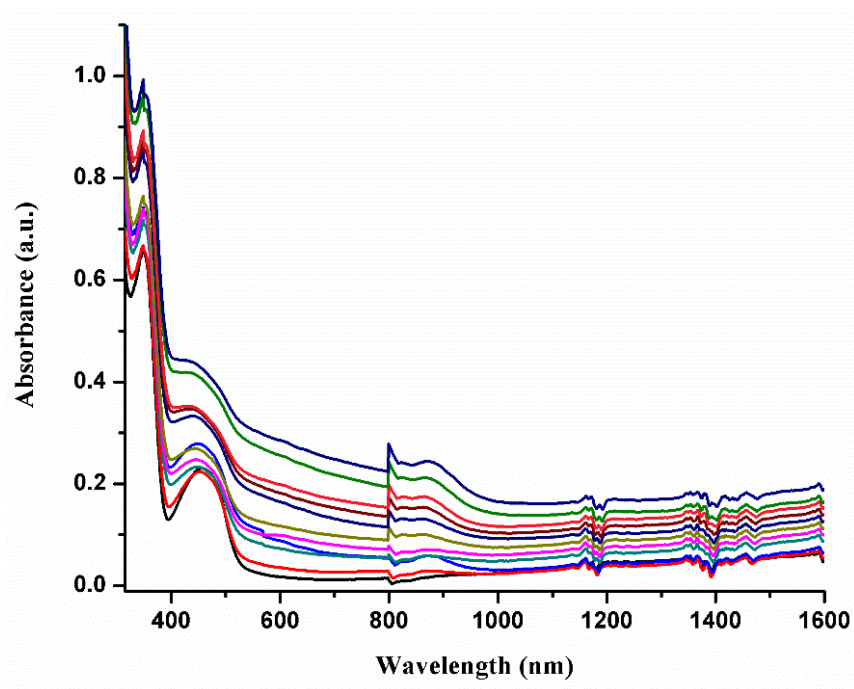
Figure 3.8 Electrochemical p-type doping electronic absorption spectra of **P3** (0-1.4V).
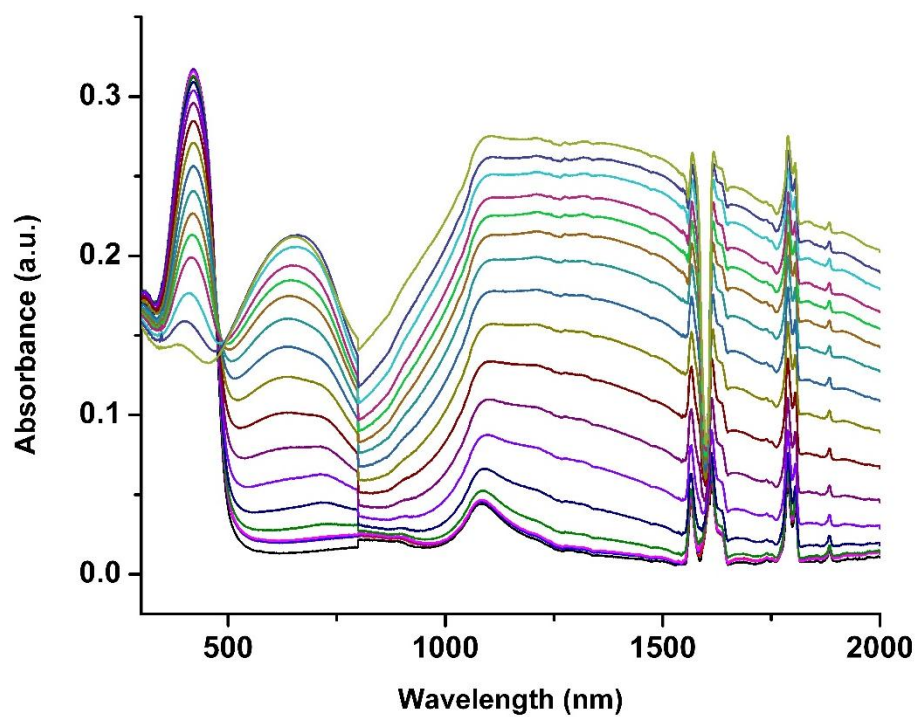
Figure 3.9 Electrochemical p-type doping electronic absorption spectra of **P4** (0-1.3V).

Table 3.1 Electrochemical and optical studies of **P1**, **P2**, **P3** and **P4**

Polymer	Oxidation Potential (V)		Reduction Potential (V)		Band Gap (eV)		Energy Levels (eV)	
	E_{ox}	$E_{ox\ onset}$	E_{red}	$E_{red\ onset}$	E_g^{ec}	E_g^{op}	HOMO	LUMO
P1	1.10	0.81	-1.94	-1.67	2.6	2.0	-5.3	-2.7
P2	1.18	0.93	-1.91	-1.74	2.7	2.2	-5.52	-2.76
P3	1.10	0.93	-1.80	-1.40	2.33	2.30	-5.98	-3.65
P4	1.08	0.91	-1.73	-1.41	2.21	2.15	-5.96	-3.75

3.4 Thermal Analysis

For the determination of decomposition temperatures (Td) and glass transition temperatures (Tg) of **P1**, **P2**, **P3** and **P4** polymers, TGA and DSC analysis were conducted as given in Appendix B and C. According to the results of the analysis, **P1** is stable up to 300 °C, and at 300 °C, a mass loss of about 5% was observed. Since the analysis was done as samples were heated up to 800 °C from room temperature, the total mass loss at 800 °C is about 67% by weight. In addition, **P1** has a Tg (glass transition temperature) value of 63.7 degrees. For **P2** polymer, a 5% mass loss at 430°C, and a 60% total mass loss at 800 °C was obtained. Tg value is 170 °C for **P2**. Therefore, at this temperature, the polymer was transformed reversibly into a more disordered structure from a uniform regular structure. The 5% mass loss for **P3** was seen at 330 °C. However, the total mass loss reached to 92% at 800 °C. Being stable up to 330 °C, the bonds were broken after this temperature. Tg of **P3** was observed at 169 °C. **P4** has a 5% mass loss at 330 °C, and a total mass loss of 70% was seen at 800°C. Tg value of P4 is 120°C. Thus, the results for **P1** and **P2** are also valid for **P3** and **P4**. In other words, after reaching the Tg value, the structure of the material changes reversibly. Consequently, the atoms gained amorphous characteristics as they were transformed into active bond structure from stationary and regular structure.

3.5 Quantum Yield (QY)

Quantum yield fundamentally corresponds to the ratio of the photons emitted to the photons absorbed. The QY experiments primarily include the measurements of the fluorescence quantum yields of the synthesized polymers prior to the WPLED production step. The method used for the fluorescence quantum yield determination was

the relative quantum yield measurement method which needed a reference characterized material [72]. This reference fluorescent material (Quinine Sulfate) has a pre-determined fluorescence quantum yield and an absorbance and fluorescence emission values that resembles to those of the synthesized polymers as much as possible. Perkin Elmer LS 55 Fluorescence Spectrometer was used together with its software FLWinlab throughout the experiments, and the samples were prepared with extremely diluted concentrations of approximately 10^{-6} M. The thicknesses of the thin films were adjusted in order to ensure optical behavior according to the Beer's law. Moreover, it is also known that the dilution of acceptor polymer increases the quantum yield as the concentration quenching and self-absorption are effectively prevented. The spectrometer recorded the fluorescence emission spectra from the respective toluene solutions. The reference material is quinine sulfate (QS) as stated and its photoluminescence efficiency (Q_{QS}) is 0.55; in H_2SO_4 [73]. Experimental results were calculated using Equation 3.2:

$$\Phi s / \Phi r = (As \ n_r \int Fr) / (Ar \ ns \int Fs) \qquad \text{Equation 3.2}$$

The optical properties are summarized in Table 3.2.

In the equation, Φs and Φr are photoluminescence efficiencies, As and Ar are the absorbance values at the excitation wavelength, Fr and Fs are fluorescence values, and n_r and ns are the refractive indexes.

It is crucial that the absorbance values have to be lower than 1 so as to prevent the self-quenching. Thus, concentrations of the solutions have to be close to the value of 10^{-6} M. Polymers were dissolved in toluene, and from the solutions that were prepared with the concentration of 0.01 mg/mL; 0.1 mL were taken and diluted to 10 mL. For the preparation of the thin film samples, the solutions were spin-coated onto the pre-cleaned glasses. The absorption spectra of the polymers were shown in **Figure 3.10**.
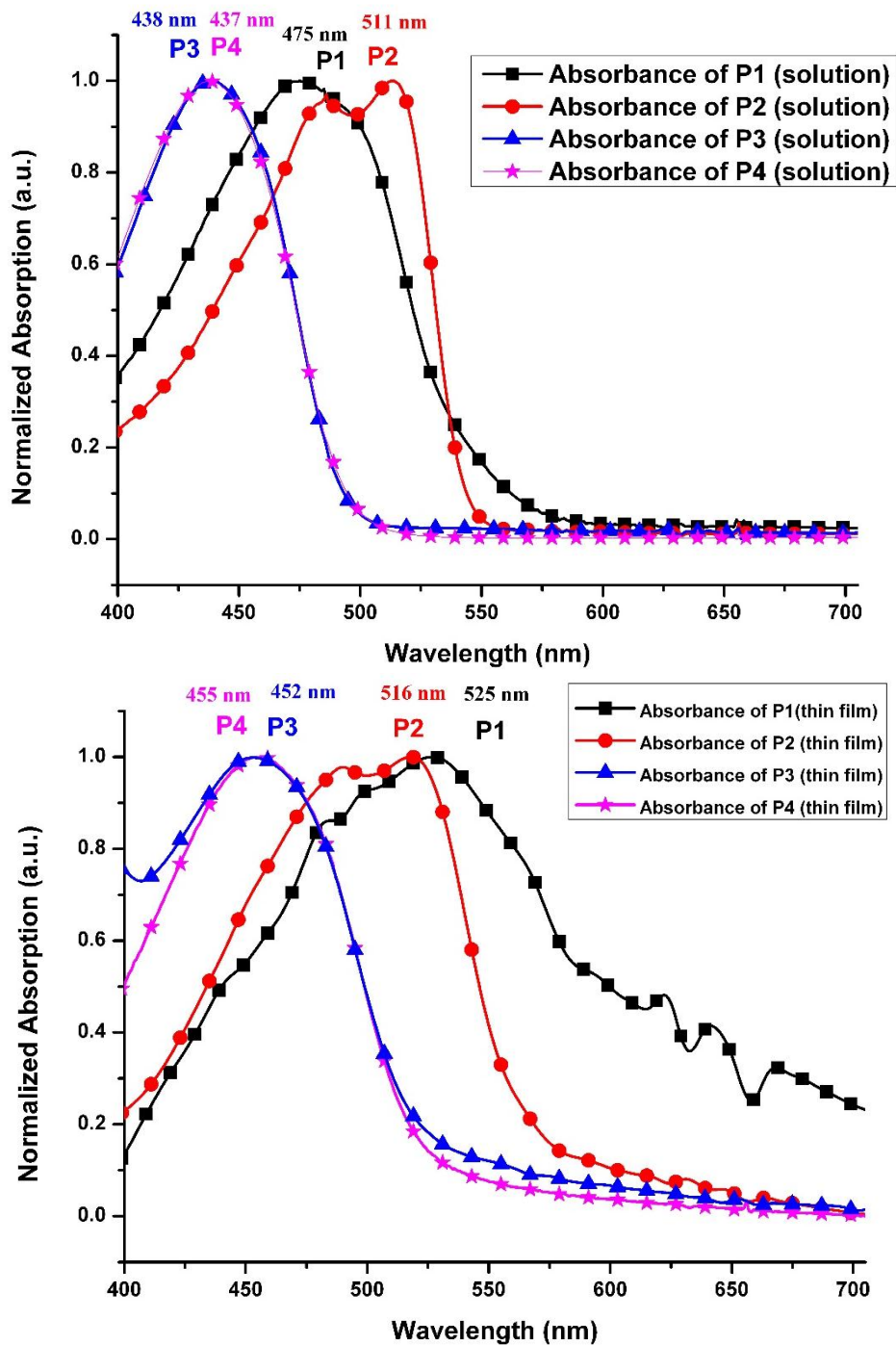
Figure 3.10 Absorption spectra for **P1**, **P2**, **P3** and **P4** (solution and thin film).

Fr and Fs fluorescence values were used in the calculations by taking the integral of the area under their curves. Throughout the preparation of the thin films for emission

56

studies, the spin-coating speed was set to 750 rpm and the duration was 60 seconds. Utilizing the Perkin Elmer Fluorescence Spectrometer, the emission values of the samples that were excited at 380 nm were depicted in the graphs below:
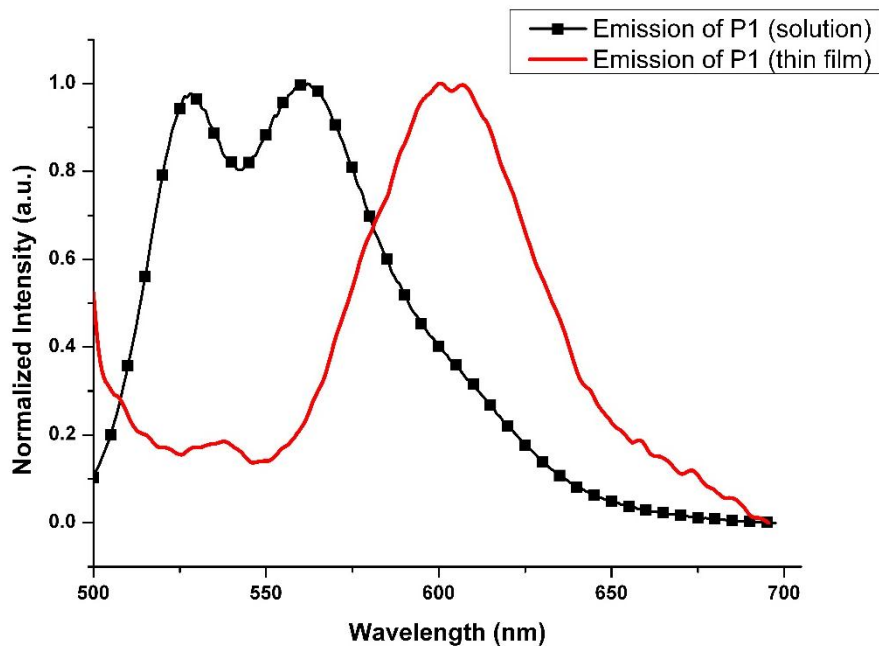
Figure 3.11 Photoluminescence spectra for **P1** (solution and thin film).
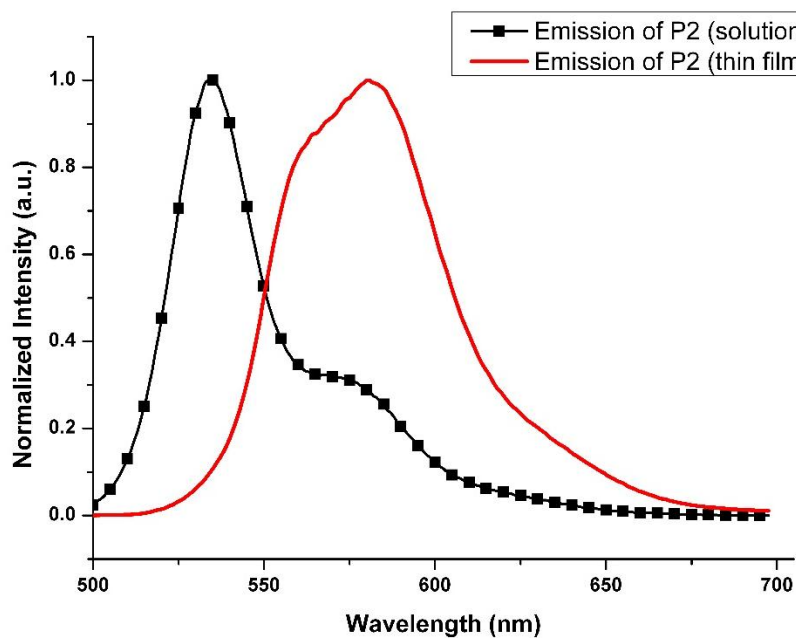
Figure 3.12 Photoluminescence spectra for **P2** (solution and thin film).
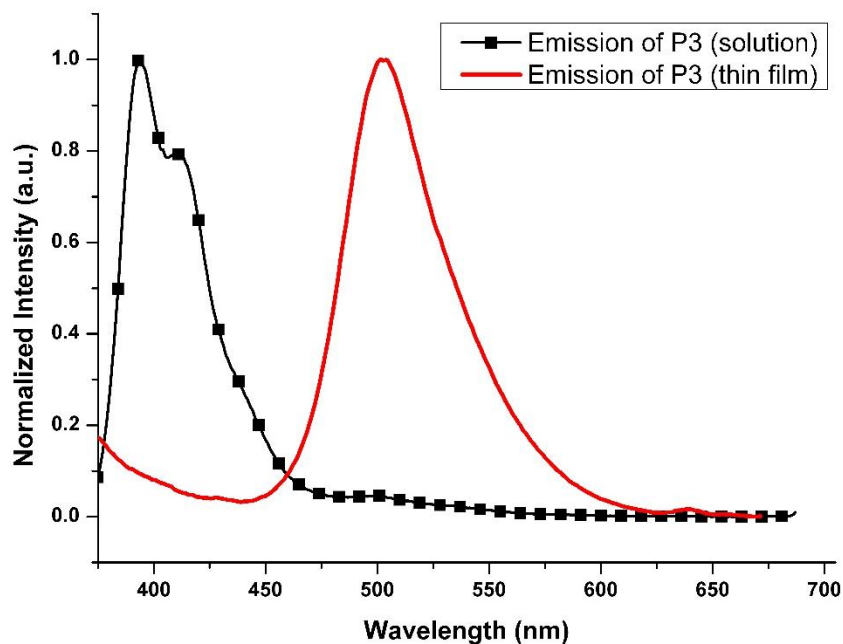
Figure 3.13 Photoluminescence spectra for **P3** (solution and thin film).

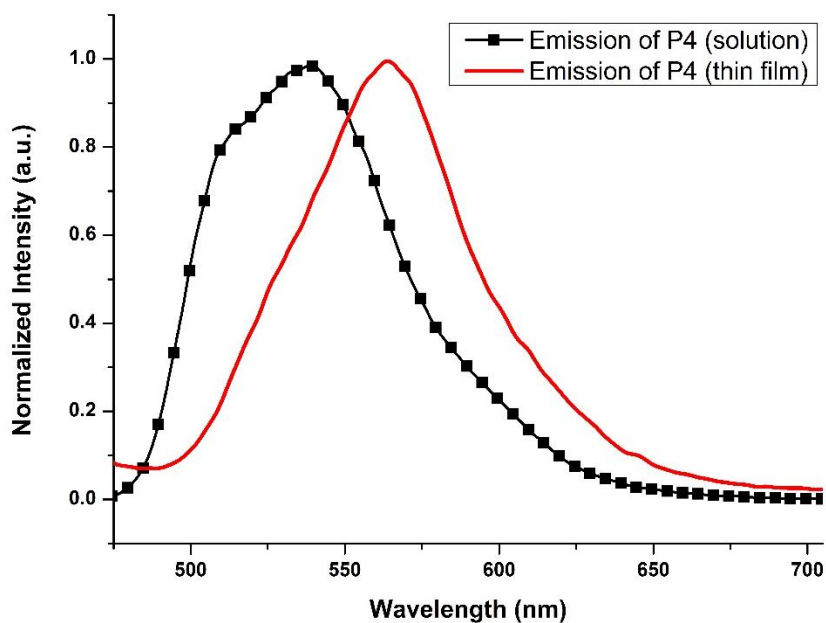**Figure 3.14** Photoluminescence spectra for **P4** (solution and thin film).

58
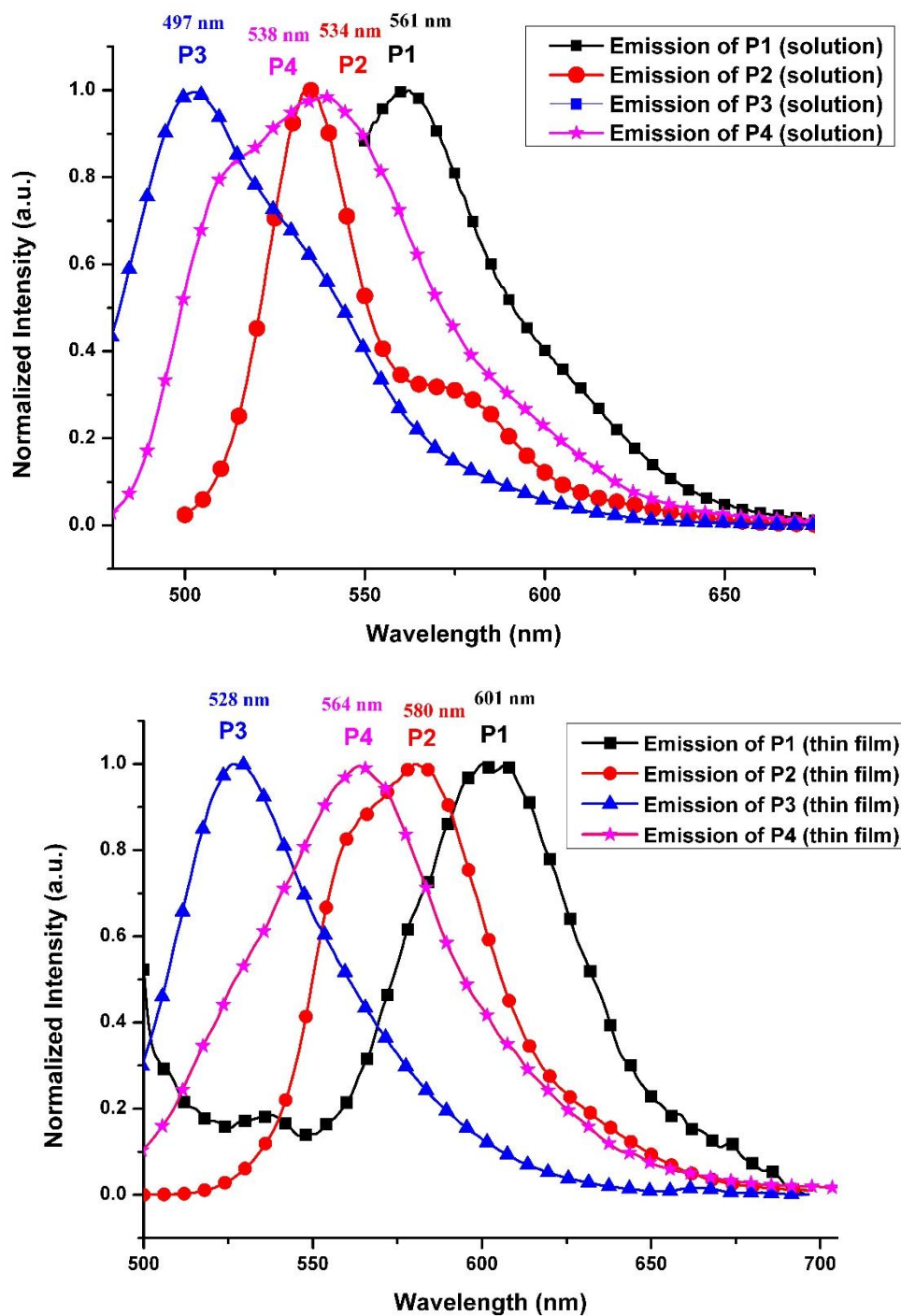
Figure 3.15 Photoluminescence spectra for **P1**, **P2**, **P3** and **P4** (solution and thin film).

In **Figure 3.15**, emission properties of **P1**, **P2**, **P3** and **P4** were evaluated. In PL, optical properties were revealed as electrons and holes are photo-excited. As a result,

light is emitted from the radiative recombination of electrons and holes. It is required to obtain the longer wavelengths for the individual acceptor thin film emissions. In energy transfer process, concerning the white light spectrum range, as the wavelength of a low band gap polymer gets longer, the light is shifted to the red end of the spectrum. **P1** has the longer red shifted emission at 601 nm and **P2** emits light at 580 nm, thus **P1** and **P2** were proved to be effective acceptor components for the white light generation. PL experiments in dilute solution and thin film showed differences in **Figure 3.11-14**; the thin film PL spectra red-shifted as compared to the solution PL which are owing to the different intermolecular interactions in the films formed.
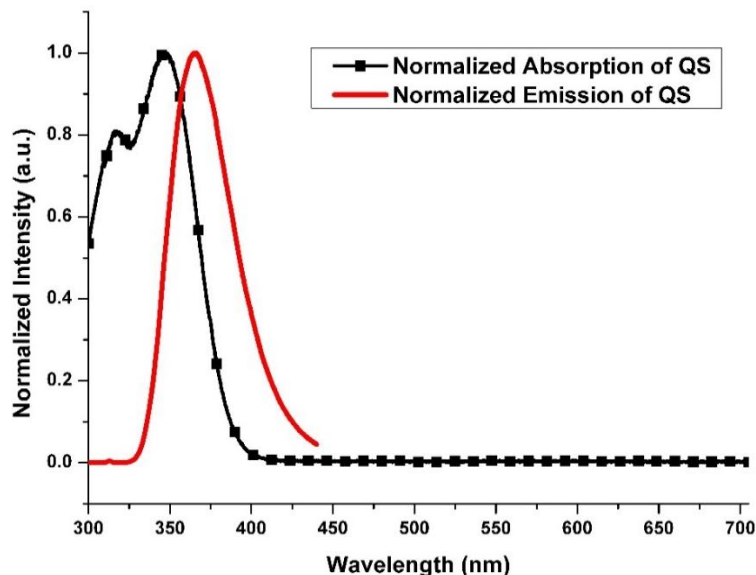
Figure 3.16 Absorption and emission spectra of Quinine sulfate in solution.

The synthesized polymers of **P1**, **P2**, **P3** and **P4** have PL quantum efficiencies of 0.63, 0.61, 0.49 and 0.54 by the calculations based on Equation 3.1. Since **P3** and **P4** do not possess the required fluorescence emission values and **P3** has a lower fluorescence quantum efficiency value; for the fabrication of the white light emitting polymer diodes, **P1** and **P2** polymers were utilized in the emissive layer of the device by blending them with the blue emitting polymers in certain ratios.

60

Table 3.2: The optical properties of **P1**, **P2**, **P3**, and **P4**

Polymers	UV	UV	PL	PL	Φ_s
	Λ_{max} (nm) (solution)	Λ_{max}(nm) (thin film)	Λ_{max}(nm) (solution)	Λ_{max}(nm) (thin film)	Quantum Efficiency
P1	475	525	528, 561	601	0.63
P2	484, 511	489, 516	534	580	0.61
P3	438	452	497	528	0.49
P4	437	455	538	564	0.54

3.6 Förster Energy Transfer

In the graphs below (**Figure 3.17 and 3.18**), as the evidences of the FRET, the overlaps of the absorbance spectrum of the **P1** and **P2** with the fluorescence emission spectrum of the blue emitting polymer (**BE3**) which has the best performance for the WPLED production is given, respectively. (An overlap of the acceptor absorption spectrum with the donor photoluminescence spectrum is one of the required principles for the FRET.)

Figure 3.17 The spectral overlap of the thin film absorption of the **P1** polymer and thin film fluorescence of the blue light emitting polymer (**BE3**).
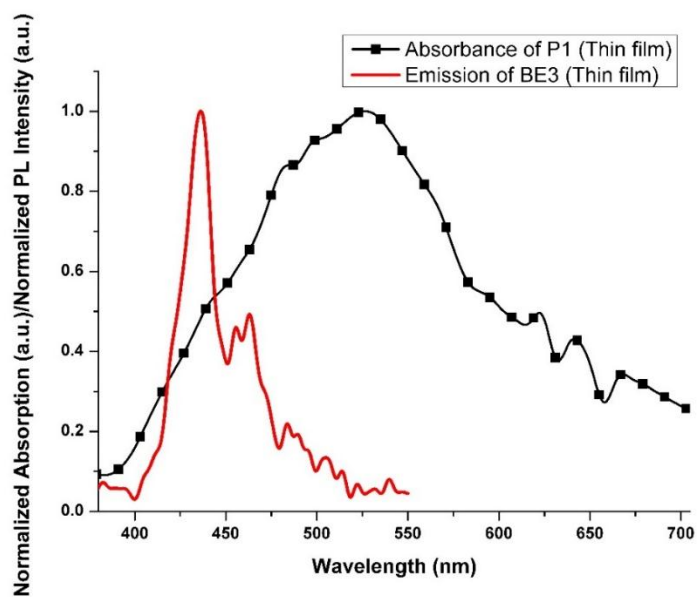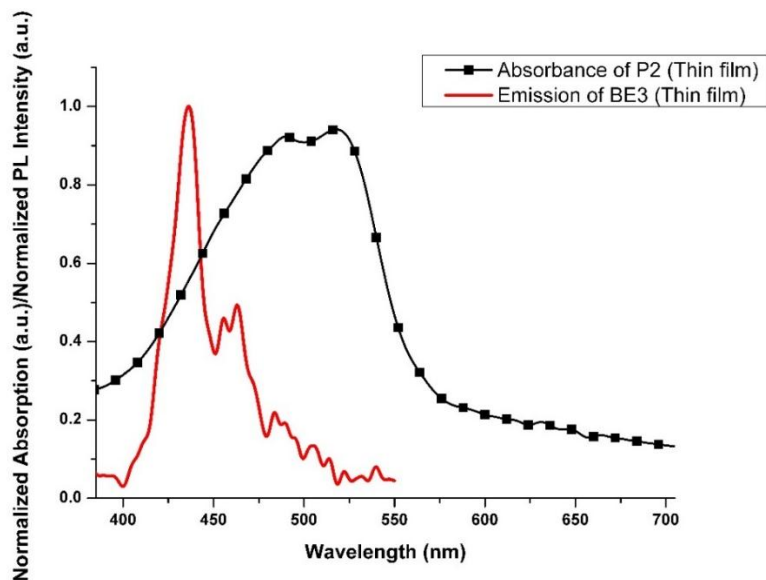
Figure 3.18 The spectral overlap of the thin film absorption of the **P2** polymer and thin film fluorescence of the blue light emitting polymer (**BE3**).

In the thesis study, the white light was achieved via blending the polymers that emit light in different wavelengths which are blended and dissolved in a common solvent in order to use them as one emissive layer with the simple spin-coating method. The two-component (binary) polymer blend was employed with a systematic change of the acceptor concentration. The photoluminescence studies and Förster non-radiative energy transfer between the donor (blue light emitting polymer) and the acceptor (orange light emitting polymer) were investigated. As the polymers were intermixed within the Förster radius, a flow of energy transfer from donor polymer to acceptor molecule took place. Particularly, in donor-acceptor blend systems, the acceptor traps the charge carriers (hole electron pairs) since HOMO level of the acceptor is above that of the donor (close to the vacuum level); at the same time, LUMO of the acceptor polymer is below that of the donor. Thus, when charge carriers are injected from the electrodes, orange acceptor emission may be preferred due to this charge trapping effect; as a result, all singlet excitons migrates to the orange emitting acceptor. Consequently; owing to the quenching of the excited state and poor charge mobility of the acceptor, orange emitting polymer concentration value needs to be maximum 5% of the donor polymer amount in order to avoid this complete energy transfer [74], in this manner, to avoid the single orange emission. Subsequently, by controlling the amount of doping of acceptor (99:1

wt. % blue donor to orange acceptor polymer weight ratio in blend), the excitation energy transfer to the acceptor polymer was prevented through an incomplete energy transfer between donor and acceptor polymer. Finally white light electroluminescence was successfully attained. Furthermore, when two light emitting polymers with higher and lower band gap energies are blended together, phase separation is also realized. Förster energy transfer may be incomplete owing to the presence of phase separated domains in the polymers, as well. In fact, since the donor-acceptor polymers used in the thesis study forms a miscible polymer blend, energy transfer is more likely to happen, and emission color could only be altered with modifying the blend ratio of the blue and orange emitting polymers. Hence, an individual study was additionally conducted in order to demonstrate the effect of the blend ratio. In 90:10% (blue to orange) wt. ratio blend, an energy transfer to the acceptor was realized. Eventually, an almost complete energy transfer occurred that prevented white light generation as depicted in **Figure 3.19**.
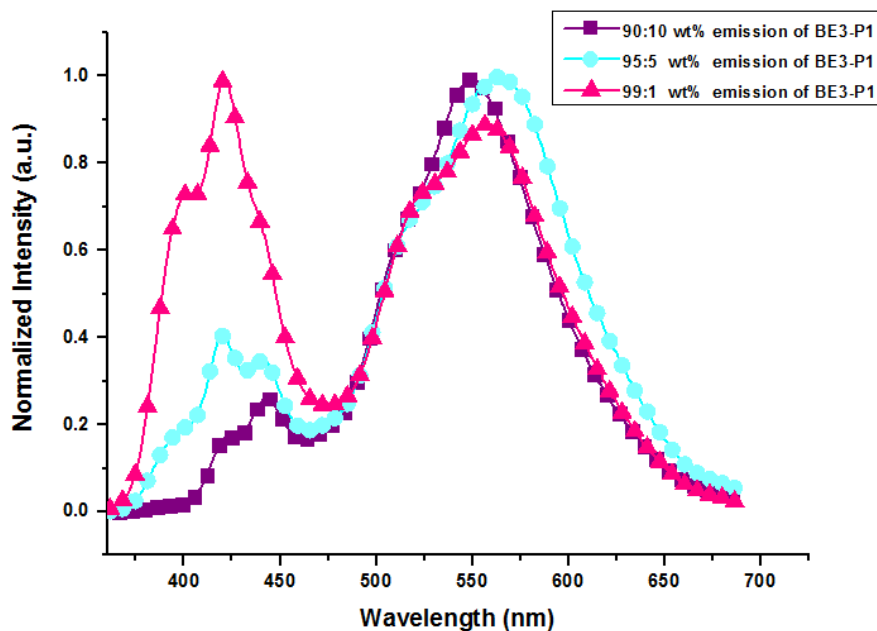

Figure 3.19 Photoluminescence spectra for 90:10 wt. %, 95:5 wt. %, and 99:1 wt. %
BE3-P1 blends.

In **Figure 3.19**, the weight ratios of the donor-acceptor polymer blends are varied in order to discover the correct ratios of blends for device fabrication experiments. By decreasing the content of the donor amount to a certain concentration, incomplete energy transfer took place rather than the complete energy transfer for one-color emission, resulting in a simultaneous emission from the acceptor and the donor. Consequently, as the amount of acceptor **P1** decreases to 1% ratio, the spectral range of each individual blue and orange color overlaps at a definite level with each other, and energy transfer was retarded which indeed stimulated a continuous spectrum very close to the white light. In particular, as can be seen in 90:10 wt. % blend's PL spectra, after 5 wt. % of acceptor amount, as predicted from the photoluminescence spectra and within the subsequent constructed device characteristics, the blue emission starts quenching and green emission starts to dominate in PL spectra, undoubtedly, also in EL spectra.

As an additional principle of the FRET, the donor blue light emitting polymer molecules are close to that of the orange light emitting polymer with a certain essential distance, accordingly, by the excitation of the acceptor, emission from the blue emitting polymer and the emission from the orange emitting polymer provided the required spectrum range for the white light generation.

In the graphs below, the FRET mechanism studies were further realized. The thin film photoluminescence studies of the blends of the blue light emitting polymers **BE1**, **BE2** and **BE3** and the orange light emitting polymers **P1** and **P2** which have the appropriate fluorescence quantum efficiencies with the required photoluminescence emission wavelengths are provided. The blends are given as **BE1-P1**, **BE1 -P2**, **BE2 -P1**, **BE2-P2** **BE3-P1**, and **BE3-P2**. In addition, through this comparative analysis of the polymer blends, the thin film photoluminescence spectrum of a blend which shows similarity to the electroluminescence of the prospective polymer white light emitting diode was determined. Consequently, it was decided to proceed with the next step which was the device fabrication with the appropriate blends offering the white light range.
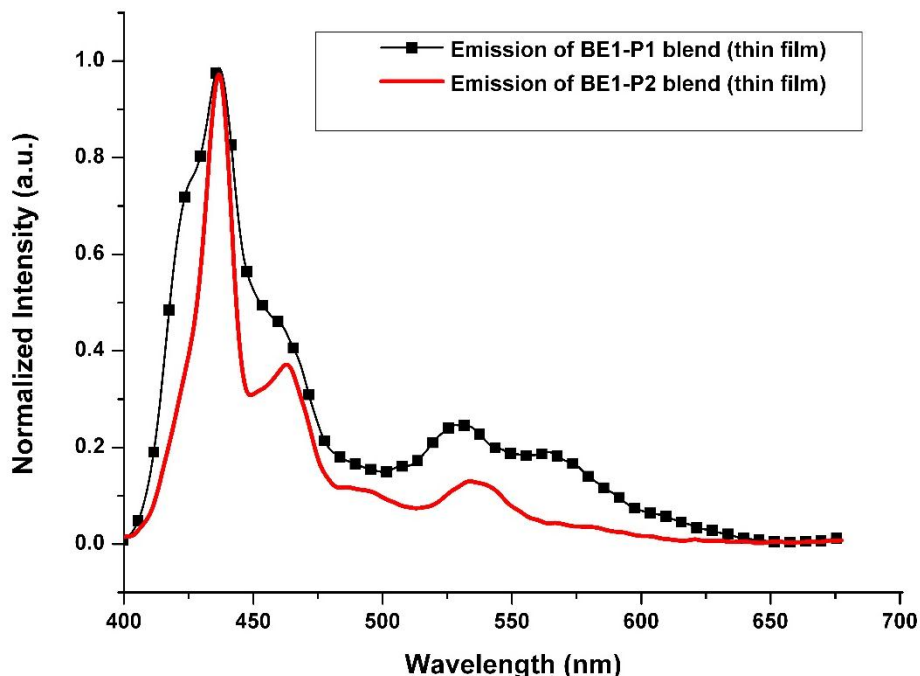
Figure 3.20 Photoluminescence spectra for **BE1-P1** and **BE1-P2** blends (99:1wt %).

As depicted in **Figure 3.20**, in the two component polymer blend which was prepared as a thin film from toluene, when the acceptor **P1** weight ratio was kept as low as 1%, a non-radiative FRET partial energy transfer was achieved. Both blue light emission from **BE1** and orange light emission from **P1** were achieved. This emission is in the range of white light covering the whole spectrum, nevertheless, since the emission from **P1** is relatively low, the equal energy white light cannot be realized. Through the reduction of the acceptor weight percentage, the photoluminescence and the electroluminescence intensity were increased and the poor charge mobility of the acceptor and quenching of the excited species were prevented. The circumstances for **P2** are the same. Thus, as a result of a study where the fluorescence emission properties were investigated, it can be conferred that the different end capper molecules of the polymers influenced the structure in different ways and they did not affect the properties of the emission of the blend as much as the individual emission mechanisms. The end capper molecule of the phenyl and tri-phenyl amine for the polymer **P1** and **P2** improved the hole-transporting and solubility performances, respectively.
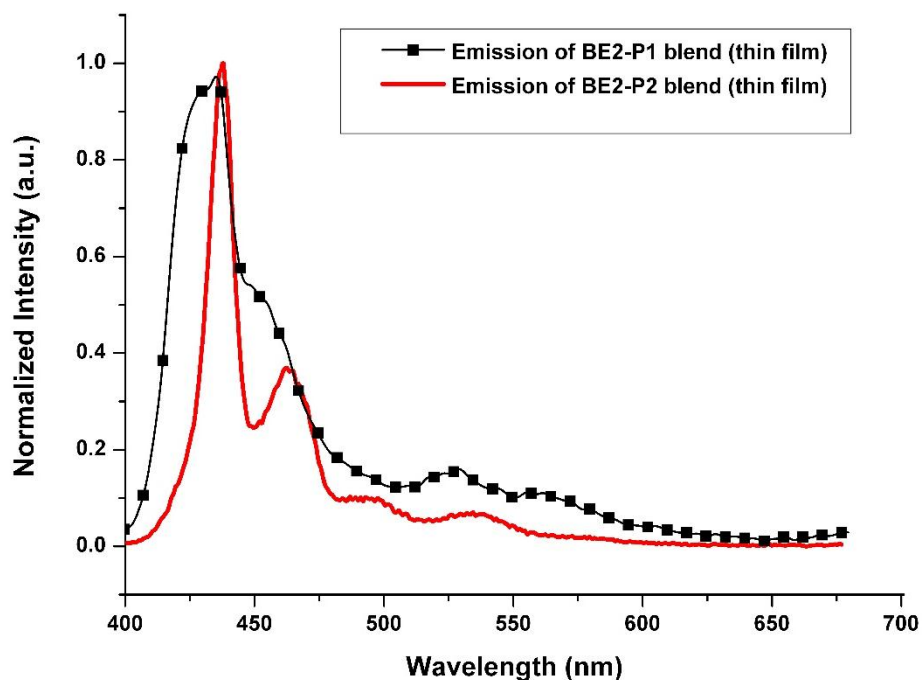
Figure 3.21 Photoluminescence spectra for **BE2-P1** and **BE2-P2** blends (99:1wt %).

As depicted in **Figure 3.21**, similarly, in the two component polymer blend which was prepared as a thin film from toluene, when the acceptor **P1** weight ratio was kept as low as 1%, a non-radiative FRET partial energy transfer was achieved. Both blue light emission from **BE2** and orange light emission from **P1** were achieved. This emission is in the range of white light covering the whole spectrum, nevertheless, since the emission from **P1** is relatively low, the equal energy white light cannot be realized. The circumstances for the **P2** are again the same. Thus, the different end capper molecules of the polymers influenced the structure, yet they did not affect the properties of the emission of the blend, remarkably. The end capper molecule of the tri-phenyl amine both for the polymer **P2** and **BE2** improved the hole-transporting performances and the solubility by reducing the aggregations in the solution.
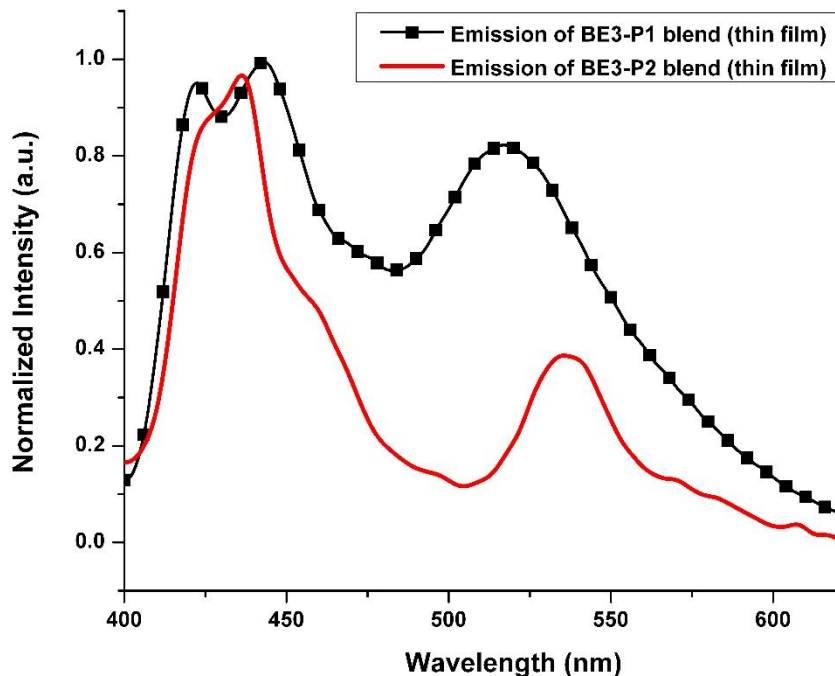
Figure 3.22 Photoluminescence spectra for **BE3-P1** and **BE3-P2** blends (99:1wt %).

As depicted in **Figure 3.22**, similarly, in the two component polymer blend which was prepared as a thin film from toluene, when the acceptor **P1** weight ratio was kept as low as 1%, a non-radiative FRET partial energy transfer was achieved. Both blue light emission from **BE3** and orange light emission from **P1** were achieved successfully. This emission is in the range of white light covering the whole spectrum, in addition, since the emission from **P1** is fairly efficient, the equal energy white light was ultimately realized. The circumstances for the **P2** are the same. Thus, as a result of a study where the fluorescence emission properties were investigated, the different end capper molecules of the polymers influenced the structure and the properties of the emission of the blends different from the cases with **BE1** and **BE2**. The blue light emitting polymer **BE3** has end capper molecules of oxadiazole which improves electron transporting property and the end capper molecule of the electron donating phenyl and tri-phenyl amine for the polymer **P1** and **P2** improved the hole-transporting abilities, respectively. Thus, an efficient recombination of the charges was reinforced. The aggregations in the solutions were diminished and the solubility was increased, as well. As a result; the best

photoluminescence performance of the polymer blend for the white light generation was achieved with **BE3** blue light emitting polymer.

Figure 3.23 Photoluminescence spectra for **BE3-P1** blends (95:5wt %)&(99:1wt %).

In **Figure 3.23**, in order to prove that the 99:1% blend ratio provided the best performance, experiments with 95:5% blend ratio were also accomplished. The dilute polymer blend solutions with 1% acceptor **P1** concentration avoided the self-absorption and the fluorescence quantum efficiency was improved. The 99:1% blend has a more stable and intense thin film PL. Moreover, the emission intensities from both blue and orange light emitting polymers are close to each other.

Figure 3.24 Photoluminescence spectra for **BE3-P2** blends (95:5wt %)&(99:1wt %).

In **Figure 3.24**, similarly, experiments with 95:5% blend ratio were also accomplished. The dilute polymer blend solutions with 1% acceptor **P2** concentration avoided the self-absorption and the fluorescence quantum efficiency was slightly improved. Emission from the orange component is at a longer wavelength in the 99:1% blend, and both blends have stable thin film PL. Moreover, the emission intensities from both blue and orange light emitting polymers are again close to each other.
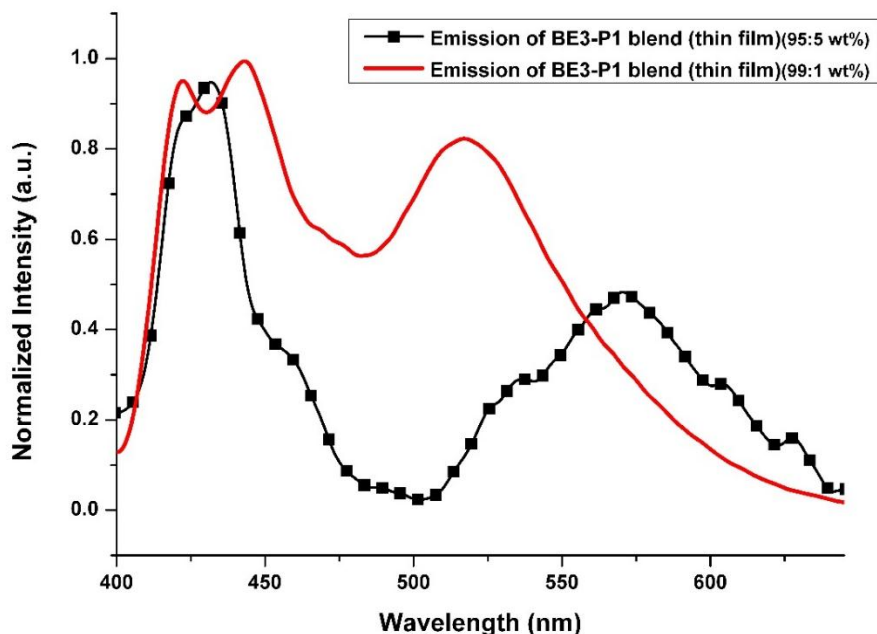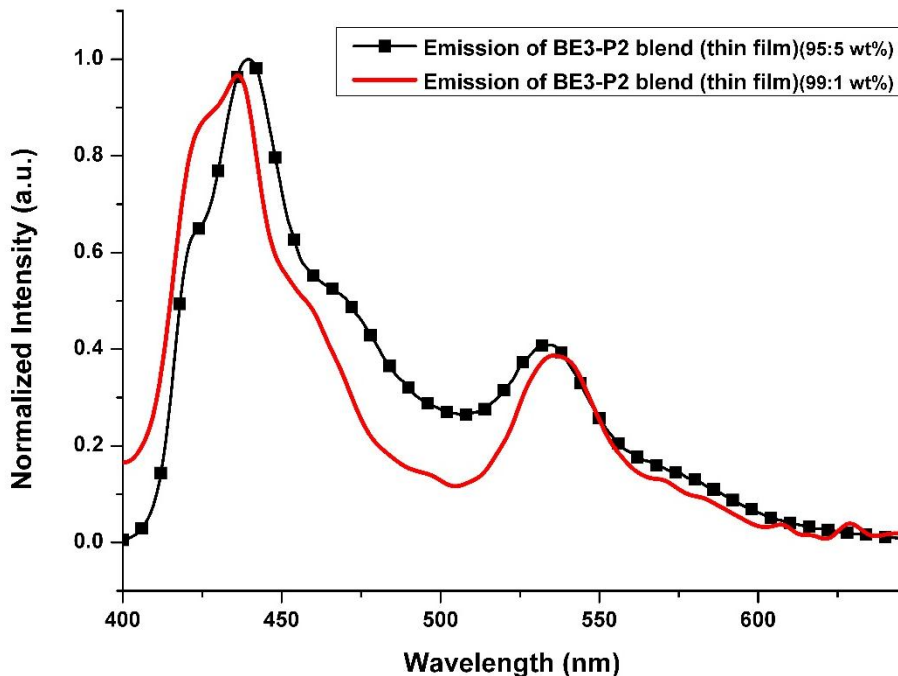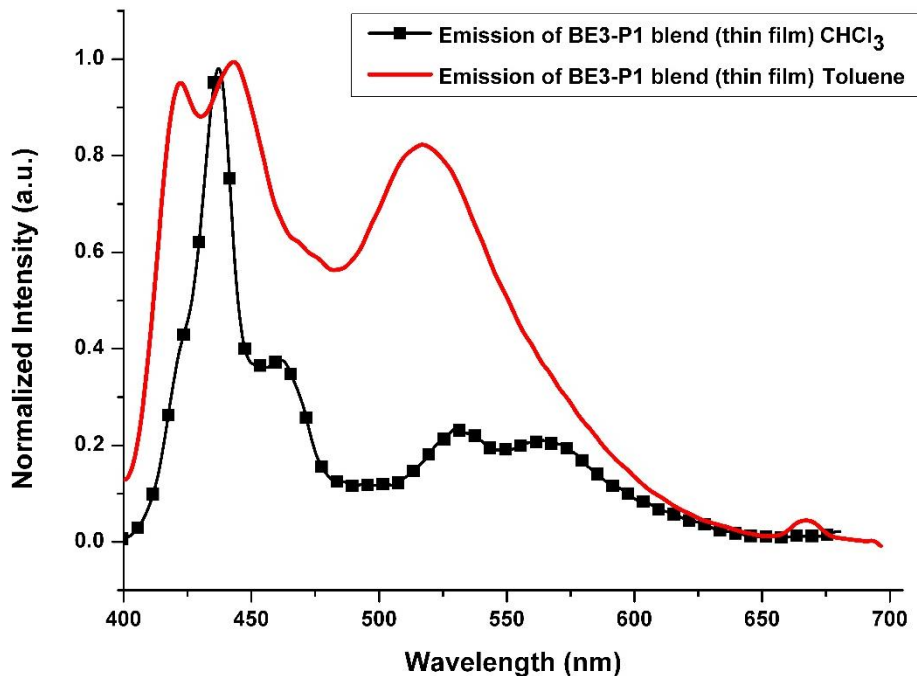
Figure 3.25 Photoluminescence spectra for **BE3-P1** blends (99:1wt %).

In **Figure 3.25**, in order to prove that the blend solution prepared from toluene provided the best performance in the thin film PL studies, experiments with $CHCl_3$ were also accomplished. In the blend where a thin film was formed by dissolving it in toluene, the phase separation was better and the self-absorption was prevented providing a high PL quantum efficiency. Moreover, the emission intensity from both blue and orange light emitting polymers are high.

The weight percentages of the polymer blends, 99:1 (**BE3**: **P1**) ratio and toluene solvent were precisely used in the device fabrication using **BE3** blue emitting polymer after the PL studies, and it was predicted that the electroluminescence spectra (EL) and the photoluminescence spectra (PL) would exhibit similarities in terms of exciton formation.

Figure 3.26 Photoluminescence spectra for **BE1-P1**, **BE2-P1**, **BE3-P1** blends (99:1wt %).

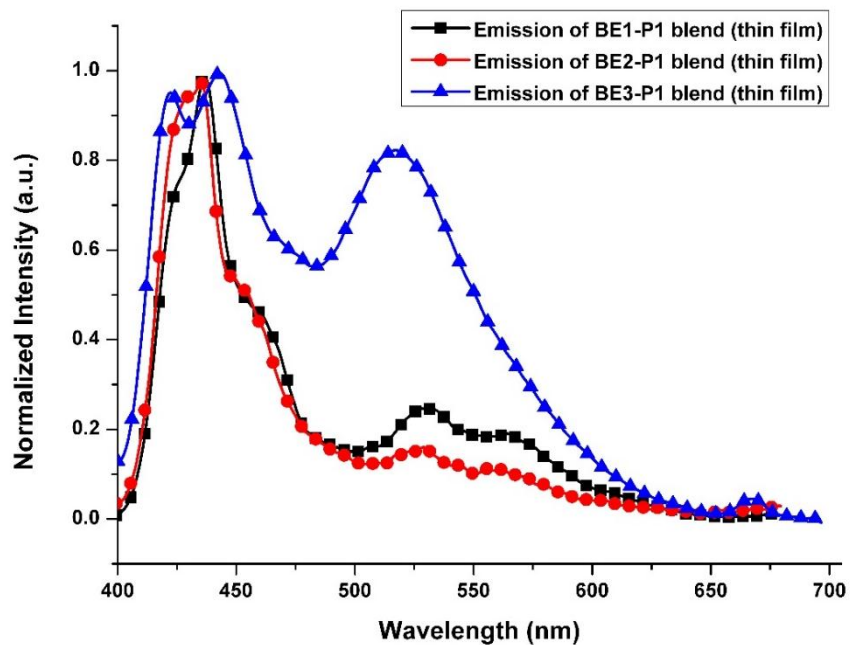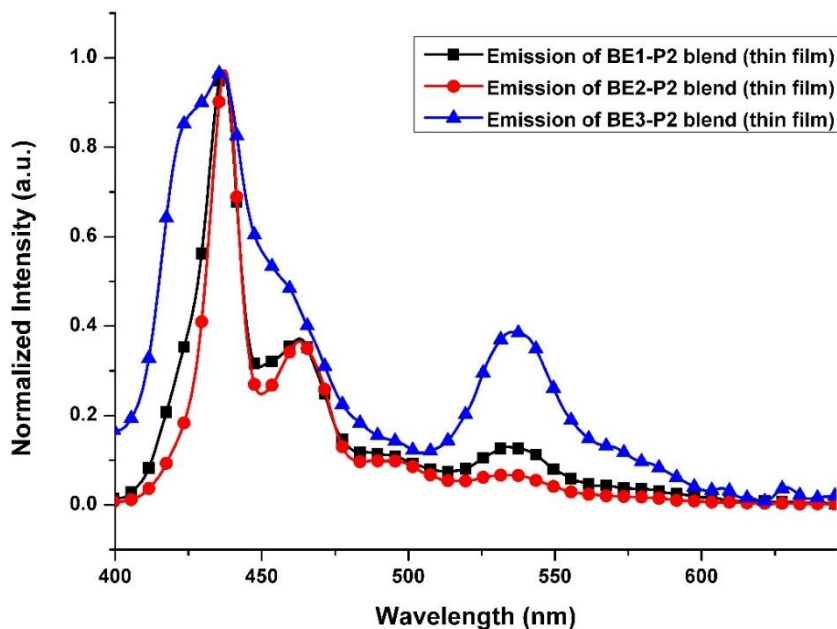

Figure 3.27 Photoluminescence spectra for **BE1-P2**, **BE2-P2**, **BE3-P2** blends (99:1wt %).

In brief, the FRET analysis studies were conducted prior to the device fabrication as a necessity for the emissive layer of the WPLED. The solid state photoluminescence spectra given for the blended blue light emitting (**BE3**) and the orange light emitting polymers (**P1** and **P2**) proved the FRET existence; and having the correct range in the spectrum, PL analysis studies and the fluorescence quantum efficiency experiments of **P1** and **P2** proposed that the best performance can be achieved with the particular blends of **BE3-P1** and **BE3-P2** for the white light generation.

3.7 Device Performance

3.7.1. ITO-Glass White Polymer Light Emitting Diodes:

The best results accomplished from the white light-emitting diodes constructed with the emissive layer of **BE3-P1** and **BE3-P2** blending systems. The polymer blend was dissolved in toluene and blended with a ratio of 99:1% wt. as stated earlier.

3.7.1.1   BE3-P1 Device

Figure 3.28 Constructed WPLEDs.
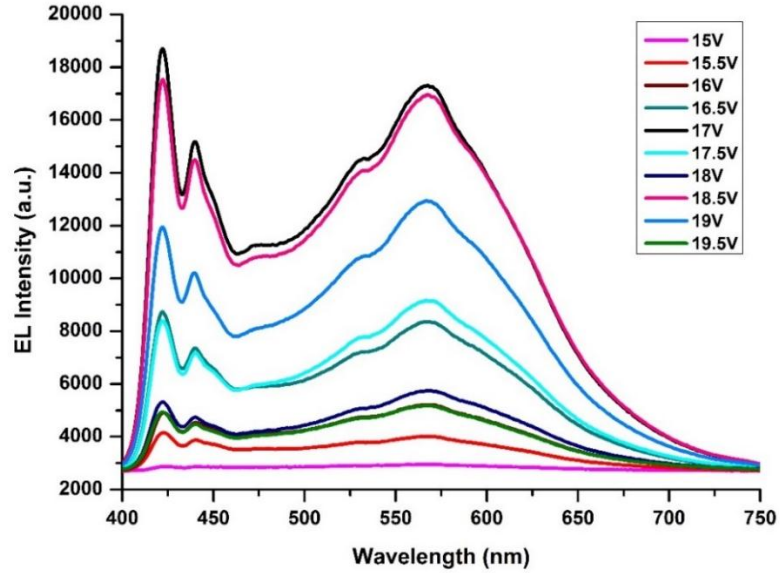
Figure 3.29 Voltage dependence of electroluminescence spectra for ITO/PEDOT:PSS/ **BE3-P1** blend/Ca/Al devices.

In **Figure 3.29**, maximum EL emission intensities corresponding to the blue emitting **BE3** and orange emitting **P1** from **BE3-P1** white PLED are observed. The spectra is similar with the corresponding PL spectra. The spectral response is insensitive to the increased voltage and driving bias, namely, white light EL spectra is quite stable for **BE3-P1**.
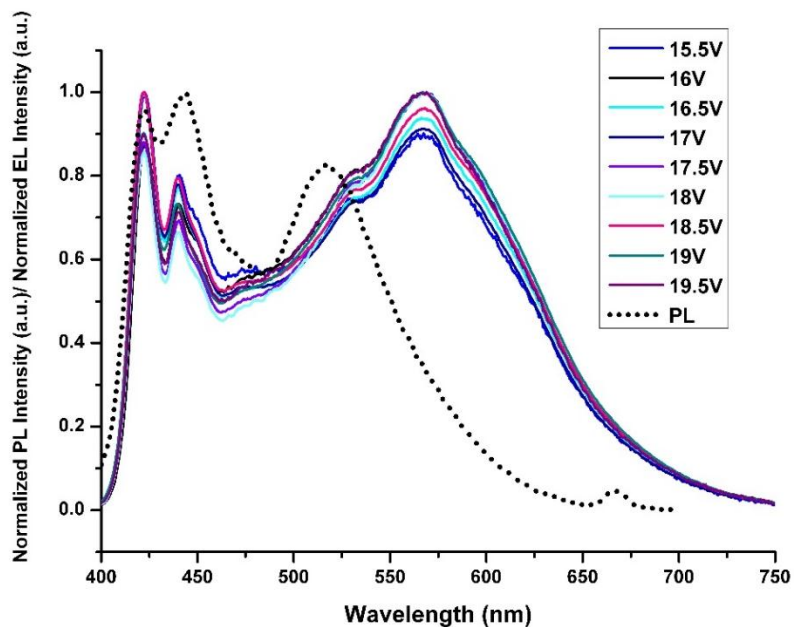
Figure 3.30 PL and EL spectra for **BE3-P1** blend.

73

Voltage dependence of electroluminescence (EL) spectra for **BE3-P1** device was compared with the photoluminescence (PL) spectra of the corresponding **BE3-P1** blend in **Figure 3.30**. The difference is mostly due to the differences in exciton formation mechanism. As excitons are formed upon applied voltage when the injected charges meet at the emissive layer during EL, the emission occurs slower and the spectra shifts accordingly. In PL, once excitons form, they have a short time to be confined on lower energy sites before they emit, whereas in EL, as the charges migrate through the device, they naturally move to the lower energy sites even before exciton formation. This additional process in EL gives a red-shift of the spectrum compared to PL as seen in **Figure 3.30**. Besides, while PL is principally determined by the optical properties of the material, EL is determined by several different factors such as the optical properties and physical structures of the optically active layers, the electrical properties of cathode and anode, and other electrical properties of hole transport and emissive layers. Thus, PL is not equivalent to EL, yet the emission properties are similar in terms of emitted light color.
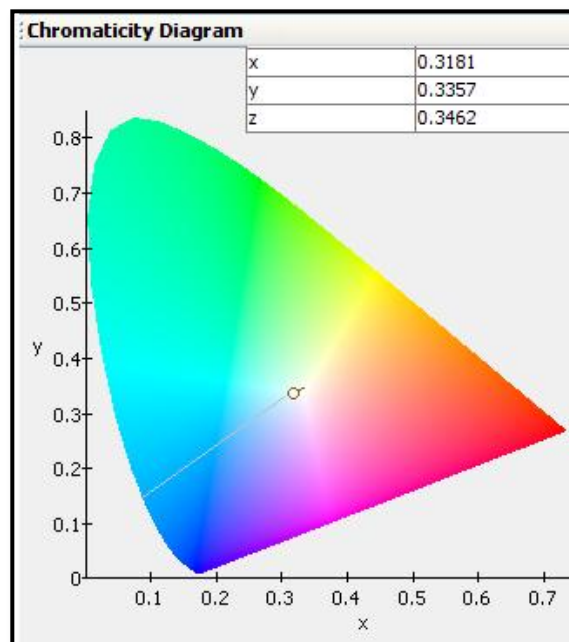

Figure 3.31 CIE chromaticity diagram for ITO/PEDOT:PSS/**BE3-P1** blend/Ca/Al devices.

74

In **Figure 3.31**, the CIE Chromaticity coordinates belonging to the **BE3-P1** white polymer light emitting diode are given as x = 0.31, y = 0.33. These coordinates are nearly pure white light (x= 0.33, y=0.33). In this study, they are the closest coordinates to the equal energy white point of the diagram that were discovered.
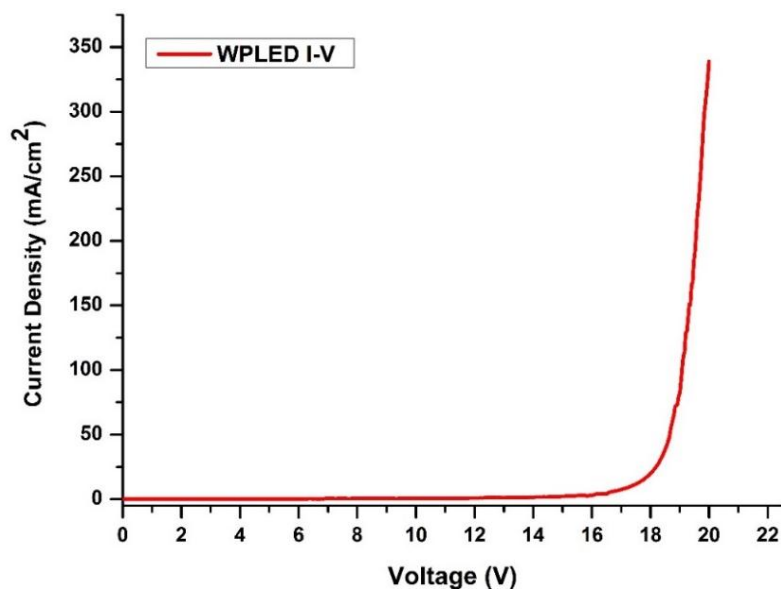
Figure 3.32 Current density vs. applied voltage for ITO/PEDOT:PSS/ **BE3-P1** blend/Ca/Al devices.

In **Figure 3.32**, the current density versus voltage characteristics (I-V) of **BE3-P1** white polymer light emitting diode was recorded. The turn-on voltage of the device is 14V. The turn-on voltages for white OLEDs are typically high due to several reasons and there are some approaches to reduce both the turn-on and working voltage. Using an inorganic electron injection or hole transport layer at organic/cathodic or organic/anodic interfaces, respectively, is one of the approaches. Incorporating an electron transport layer (ETL) and hole transport layer (HTL) were also analyzed in the thesis study. Nevertheless, by means of ETL and HTL incorporation, although the turn-on voltages were decreased remarkably, the color coordinates were shifted significantly farther than the equal energy white point. In

consequence, for the following PLED experiments, ETL and HTL materials were eliminated and the device architecture remained without any additional layers.

In this thesis work, the high turn-on voltages were mainly due to the required emission from blue donor polymer for white light emission. The energy barriers for the injection of both electrons and holes are high for a higher band gap blue emitting polymer, although it is much easier for electrons and holes to be injected into the lower band gap polymer. Therefore, the emission from higher band gap blue polymer can only be fulfilled at higher voltages. In addition, even though the turn-on voltages are high from the device of **BE3-P1** polymer blend, the increasing voltage do not cause any color impurities due to the well-mixed performance of the blend.
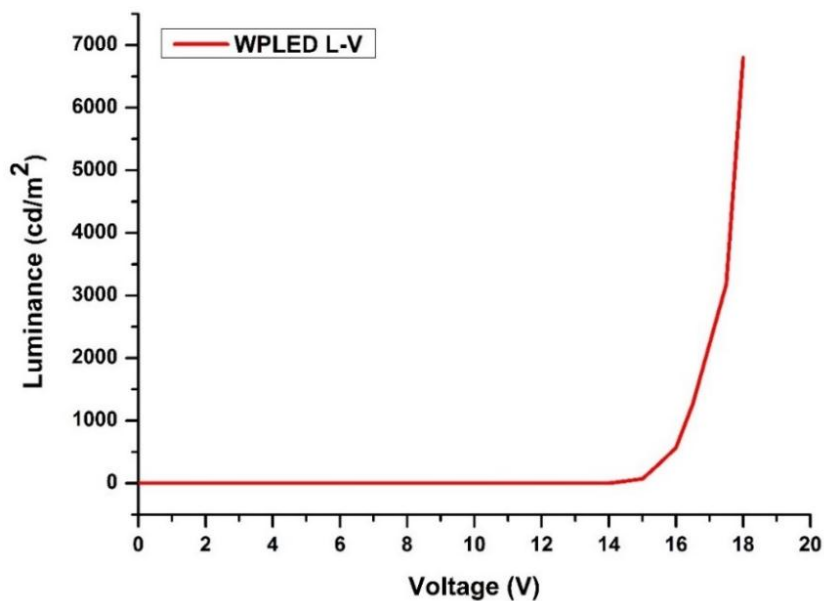

Figure 3.33 Luminance vs. applied voltage for ITO/PEDOT:PSS/**BE3-P1** blend/Ca/Al devices.

In **Figure 3.33**, the luminance against voltage characteristics (L-V) of **BE3-P1** white polymer light emitting diode were investigated. At the working voltage of 17V, the luminance was 2000 cd/m^2 which is a highly efficient brightness.

3.7.1.2 BE3-P2 Device
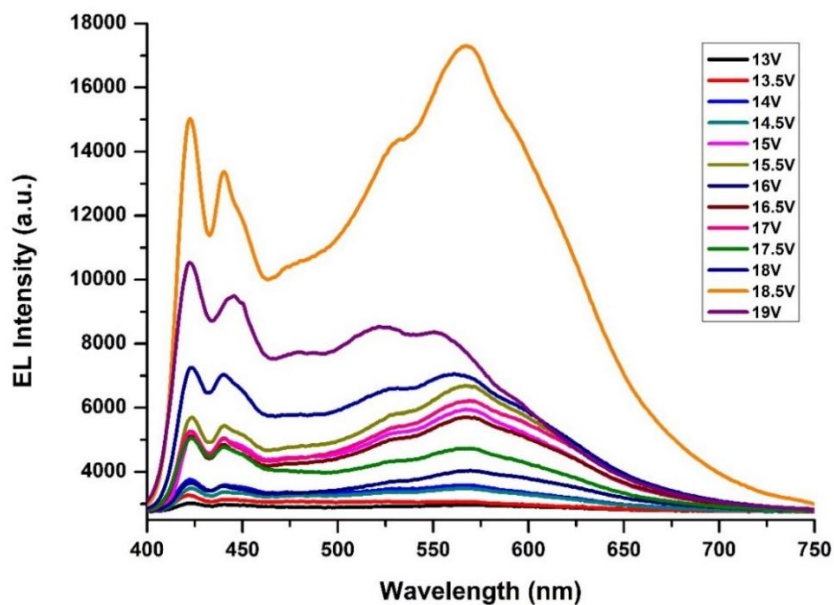
Figure 3.34 Voltage dependence for electroluminescence spectra for
ITO/PEDOT:PSS/**BE3-P2** blend/Ca/Al devices.

In **Figure 3.34**, maximum EL emission intensities corresponding to the blue emitting **BE3** and orange emitting **P2** from **BE3-P2** white polymer light emitting device are observed. The spectra is similar with the corresponding PL spectra. EL spectra is less stable to the increased voltage than that of **BE3-P1** device. This may be ascribed to the different mixing properties of **BE3** and **P2**. Although the solubility of **P1** and **P2** in toluene is good, **P2** is a slightly less soluble in toluene than **P1** to a small extent. Thus, the immiscibility characteristics of the polymers dominated their well-mixed behavior, and as the voltage increased, color impurities are formed in **BE3-P2** blend. In this case, Förster energy transfer became more difficult, and the emission not only depended on the blend ratio, but also on the solubility of components, solvent-polymer interactions,

and solvent vapor pressure. Nevertheless, due to the same reasons, the phase separation in the emissive layer of **BE3-P2** polymer blend was enhanced. Hence, white light generation was once more successful and EL intensity is high.
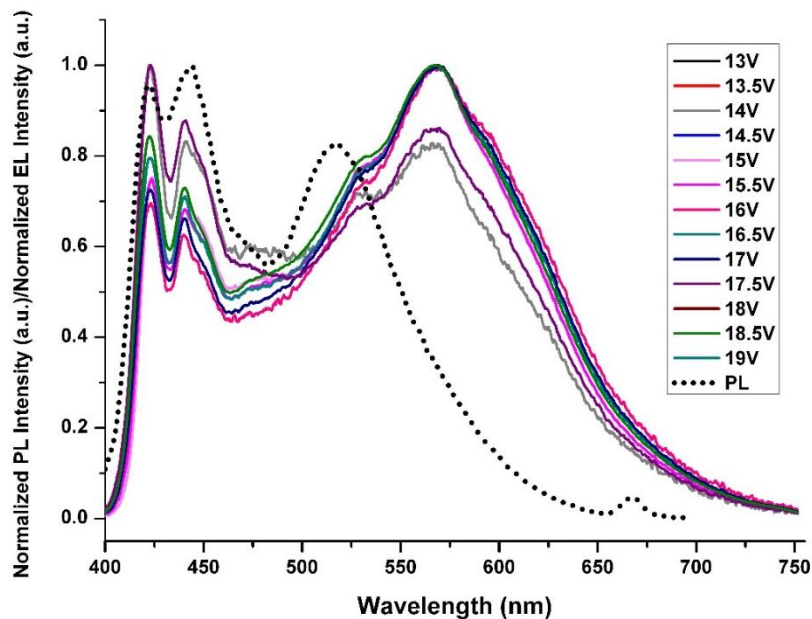
Figure 3.35 PL and EL spectra for **BE3-P2** blend.

Voltage dependence of electroluminescence spectra for **BE3-P2** device was compared with the photoluminescence spectra of the corresponding **BE3-P2** blend in **Figure 3.35**. Once again, the EL and PL spectra are not equivalent, yet similar in terms of the emitted light color. Since the exciton binding energy is 0.5 eV in organic materials, its dissociation into free charges is difficult. The differences of PL and EL spectra is also originated from this argument. The coulombically bound electron-hole pair migrates through the device in EL process, and as stated earlier, it moves to the lower energy sites even before molecular exciton formation. Thus, excited state lifetimes of EL emission is much longer, and the EL spectra was red-shifted with respect to the corresponding PL spectra as given in **Figure 3.35**.
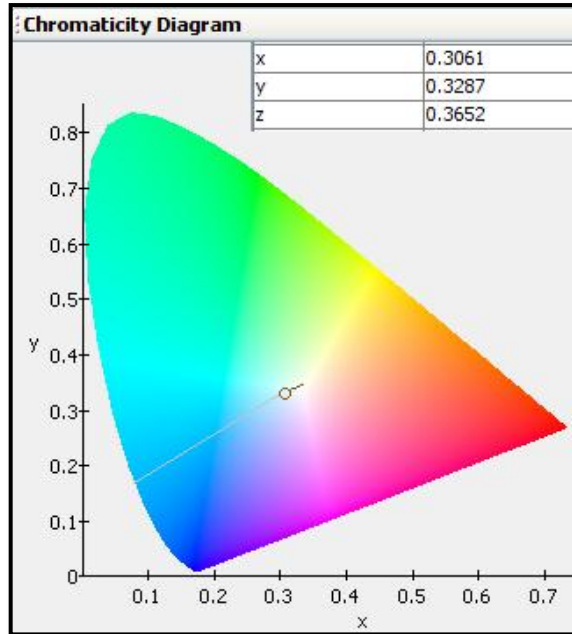
Figure 3.36 CIE chromaticity diagram for ITO/PEDOT:PSS/**BE3-P2** blend/Ca/Al devices.

In **Figure 3.36**, the CIE Chromaticity coordinates belonging to the **BE3-P2** white polymer light emitting diode is given as x =0.30, y =0.32. These coordinates are nearly pure white light (x= 0.33, y=0.33) and very close to the equal energy white point of the diagram.
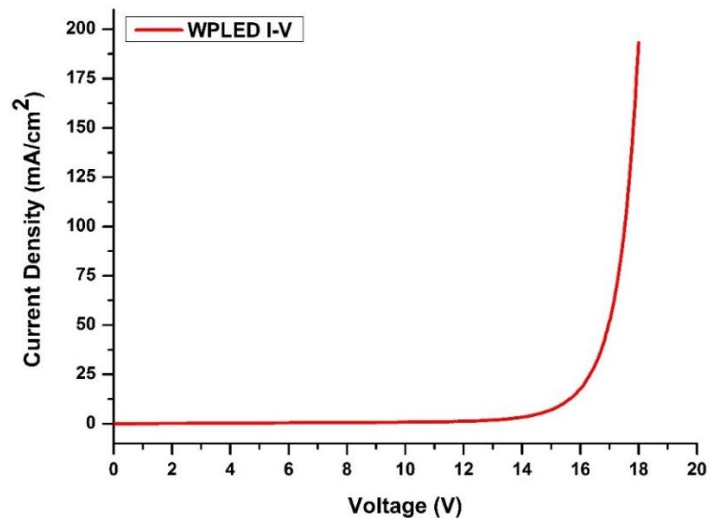
Figure 3.37 Current density vs. applied voltage for ITO/PEDOT:PSS/ **BE3-P2**
blend/Ca/Al devices.

In **Figure 3.37**, the current density versus voltage (I-V) characteristics of **BE3-P2**
white polymer light emitting diode was recorded. Since the turn-on voltage depends
mostly on the band gap of the acceptor component and on the work function of the
electrodes; it may be stated that **P2** having a slightly larger band gap than **P1**, has a
higher turn-on voltage (15V) as the charge trapping and FRET mechanisms in **BE3-P2** device were affected accordingly.
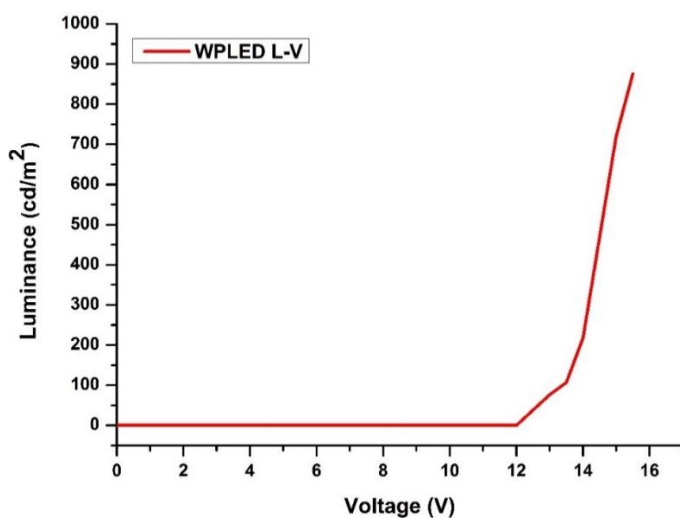
Figure 3.38 Luminance vs. applied voltage for ITO/PEDOT:PSS/**BE3-P2**
blend/Ca/Al devices.

In **Figure 3.38**, the luminance against voltage characteristics (L-V) of the **BE3-P2** white polymer light emitting diode were investigated. Luminance is 900 cd/m^2 at working voltage of 17.5V.

3.7.2. ITO-PEN Flexible White Polymer Light Emitting Diodes:

3.7.2.1 P1-BE3 Flexible Device
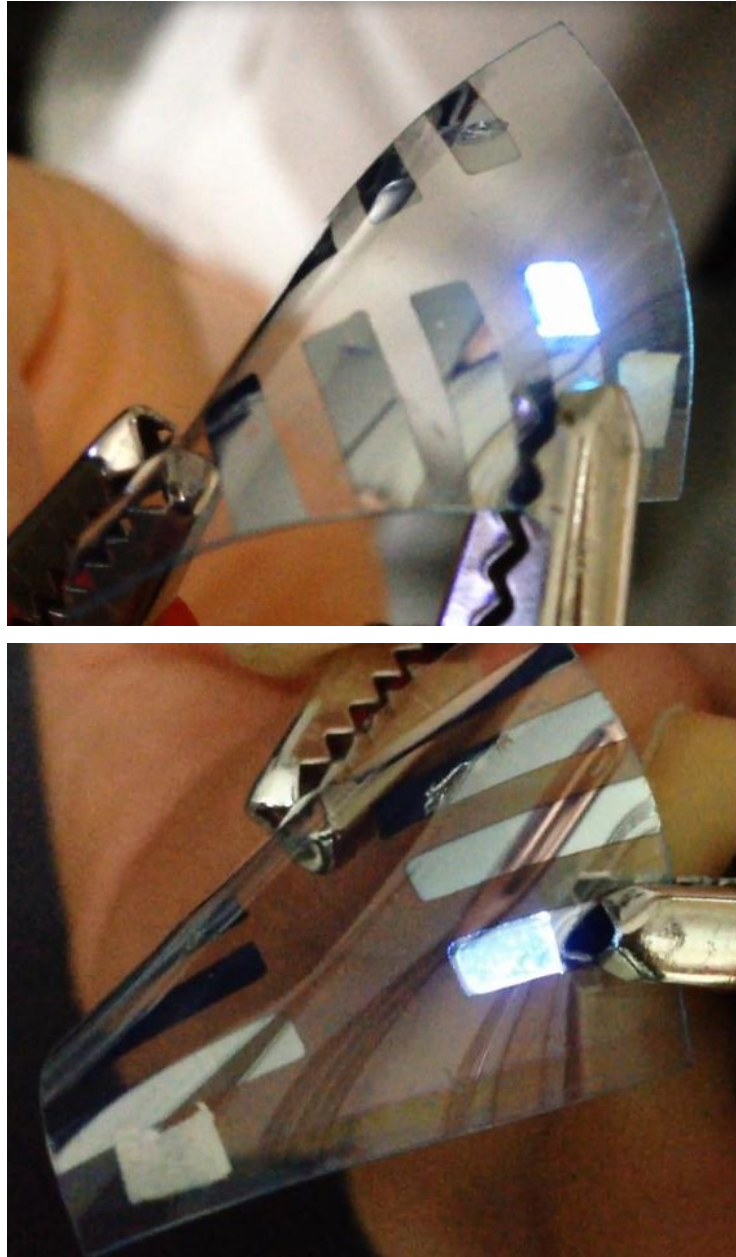
Figure 3.39 Constructed **BE3-P1** FWPLEDs.

A flexible white polymer light emitting diode employing the same binary blend of **BE3-P1** as the emitting layer (with the best performance on ITO-glass devices) was prepared in the thesis study, as well. Figure 3.40 shows the EL spectra of the device measured at various voltages similar to the measurements of ITO-glass WPLED devices.
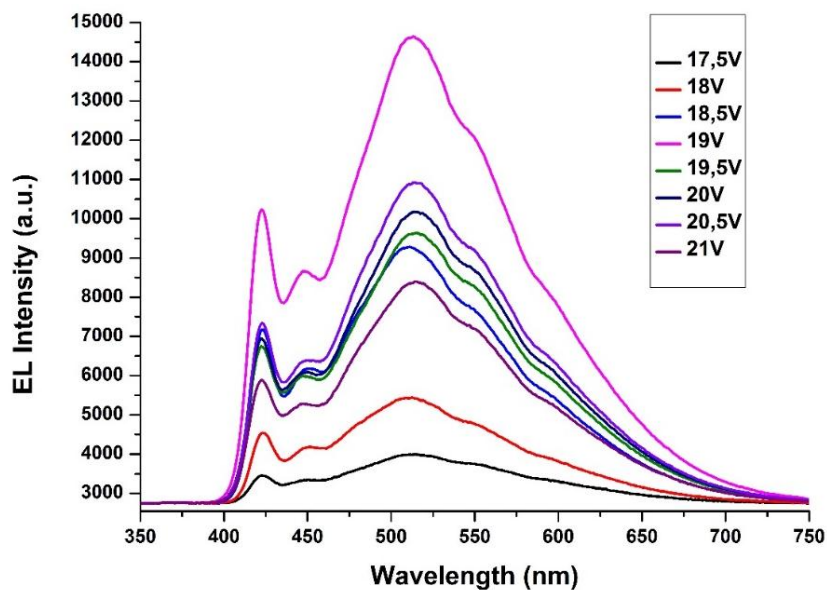
Figure 3.40 Voltage dependence for electroluminescence spectra for
ITO/PEDOT:PSS/**BE3-P1** blend/Ca/Al flexible devices.

In **Figure 3.40**, EL emission intensities corresponding to the blue emitting **BE3** and orange emitting **P1** from **BE3-P1** flexible white polymer light emitting device are observed which are also consistent with their PL spectra.
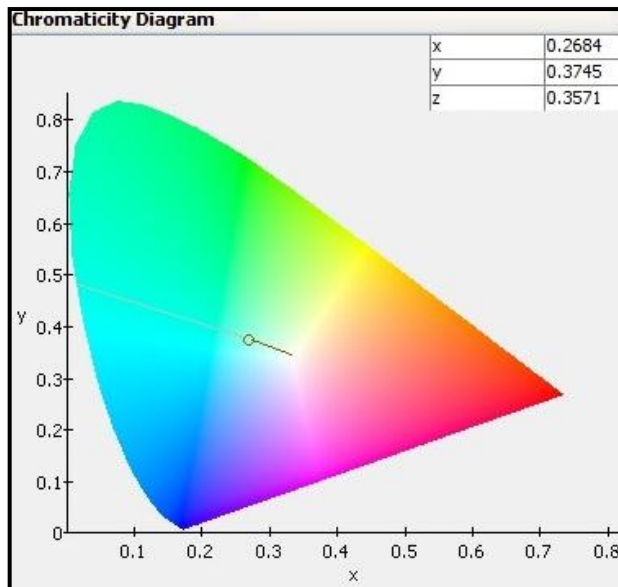
Figure 3.41 CIE chromaticity diagram for ITO/PEDOT:PSS/**BE3-P1** blend/Ca/Al
flexible devices.

In **Figure 3.41**, the CIE Chromaticity coordinates belonging to the **BE3-P1** flexible
white polymer light emitting diode is given as x = 0.26, y = 0.37. These emission
coordinates belonged to the white emission zone in the CIE diagram and close to the
equal energy white point of the diagram (x= 0.33, y=0.33).

The pure white color was unable to achieve from the flexible devices. There are a
variety of reasons for the outcomes of the flexible WPLED experiments. First of all, ITO
is not resistant to the mechanical bending due to its brittleness, thus it is detrimental to
flexible OLEDs to some extent. Moreover, the high processing of temperature of ITO
makes it difficult to form a high quality anode on flexible substrates such as PEN. It is
also difficult to easily adopt ITO-PEN to the solution process. Therefore, due to the
significant differences in processing of ITO-PEN as compared to ITO-glass, the flexible
device performance was also affected despite the usage of the same blue and orange
emitter polymer blend (**BE3-P1**) as EML.
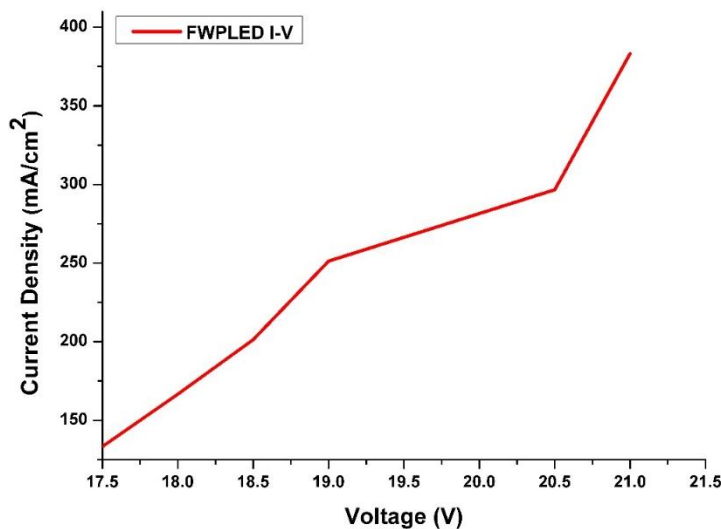
Figure 3.42 Current density vs. applied voltage for ITO/PEDOT:PSS/ **BE3-P1** blend/Ca/Al flexible devices.

In **Figure 3.42**, the current density versus voltage characteristics (I-V) of **BE3-P1** flexible white polymer light emitting diode was recorded. The turn-on voltage of the device is 17.5 V. The same reasons affecting the turn-on voltage devices are valid in flexible devices, as well. Besides, the ITO anode of the flexible device has different properties. The ITO-sheet resistance could be slightly different than that of ITO-glass. Although both of them are purchased having a resistance of 15ohm/sq, the etching and cleaning steps may change the surface properties, hence alter the turn-on voltage and working voltage.
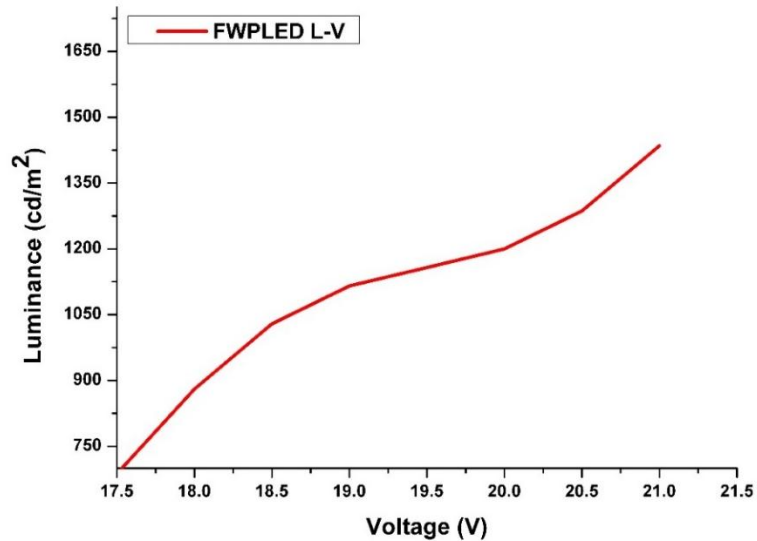
Figure 3.43 Luminance vs. applied voltage for ITO/PEDOT:PSS/**BE3-P1** blend/Ca/Al flexible devices.

In **Figure 3.43**, the luminance against voltage characteristics (L-V) of the **BE3-P1** flexible white polymer light emitting diode were investigated. The flexible WPLED operated at higher voltages, yet the working voltage range was especially narrow, at 19V, the luminance is 1100 cd/m². A summary of the constructed White PLEDs are given along with the luminance efficiencies (LE) as calculated from the L-V and I-V characteristics of the WPLEDs in Table 3.3.

Table 3.3 White PLED and Flexible White PLED Performances

Device No.	Blend Type (99:1 wt %) (toluene)	Turn-On Voltage	Working Voltage	CIE at W. Voltage	Luminance Eff. (cd/A) at W. Voltage
1. ITO-Glass WPLED	**BE-3:P1** 20mg/mL	14 V	17 V	X: 0.31, Y: 0.33	3.42
2. ITO-Glass WPLED	**BE-3:P2** 20mg/mL	15 V	17.5 V	X: 0.30, Y: 0.32	2.45
3. ITO-PEN FWPLED	**BE-3:P1** 20mg/mL	17.5 V	18.5 V	X: 0.26, Y: 0.37	0.90

CHAPTER 4

CONCLUSION

Different blue (**BE1**, **BE2**, **BE3**) and orange emitting polymers (**P1**, **P2**, **P3** and **P4**) with different end cappers were used in this study. The benzotriazole derivatives were used as the orange emitting polymers. As the alkyl chain attached to the triazol unit has a great contribution to the solubility of the polymer, the polymers containing benzotriazole and thiophene derivatives showed high optical and thermal stabilities. **P1**, **P2**, **P3** and **P4** were synthesized chemically via Suzuki cross coupling poly-condensation reaction. The structural characterizations of the polymers were carried out by NMR analysis. Physical properties of the polymers were characterized by GPC, TGA, and DSC techniques. Thermal studies showed that **P1** and **P2** have higher thermal stability then **P3** and **P4** as their total mass losses at decomposition temperatures are concerned. Electrochemical characterizations were also done by cyclic voltammetry (CV) and spectroelectrochemistry experiments. Subsequently, the optimization of the polymers that are to be used in device fabrications were conducted. First of all, quantum yield and photoluminescence (PL) experiments were accomplished prior to the PLED experiments. PL experiments in solution and thin film showed certain differences; the thin film PL spectra red-shifted as compared to the solution PL which are owing to the different intermolecular interactions in the films formed. Then, Förster energy transfer mechanism in PL and electroluminescence (EL) were investigated. Spectral overlap of the absorption of acceptor and the emission of donor were observed, and as the polymers were mixed within the Förster radius, an incomplete energy transfer occurred as proved by the outcomes of PL and EL spectra. Principally, for the generation of white EL in WPLEDs, the simultaneous emission of light from blue and orange emitting polymers were obtained in PL and EL from different polymer blends.

During this thesis work, arrangement of emitters in a well-mixed blend required a proper optimization of energy transfer process that transfer excitons from the higher band gap blue emitter to the lower band gap orange emitter, ultimately resulting in a co-existed emission. Since excitons favorably are formed in lower band gap components, thereby acting as traps for charge carriers, the weight percent ratio of blue to orange was set to 99:1 wt. % for this optimization. For the purpose of precise introduction of orange acceptor polymer with a very small amount of 1 wt. %, firstly, the orange emitter was dissolved in toluene, and then pre-calculated portions of the solutions were mixed with the blue donor polymer. Eventually, the lower band gap polymer amount was minimized in order to prevent higher exciton formation. This is also owing to the sensitivity of the energy transfer towards a minor change in the concentrations of the acceptor components. In PL experiments, most importantly, as the amount of acceptor polymer increased further above 5%, the peak from blue emitter was decreased significantly as compared in 90:10%, 95:5% and 99:1% blending ratios. This may be mostly due to the quenching of the excited state and poor charge mobility of the acceptor.

It was widely accepted that controlling an energy transfer process to ensure simultaneous emission is a critical issue in all methods for achieving white light, and in the thesis study, the successful results were achieved via proper molecular design and choice of single emitting polymers, regulation of their amounts, and controlling their interactions with each other on molecular level and on finished device. On molecular level, high PL efficiency is necessary yet not sufficient for efficient PLED performance. The device fabrication steps were critical, as well. WPLEDs and Flexible WPLEDs were constructed methodically and characterized successfully. The device configuration is as follows; ITO/PEDOT:PSS/emissive layer/Ca/Al. The motivations for choosing the polyfluorene derivatives (PFs), **BE1**, **BE2**, and **BE3** as blue emitting polymers were confirmed as they were revealed to be suitable for the device fabrication. Their high photoluminescence quantum efficiency, solubility, charge carrier mobility and thermal stability properties were found to be sound. Phenyl, triphenylamine and oxadiazole groups in the end groups of the polymers exhibited different effects to the WPLED efficiency. Their effect on charge transportation, stability, life time and WPLED

efficiency were discussed. The electron donating phenyl and triphenylamine group increased the hole transporting ability of orange emitters and oxadiazole end capper enhanced the electron transporting property of donor blue polymer. As a result, it was revealed that the best performance was obtained from the constructed device consists of an emissive layer of the mixture of blue emitting polymer **BE3** and orange emitting polymer **P1** (**BE3-P1** blend). From cyclic voltammetry experiments, **P1** having a less deeper HOMO level than **P2** promoted more hole injection and due to its higher stability, its device application ITO-glass based **BE3-P1** WPLED exhibited a stable white EL and CIE pure white color coordinates. The best luminance efficiency was achieved as 3.42cd/A, and the best white color coordinates are x= 0.31, y=0.32. The ITO-PEN based flexible white polymer light emitting diode showed efficient performance, as well. The luminance efficiency was achieved as 0.9 cd/A. The color coordinates are x=0.26, y=0.37.

REFERENCES

[1] C. K. Chiang, C. R. Fincher, Y. W. Park, A. J. Heeger, H. Shirakawa, E. J. Louis, S. C. Gau, and A. G. MacDiarmid, Electrical conductivity in doped Polyacetylene, *Phys. Rev. Lett.*, 39, 1098–1101, 1977.

[2] O.V. Mikhnenko, P. W. M. Blom, and T. Nguyen, Exciton diffusion in organic semiconductors, *Energy Environ. Sci.,* 8, 1867-1888, 2015.

[3] *Principles of Polymerization*, John Wiley and Sons, 2004.

[4] C. R. McNeill and N. C. Greenham, Conjugated-Polymer Blends for Optoelectronics, *Adv. Mater.*, 21, 3840–3850, 2009.

[5] *Electroluminescence of Polymers*, Universität Potsdam, Institute of Physics and Astronomy, 2014.

[6] Q. Pei., Light-Emitting Polymers, *Material Matters*, 26, 2 (3), 2007.

[7] B.Valeur and M.N. Berberan-Santos, A Brief History of Fluorescence and Phosphorescence before the Emergence of Quantum Theory, *J. Chem. Educ.*, 88, 731–738, 2011.

[8] Nanonews, http://www.nanonewsnet.ru/NanocoTechnologies/SciencePhoto Library, last visited on September 1, 2015.

[9] *Principles of Fluorescence Spectroscopy*, Springer Science and Business Media, 2006.

[10] N. T. Kalyani and S.J. Dhoble, Organic light emitting diodes: Energy saving lighting technology, *Renewable and Sustainable Energy Reviews*, 16, 2696– 2723, 2012.

[11] National Programme on Technology Enhanced Learning, http://nptel.ac.in/courses/102103044/module2/lec6/images/1.png, last visited on August 30, 2015.

[12] *Structure and Dynamics of Macromolecules: Absorption and Fluorescence Studies*, Elsevier B.V., 2004

[13] *Basic Mechanisms of Photoluminescence*, Springer Series in Materials Science, 2013.

[14] H. J. Round, A note on carborundum, *Electrical World*, 49, 309, 1907.

[15] J. L. Katz, S. A. Rice, S. Choi, and J. Jortner, On the Excess Electron and Hole Band Structures and Carrier Mobility in Naphthalene, Anthracene, and Several Polyphenyls, *J. Chem. Phys.*, 39, 1683, 1963.

[16] J. Kalinowski, J. Godlewski, and R. Signerski, Electroluminescence in Tetracene Crystals, *Molecular Crystals and Liquid Crystals*, 33, 247-259, 1976.

[17] R.H. Partridge, Electroluminescence from polyvinylcarbazole films, *Polymer*, 24, 733-762, 1983.

[18] C.W. Tang and S.A. Van Slyke, Organic electroluminescent diodes, *Applied Physics Letters*, 51, 913-915, 1987.

[19] J.H. Burroughes, D.D.C. Bradley, A.R. Brown, R.N. Marks, K. Mackay, R.H. Friend, P.L. Burns, and A.B. Holmes, Light-Emitting-Diodes Based on Conjugated Polymers, *Nature*, 347, 539-541, 1990.

[20] *In Solid State Physics*, Academic Press, 1995.

[21] M. Hack, R. Hewitt, K. Urbanik, A. Chwang, and J.J. Brown, Full colour top emission AMOLED displays on flexible metal foil, *Proceedings of the IMID/IDMC'06 Digest Conference*, 305-307, 2006.

[22] C. H. Cheung, A.B. Djurisic, C. Y. Kwong, Hoi-Lam Tam, K. W. Cheah, Z. T. Lui, W K Chan, P. C. Chui, J. Chan, and A.D. Rakic, Change of the Emission Spectra in Organic Light-Emitting Diodes by Layer Thickness Optimization, *Applied Physics Letters*, 85, 2944-2946, 2004.

[23] C. Zhang, Y. S. Zhao, and J. Yao, Organic composite nanomaterials: energy transfers and tunable luminescent behaviors, *New J. Chem.*, 35, 973–978, 2011.

[24] T. Förster, Zwischenmolekulare energiewanderung und fluoreszenz, *Annalen der Physik*, 437, 55–75, 1948.

[25] J. Heine and K. Müller-Buschbaum, Engineering metal-based luminescence in coordination polymers and metal–organic frameworks, *Chem. Soc. Rev.*, 42, 9232, 2013.

[26] Y. Tao, C. Yang, and J. Qin, Organic donor materials for phosphorescent organic light-emitting diodes, *Chem. Soc. Rev.*, 40, 2943–2970, 2011.

[27] Y.K. Huang, T.H. Jen, Y.T. Chang, N.J. Yang, H.H. Lu, and S.A. Chen, Enhancing Shielding of Triplet Energy Transfer to Poly(p-phenylene)s from Phosphor Acceptor by Addition of Branched Alcohol for Highly Efficient Electrophosphorescence, *ACS Appl. Mater. Interfaces*, 2, 1094-1099, 2010.

[28] C. Berney and G. Danuser, FRET or no FRET: A Quantitative Comparison, *Biophys. J.*, 84, 3992-4010, 2003.

[29] C.B. Murphy, Y. Zhang ,T. Troxler ,V. Ferry , J. J. Martin , and W. E. Jones , Jr., Probing Förster and Dexter Energy-Transfer Mechanisms in Fluorescent Conjugated Polymer Chemosensors, *J. Phys. Chem. B*, 108, 1537–1543, 2004.

[30] S. H. Lin, W. Z. Xiao, and W. Dietz, Generalized Förster-Dexter theory of photoinduced intramolecular energy transfer, *Phys. Rev. E*, 47, 3698, 1993.

[31] *Organic Electronics: Materials, Manufacturing and Applications*, Wiley-VCH Verlag GmbH & Co, 2006.

[32] *Solid-State Lighting Research and Development:Multi-Year Program Plan*, Navigant Consulting, Inc., 2012.

[33] D. Volz, M. Wallesch, C. Fléchon, M. Danz, A. Verma, J. M. Navarro, D. M. Zink, S. Bräse, and T. Baumann, From iridium and platinum to copper and carbon: new avenues for more sustainability in organic light-emitting diodes, *Green Chem.*, 17, 1988, 2015.

[34] *WOLEDs and Organic Photovoltaics*, Springer-Verlag Berlin Heidelberg, 2010.

[35] B. Geffroy, P. le Roy, and C. Prat, Organic light-emitting diode (OLED) technology: materials, devices and display technologies, *Polym Int*, 55, 572–582, 2006.

[36] R. Schlaf, H. Murata, and Z.H. Kafaf, Work function measurements on indium tin oxide films, *Journal of Electron Spectroscopy and Related Phenomena*, 120, 149–154. 2001.

[37] M. Stössel J. Staudigel1, F. Steuber, J. Simmerer, and A. Winnacker, Impact of the cathode metal work function on the performance of vacuum-deposited organic light emitting-devices, *Appl. Phys. A*, 68, 387–390, 1999.

[38] S. E. Shaheen, G. E. Jabbour, M. M. Morrell, Yutaka Kawabe, Bernard Kippelen, N. Peyghambarian, M. F. Nabor, Rudy Schlaf, E. A. Mash, and N. R. Armstrong, Bright blue organic light-emitting diode with improved color purity using a LiF/Al cathode, J. *Appl. Phys.* 84, 2324, 1998.

[39] J. H. Cook, H.A. Al-Attar, and A. P. Monkman, Effect of PEDOT–PSS resistivity and work function on PLED performance, *Organic Electronics*, 15, 245–250, 2014.

[40] *Transparent Conducting Thin Films,* Organic Light-Emitting Diodes (OLEDs): Materials, Devices and Applications, 2013.

[41] *OLED Fundamentals: Materials, Devices, and Processing of Organic Light-Emitting Diodes*, CRC Press Book, 2015.

[42] *OLED Display Fundamentals and Applications*, John Wiley and Sons, 2012.

[43] Rensselaer Polytechnic Institute, http://www.ecse.rpi.edu/~schubert/Light-Emitting-Diodes-dot-org/cha**P1**7/F17-04%20Chromaticity%20diagram.jpg, last visited on September 10, 2015.

[44] M. Shukla, N. Brahme, R.S. Kher, and M.S.K. Khokhar, Elementary approach to calculate quantum efficiency of polymer light emitting diodes, *Indian Journal of Pure and Applied Physics*, 49, 142-145, 2011.

[45] Q. Yue, W. Li, F. Kong, and K. Li, Enhancing the Out-Coupling Efficiency of Organic Light-Emitting Diodes Using Two-Dimensional Periodic Nanostructures, *Advances in Materials Science and Engineering*, 2012.

[46] S. R. Forrest, The road to high efficiency organic light emitting devices, *Organic Electronics*, 4, 45–48, 2003.

[47] E. Polikarpov and M. E. Thompson, Achieving High Efficiency in Organic Light-Emitting Devices, *Material Matters*, 2-3, 2007.

[48] S. Reineke, M. Thomschke, B. Lüssem, and K. Leo, White organic light-emitting diodes: Status and perspective, *Rev. Mod. Phys*., 85, 1245, 2013.

[49] *Organic Light Emitting Diodes (OLEDs) for General Illumination Update 2002,* OIDA, 2002.

[50] Wonderful Engineering,
 http://cdn.wonderfulengineering.com/wp-content/uploads/2014/01/LG-and-OLED-610x457.jpg, last visited on September 2, 2015.

[51] How OLEDs Work, http://electronics.howstuffworks.com/oled.htm, last visited on September 2, 2015.

[52] *How OLEDs Work*, F. Craig., 2005.

[53] Sammobile,
 http://www.sammobile.com/wp-content/uploads/2012/11/3186-samsung-flex.jpg, last visited on September 1, 2015.

[54] J. W. Hamer, A. D. Arnold, M. L. Boroson, M. Itoh, T. K. Hatwar, M.J. Helber, K. Miwa, C.I. Levey, M. Long, J.E. Ludwicki, D.C. Scheirer, J.P. Spindler, and S.A. Van Slyke, System design for a wide-color-gamut TV-sized AMOLED display, *Journal of the Society for Information Display*, 16 (3), 2008.

[55] *International OLED Technology Roadmap*, U.S. Display Consortium, 2010.

[56] *Solid-State Lighting Multi-Year Market Development Support Plan*, U.S. Department of Energy, 2012.

[57] Philips demonstrates world's first mains-powered white-light OLED module, http://www.newscenter.philips.com/pwc_nc/main/standard/resources/corporate/press/20 10/OLED/Philips_%20AC-OLED_hand_560.jpg, last visited on September 8, 2015.

[58] J. Kalinowski, M. Cocchi, D. Virgili, V. Fattori, and J.A.G. Williams, Mixing of excimer and exciplex emission: a new way to improve white light emitting organic electrophosphorescent diodes, *Advanced Materials*, 19, 4000-4005, 2007.

[59] A. Misra, P. Kumar, M. N. Kamalasanan, and S. Chandra, White organic LEDs and their recent advancements, *Semiconductor Science and Technolog*y, 21, 7, 2006.

[60] J. Huang, W. Hou, J. Li, G. Li, and Y. Yang, Improving the power efficiency of white light-emitting diode by doping electron transport material, *Appl Phys Lett*, 89, 133509, 2006.

[61] F. Liu, C. Tang, Q. Chen, F. Shi, H. Wu, L. Xie, B. Peng, W. Wei, Y. Cao, and W. Huang, *J Phys Chem C*, 113:4641, 2009.

[62] B. W. D'Andrade, M. E. Thompson, and S. R. Forrest, Controlling Exciton Diffusion in Multilayer White Phosphorescent Organic Light Emitting Devices, *Adv. Mater.*, 14-2, 2002.

[63] Y. Karzazi, Organic Light Emitting Diodes: Devices and applications, *J. Mater. Environ. Sci.* 5, 1-12, 2014

[64] A. Köhnen, M. Irion, M. C. Gather, N. Rehmann, P. Zacharias, and K. Meerholz, Highly color-stable solution-processed multilayer WOLEDs for lighting application, *J. Mater. Chem.*, 20, 3301–3306, 2010.

[65] J. Zou, J. Liu, H. Wu, W. Yang, J. Peng, and Y. Cao, High-efficiency and good color quality white light-emitting devices based on polymer blend, *Organic Electronics*, 10, 843–848, 2009.

[66] B. B. Zhang, C. Qin, J. Ding, L. Chen, Z. Xie, Y. Cheng, and L. Wang, High-Performance All-Polymer White-Light-Emitting Diodes Using Polyfluorene Containing Phosphonate Groups as an Efficient Electron-Injection Layer, *Adv. Funct. Mater.*, 20, 2951–2957, 2010.

[67] E. R. Kötz, H. Neff, and K. J. Müller, *Electroanal. Chem.*, 215, 331, 1986.

[68] E. Kaya, A. Balan, D. Baran, A. Cirpan, and L. Toppare, Electrochromic and optical studies of solution processable benzotriazole and fluorene containing copolymers, *Organic Electronics*, 12, 202–209, 2011.

[69] T. Kaya Deniz, A. Goycek Nurioglu, N. Akbasoglu Unlu, M. Sendur, L. Toppare, and A. Cirpan, Syntheses, electrochemical and photophysical properties of biphenyl containing conjugated copolymers, *Polymer*, 54, 2243-2249, 2013.

[70] R. S. Nicholson, Theory and Application of Cyclic Voltammetry for Measurement of Electrode Reaction Kinetics, *Analytical Chemistry*, 37, 1351-1355, 1965.

[71] C.Q. Ma, M. Fonrodona, M.C. Schikora, M.M. Wienk, R.A.J. Janssen, and P. Bauerle, *Adv. Funct. Mater.*, 18, 3323, 2008.

[72] *Measurement of Fluorescence Quantum Yields*, Thermo Fisher Scientific, 2010.

[73] *Standard Reference Materials: A Fluorescence Standard Reference Material: Quinine Sulfate Dihydrate*, National Bureau of Standards Special Publication, 1980.

[74] T. Lee, J. H. Park, O. O. Park, J. Lee, Y. C. Kim, A systematic doping strategy to control the emission spectrum of ternary luminescent polymer blends for white emission, *Optical Materials*, 30, 486–491, 2007.
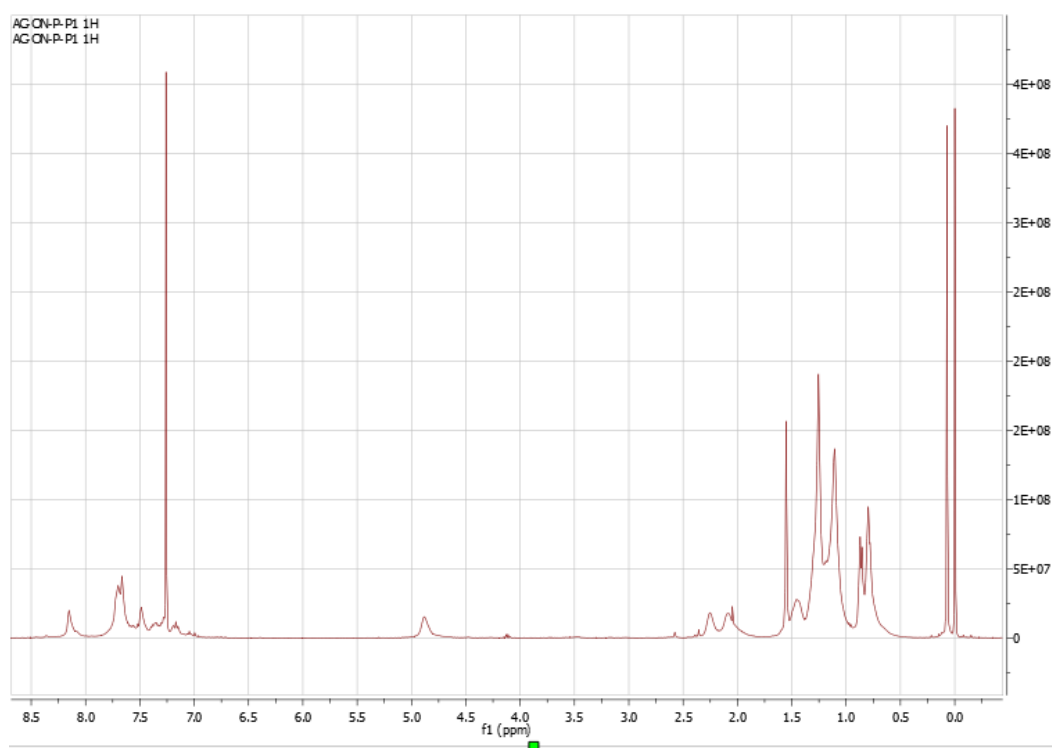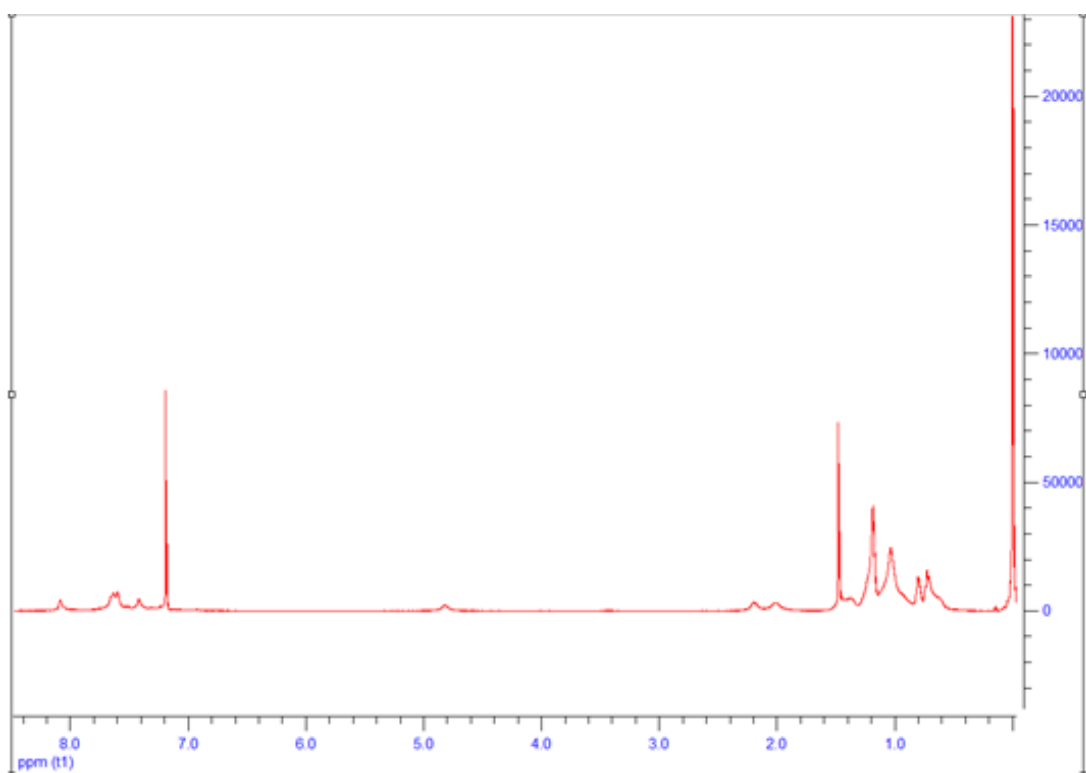
A.1 ^{1}H NMR of P1

Figure A.1 ^{1}H NMR of poly-(9,9-dioctylfluorene)-2,7-diyl-(4,7 bis(thien-2-yl)2-dodecyl- benzo[1,2,3]triazole)) end capped with phenyl (**P1**).
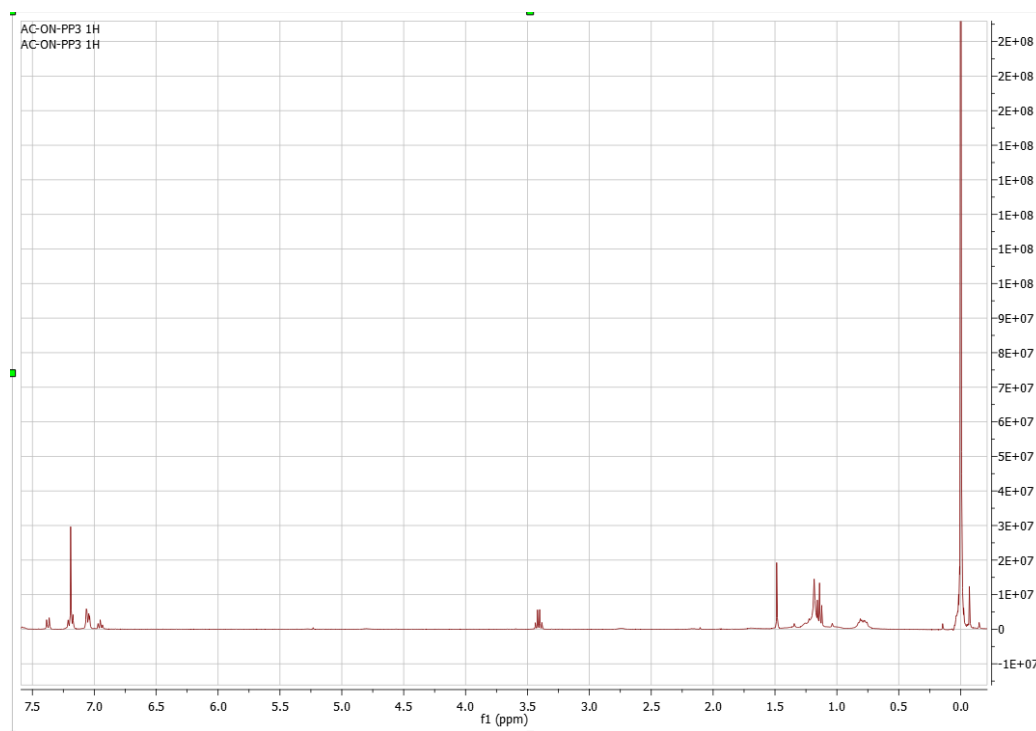
Figure A.2 ^{1}H NMR of poly-(9,9-dioctylfluorene)-2,7-diyl-(4,7 bis(thien-2-yl)2-dodecyl- benzo[1,2,3]triazole)) end capped with triphenylamine (**P2**).

A.3 ¹H NMR of P3

Figure A.3 ¹H NMR of poly ((4-(5-(biphenyl-4-yl)-4-hexylthiophenyl-2-yl)-2-dodecyl-7-(4-   hexylthiophen-2-yl)-2H-benzo[d][1,2,3]triazole)) end capped with phenyl (**P3**).

A.4 ^{1}H NMR of P4
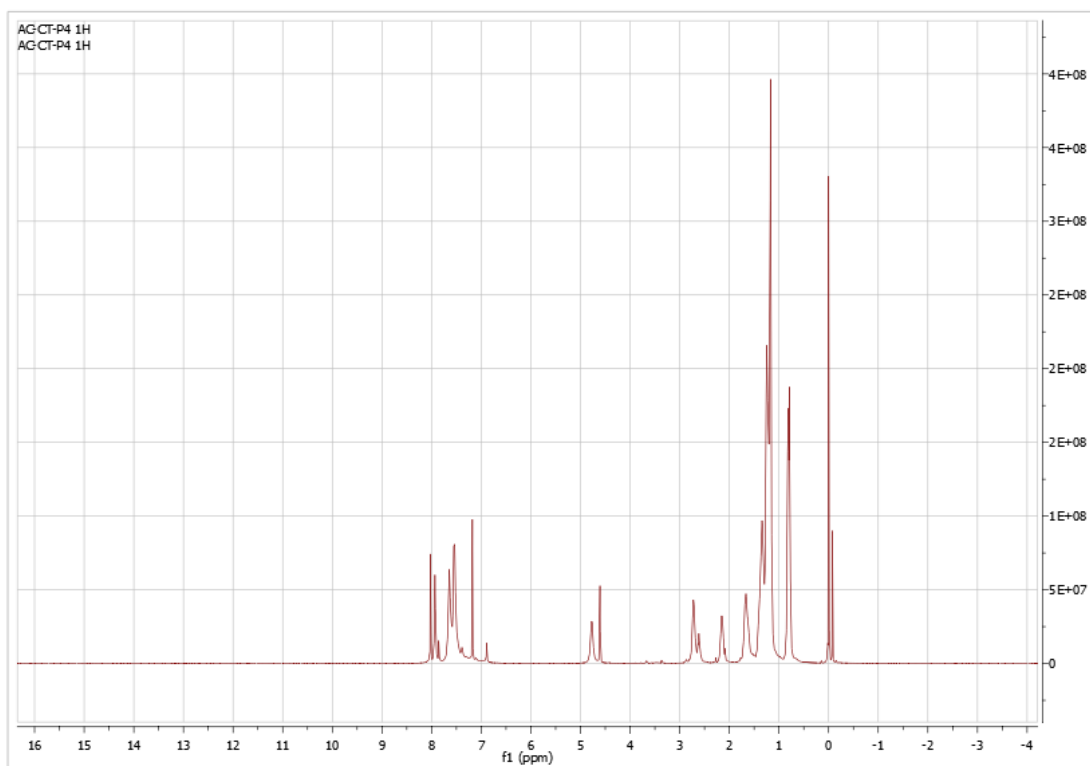
Figure A.4 ^{1}H NMR of poly ((4-(5-(biphenyl-4-yl)-4-hexylthiophenyl-2-yl)-2-dodecyl-7-(4-hexylthiophen-2-yl)-2H-benzo[d][1,2,3]triazole)) end capped with triphenylamine (**P4**).

APPENDIX B

B.1 Differential Scanning Calorimetry (DSC) of P1
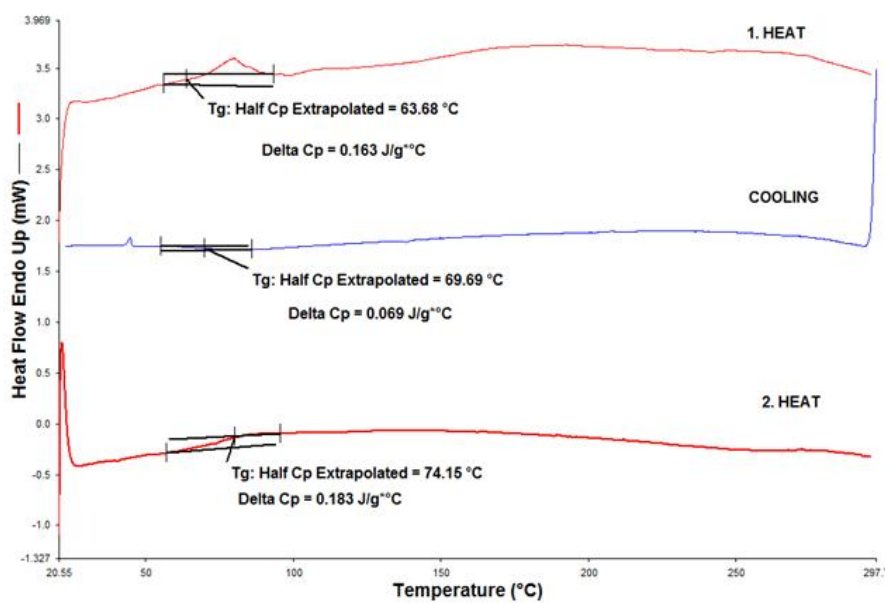
Figure B.1 Differential Scanning Calorimetry (DSC) of **P1.**
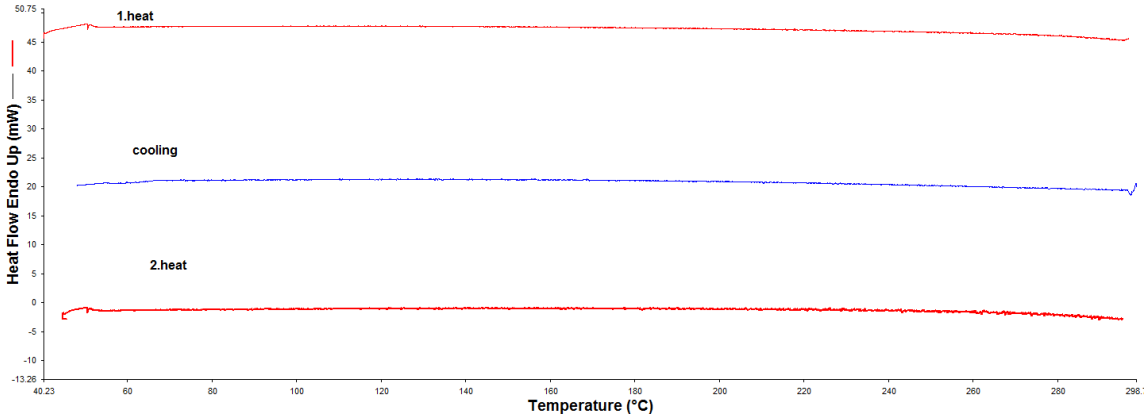
B.2 Differential Scanning Calorimetry (DSC) of P2
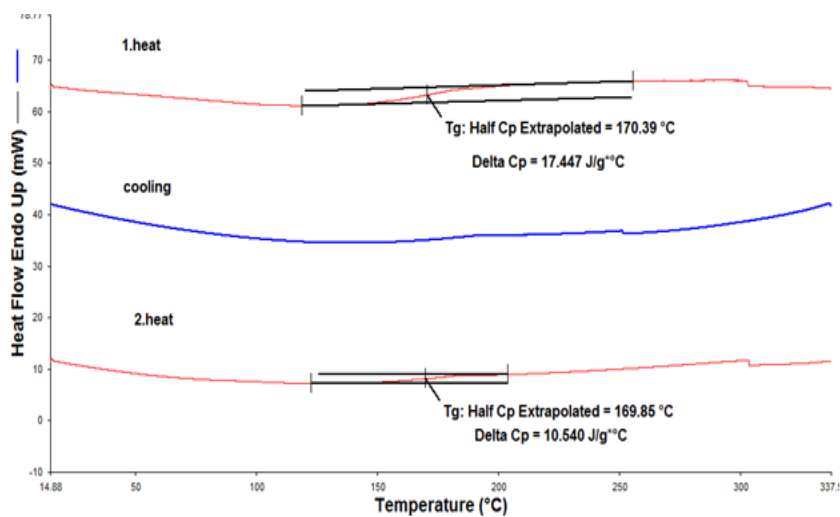
Figure B.2 Differential Scanning Calorimetry (DSC) of **P2.**

B.3 Differential Scanning Calorimetry (DSC) of P3
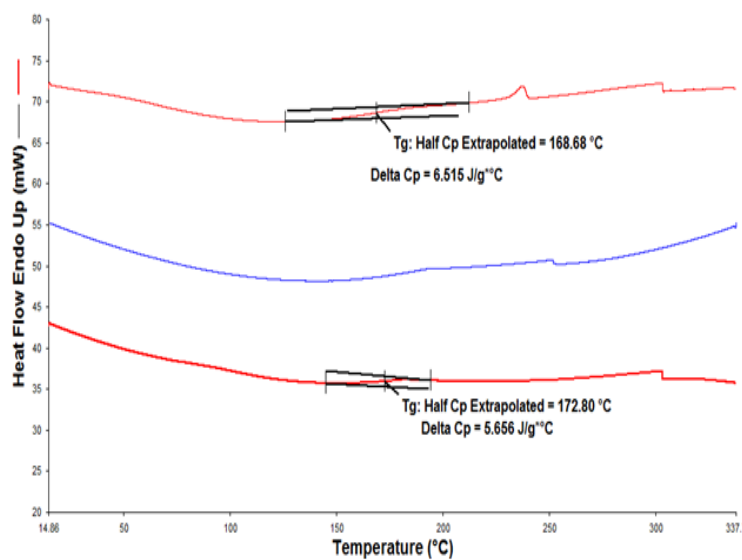
Figure B.3 Differential Scanning Calorimetry (DSC) of **P3.**

B.4 Differential Scanning Calorimetry (DSC) of P4

Figure B.4 Differential Scanning Calorimetry (DSC) of **P4.**

APPENDIX C

C.1 Thermogravimetric Analysis (TGA) of P1

%Kayıp= 67.021%
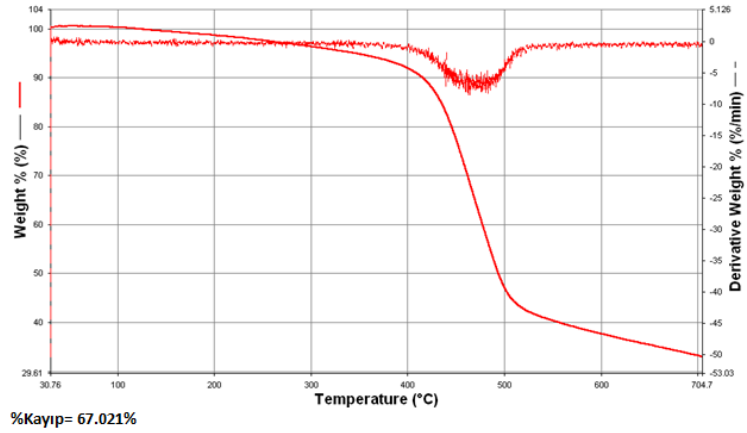
Figure C.1 Thermogravimetric Analysis (TGA) of **P1.**

C.2 Thermogravimetric Analysis (TGA) of P2

%Kayıp= 60.419%
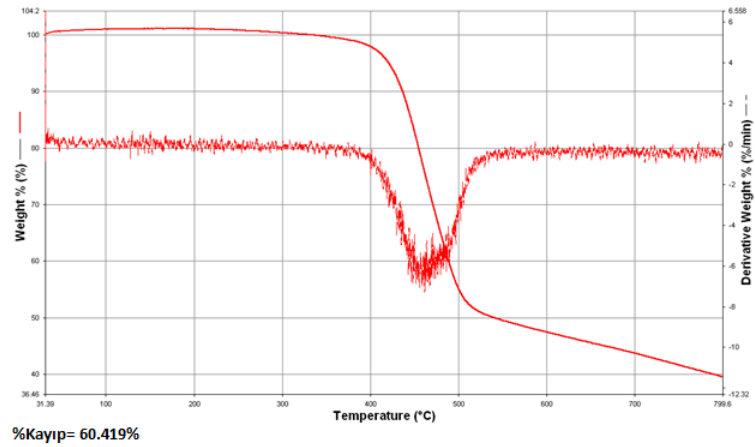
Figure C.2 Thermogravimetric Analysis (TGA) of **P2.**

C.3 Thermogravimetric Analysis (TGA) of P3

%Kayıp=92.166 %
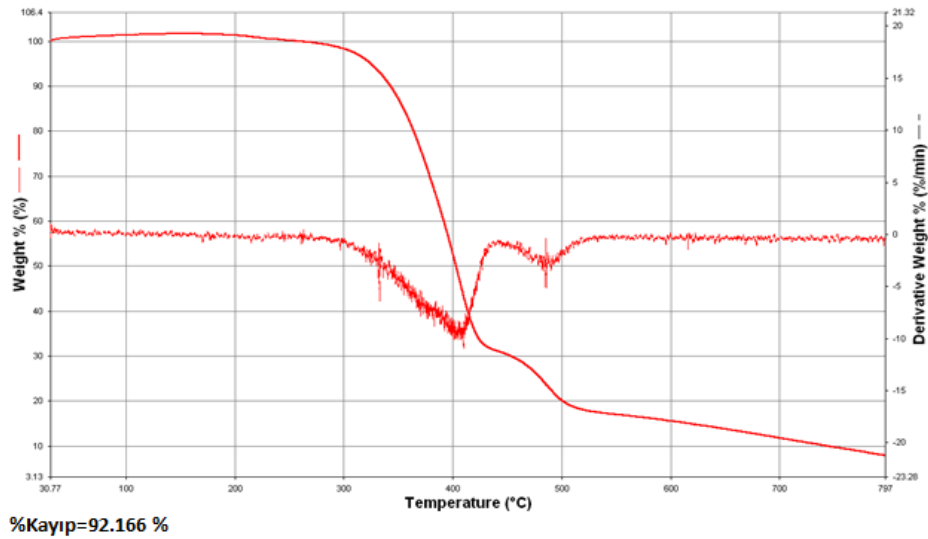
Figure C.3 Thermogravimetric Analysis (TGA) of **P3.**

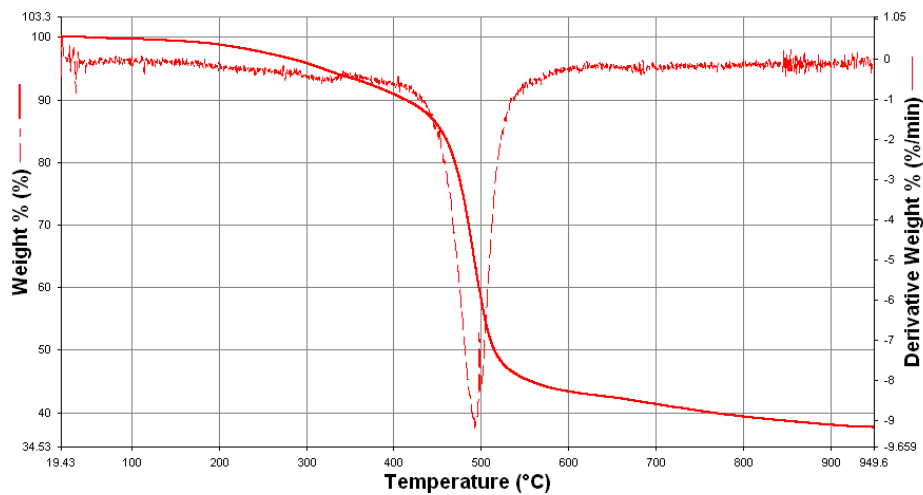## C.4 Thermogravimetric Analysis (TGA) of P4

Figure C.4 Thermogravimetric Analysis (TGA) of **P4.**

APPENDIX D

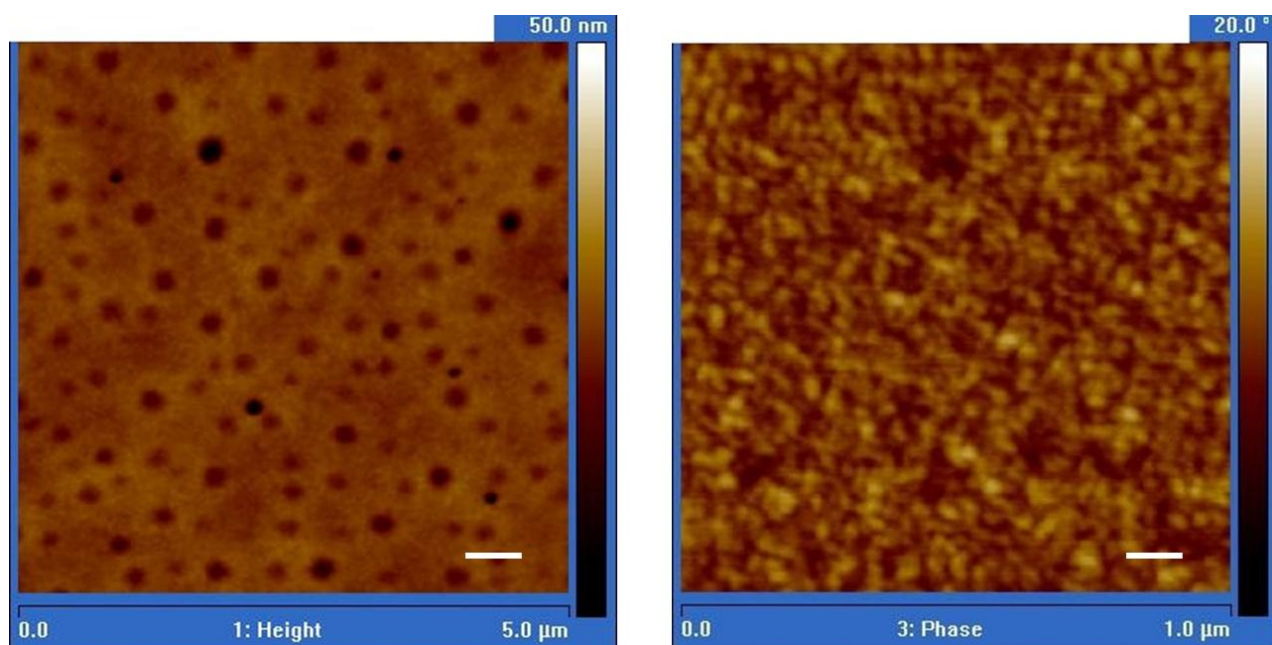**D.1 AFM height and phase images of polymer blend BE3-P1 (toluene) on ITO/PEDOT:PSS**

Figure D.1 AFM height and phase images of polymer blend **BE3-P1** (toluene) on ITO/PEDOT:PSS (scale bar is 100 nm).

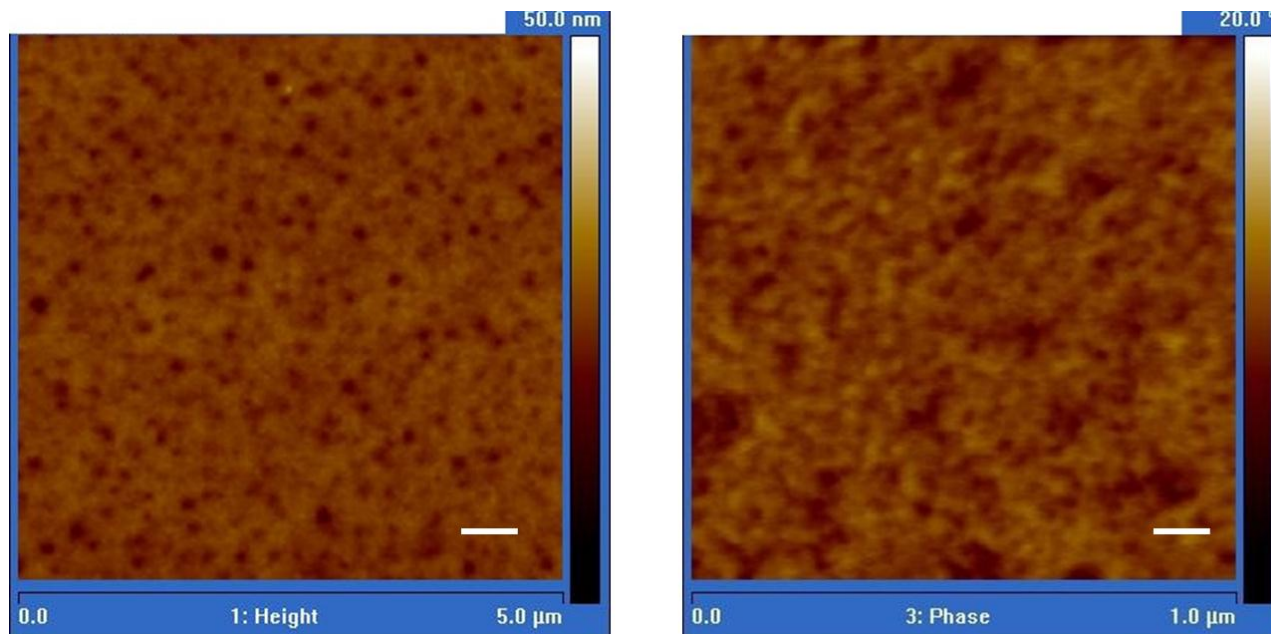## D.2 AFM height and phase images of polymer blend BE3-P1 (CHCl₃) on ITO/PEDOT:PSS

Figure D.2 AFM height and phase images of polymer blend **BE3-P1** (CHCl$_3$) on ITO/PEDOT:PSS (scale bar is 100 nm).

APPENDIX E

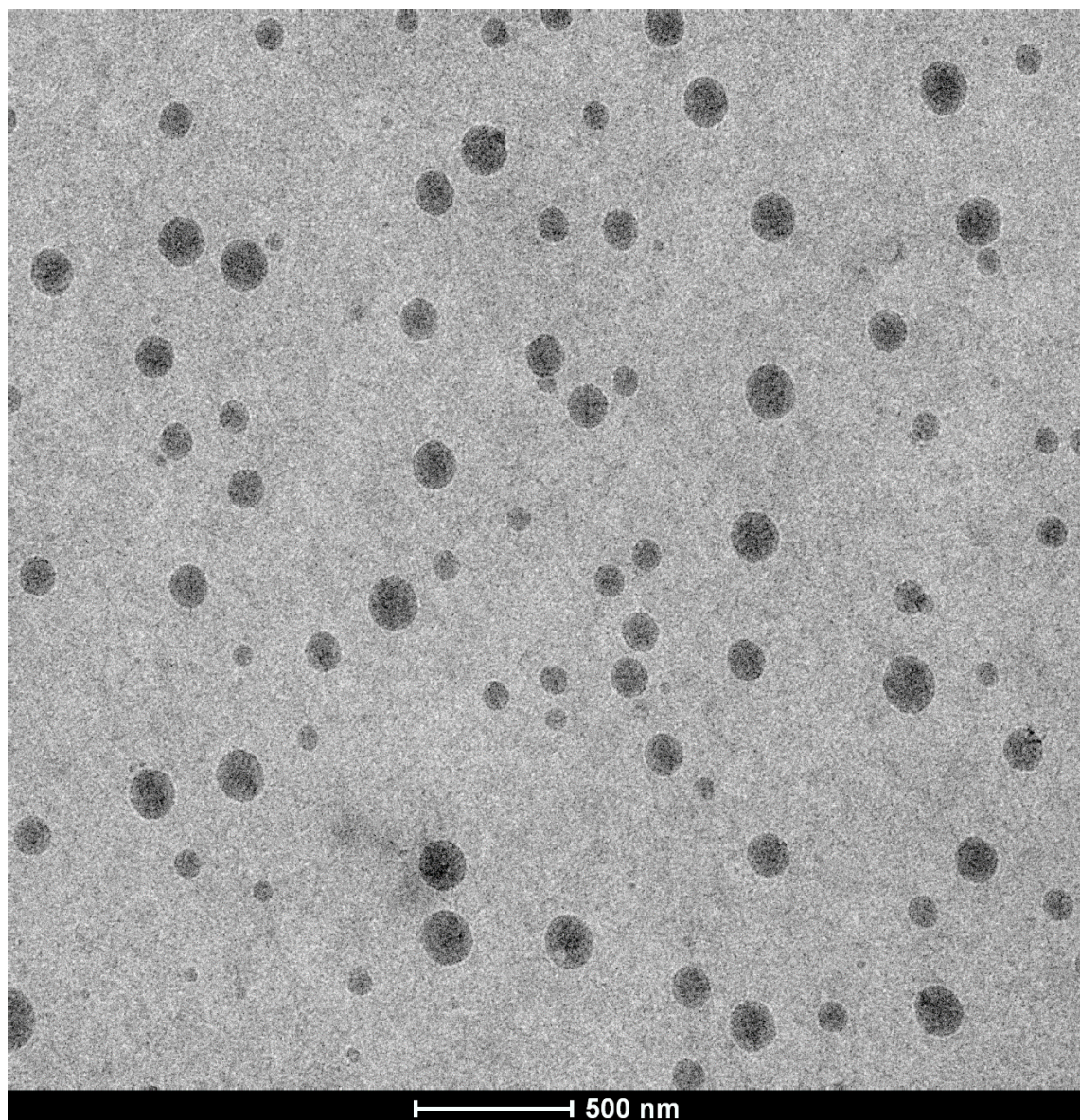**E.1 Transmission Electron Microscopy Image (TEM) of BE3-P1 Blend Active Layer (Toluene) 500 nm**

Figure E.1 Transmission Electron Microscopy Image (TEM) of **BE3-P1** Blend Active
Layer (Toluene) 500 nm.

E.2 Transmission Electron Microscopy Image (TEM) of BE3-P1 Blend Active Layer (Toluene) 100 nm
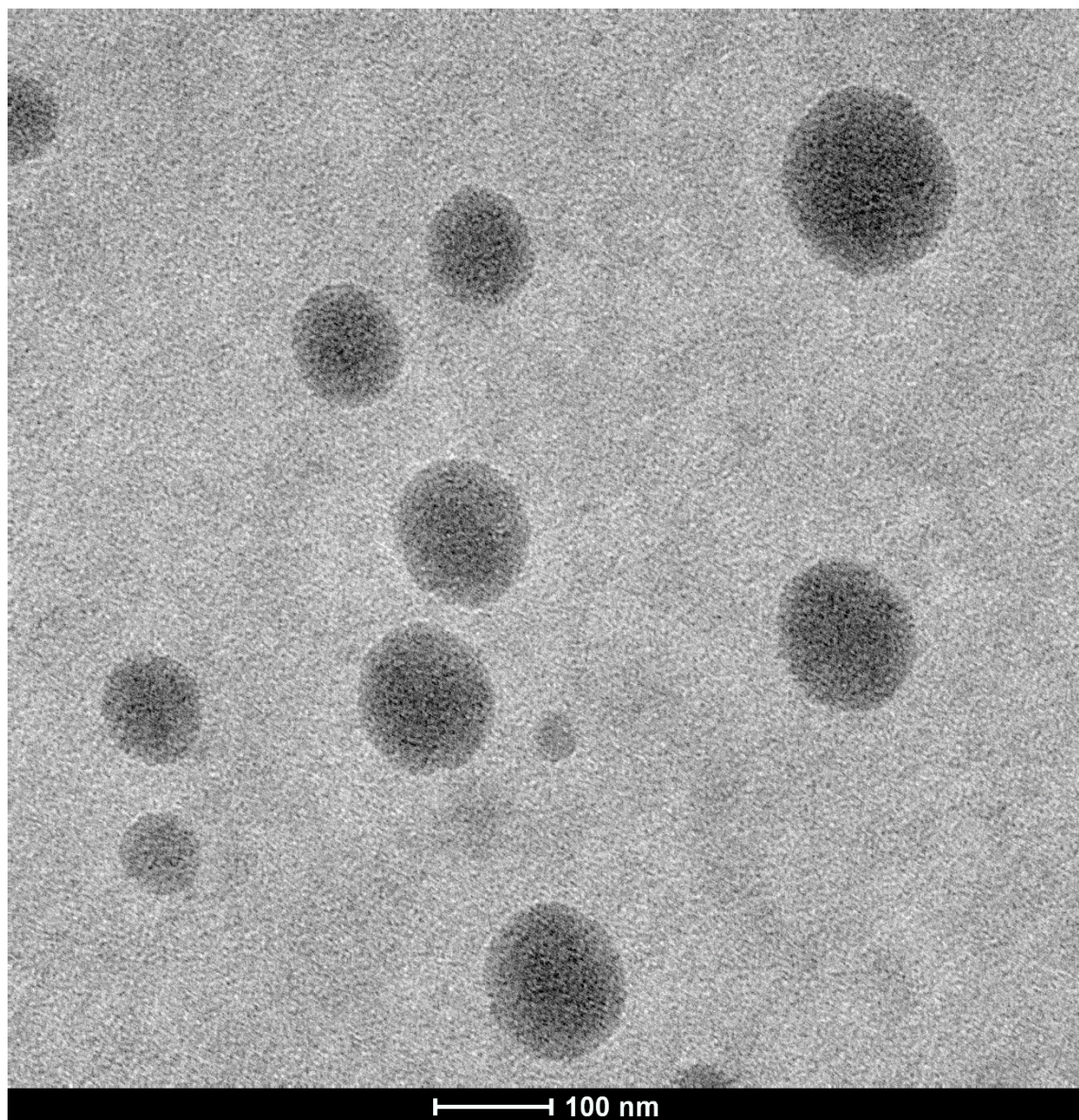

Figure E.2 Transmission Electron Microscopy Image (TEM) of **BE3-P1** Blend Active Layer (Toluene) 100 nm.

APPENDIX F

F.1 Gel Permeation Chromatography (GPC) Results of P1, P2, P3 and P4

Table F.1 Average molecular weight determination of **P1**, **P2**, **P3** and **P4**

Polymers	Mn	Mw	PDI
P1	15700	27900	1.7
P2	6900	17500	2.5
P3	8600	32600	3.8
P4	45000	183000	4.1